

Dear Prof. Kimitaka Kawamura and referees:

Thank you very much for your thoughtful and constructive comments on our manuscript. We have revised the manuscript accordingly. The detailed responses are given below point by point (in blue), and the revised manuscript is shown in red.

Response to Referee #1

Review of “One year monitoring of volatile organic compounds (VOCs) from an oil-gas station in northwest China. The authors of this paper have collected real-time high-resolution VOC concentration data for 56 VOCs in a location in China that is near high density oil and gas and petrochemical activity. VOC concentration data from oil and gas rich regions have been collected and published before, but the data are novel in that they were collected at a region where no such studies that targeted oil and gas emissions were conducted. The data and some of the discussion/comparison presented in the paper are valuable, however, there are a lot of redundant information in the paper and some parts that need additional clarification. There is also a lot of grammatical errors in the paper that need to be addressed before the paper is ready for publication. I recommend publication of the paper after major revisions. We thank the referee for the constructive evaluation and improving suggestions which were considered in revising the manuscript.

General comments:

Throughout the paper, the term oil-gas or oil and natural gas have been used. Unless the authors are specifically directing attention to wet gas (which is a combination of oil and gas from the same well), they should use the term oil and gas.

Thanks for the referee’s rigorous suggestion. We confirm that the oil and gas in the study area is not from the same well. Therefore, the term oil and gas instead of oil-gas is used in the revised manuscript.

The abstract needs major revisions (see Specific comments).

We have revised the abstract.

Oil and natural gas are important for energy supply around the world. The exploring, drilling, transportation and processing in oil and gas regions can release a lot of volatile organic compounds (VOCs). To understand the VOC levels, compositions and sources in such region, an oil and gas station in northwest China was chosen as the research site and fifty-seven VOCs designed as the photochemical precursors were continuously measured for an entire year (September 2014–August 2015) using an on-line monitoring system. The average concentrations of total VOCs were

297 ± 372 ppbv and the main contributor was alkanes, accounting for 87.5% of the total VOCs. According to the propylene-equivalent concentration and maximum incremental reactivity methods, alkanes were identified as the most important VOC groups for the ozone formation potential. Positive matrix factorization (PMF) analysis showed that the annual average contributions from natural gas, fuel evaporation, combustion sources, oil refining process and asphalt (anthropogenic and natural sources) to the total VOCs were 62.6 ± 3.04%, 21.5 ± .99%, 10.9 ± 1.57%, 3.8 ± 0.50% and 1.3 ± 0.69%, respectively. The five identified VOC sources exhibited various diurnal variation patterns due to their different emission patterns and the impact of meteorological parameters. Potential source contribution function (PSCF) and contribution weighted trajectory (CWT) models based on backward trajectories indicated that the five identified sources had similar geographic origins. Raster analysis based on CWT analysis indicated that the local emissions contributed 48.4–74.6% to the total VOCs. Based on the high-resolution observation data, this study clearly described and analyzed the temporal variation of VOC emission characteristics at a typical oil and gas field, which exhibited different atmospheric behaviors compared with that in urban and industrial areas.

Section 3.3: The authors do a lot of correlation comparisons in the paper. This is noted in the abstract too. A correlation ($r=0.19$) is not a good correlation. Furthermore, the authors do not discuss what this actually would mean in the physical sense. This is noted in the abstract (for correlation with pressure) and page 8 and 9 (Section 2.2). What exactly does a negative correlation of $r=-0.29$ between VOCs and temperature? Which VOCs were correlated? Were some better or worse? Are we looking at total VOCs? If yes, this does not make sense as some VOCs are broken down by UV or other atmospheric constituents in place because of sunlight. This section needs a lot of revising and some deletion of information that is not relevant or useful.

Thanks for your constructive comments. The physical meaning of the relationship between total VOCs and meteorological data are discussed in the manuscript. In addition, the relations between some VOC species (the representative species of VOCs groups, i.e., ethane, ethylene, acetylene and benzene) were explored by Pearson correlation analysis (Table S2) and we find that meteorological condition have different impacts on different VOCs species. Some irrelevant information is also deleted. We revised this section as shown below:

Fig. 6 shows the temporal variation of ethane, ethylene, acetylene and benzene in different timescales. Though differences exist, the selected compounds broadly represent the respective alkanes, alkenes, alkynes and aromatics (Lyu et al., 2016). Significant differences were found between the meteorological parameters in different seasons ($p < 0.01$) and the highest concentrations of these species in winter were observed. The seasonal variation of VOCs is

controlled by meteorological conditions, photochemical activities and source emissions. The highest values in winter was due to inhibited photochemical activities under suppressed dispersion conditions and low temperature. For instance, all these species were negatively correlated to BLH with higher VOCs levels under lower BLH (Fig. 6). The wind speed and temperature were also found negatively correlated to VOCs concentrations and ethylene showed the highest negative correlation to these parameters (Table S2). The less photochemical reactions also resulted in high concentrations in winter, which was proved by negative correlation between VOCs and O₃ (Table S2). Additional sources (i.e., combustion) may be also present, in view of the obvious increase of acetylene (Fig. 6c) from summer (0.87 ± 1.00 ppbv) to winter (10.5 ± 8.51 ppbv). Conversely, the high temperature, wind speed and BLH favor the dilution and dispersion of ambient VOCs and the photochemical depletion in summer. Therefore, lowest VOCs concentrations were observed in summer.

The diurnal variations of VOCs and trace gases (NO₂ and O₃) related to photochemical reaction are shown in Fig. 7. The VOCs had a reverse trend with O₃ ($r = -0.82$, $p < 0.01$). The lower BLH and less photochemical activities resulted in peak values for VOCs and low O₃ concentrations before sunrise (6:00 local time). After sunrise, with the initiation of photochemical oxidation and the increasing of BLH, the concentrations of VOCs decreased while the O₃ increased rapidly. The minimum of VOCs and occurred at about 12:00–14:00 LT was resulted from both dispersion or dilution conditions and photochemical reactions (with highest O₃ concentrations at 14:00 LT) in the afternoon. The diurnal variation of NO₂ was controlled by BLH, O₃ and photochemical reactions (i.e., OH radical) and showed a double peak. The similar diurnal patterns of different atmospheric lifetime compounds including ethane, ethylene, acetylene and benzene (the most abundant contributors to its categories) were also found (Fig. S4). To better understand the effects of BLH and photochemical reactions on VOCs, the diurnal variations of VOCs, BLH and O₃ in winter and summer were analyzed (Fig. 7b, c). VOC concentrations in winter (213 ± 97.7 ppbv) were significantly higher than those in summer (130 ± 100 ppbv). However, the VOCs in summer and winter decreased by 8.3 times and 2.3 times, respectively, from maximum to minimum. This was due to the BLH increased by 8.2 times in summer while the BLH in winter only increased by 2.3 times. The effects of photochemical reactions on VOCs in two seasons were comparable, which was explained by similar O₃ increment in winter (0.78 times up) and summer (0.71 times up). Therefore, we can conclude that the role of BLH variation was more important than the photochemical reaction for the diurnal variation of VOCs.

Table S2 Pearson correlation between VOCs, meteorological data and trace gases (O3 and NO2)

Species	Temperature	Wind speed	BLH	O3	NO2
Ethane	-0.393**	-0.436**	-0.524**	-0.414**	0.633**
Ethylene	-0.590**	-0.530**	-0.653**	-0.500**	0.642**
Acetylene	-0.541**	-0.370**	-0.481**	-0.197**	0.321**
Benzene	-0.440**	-0.392**	-0.473**	-0.377**	0.418**
VOCs	-0.286**	-0.391**	-0.444**	-0.361**	0.603**

** . Correlation is significant at the 0.01 level (2-tailed).

* . Correlation is significant at the 0.05 level (2-tailed).

The authors have collected data in China and the value of the data is that such data have not been collected in this area. The way they introduce this concept in the introduction is very-very confusing. I suggest the authors discuss the studies done in China in more detail (when justifying this research) and then when comparing their results with other oil and gas basins, discuss location other than China where there have been a multitude of such studies and data presented.

Thanks for this comment, we have revised the expression accordingly.

Was there a reason the authors did not use HYSPLIT for the back-trajectory analysis?

Due to our vague description, which made the readers confusing the method for back-trajectory analysis. In fact, the back-trajectory analysis was conducted using HYSPLIT, which was run by TrajSta-MeteoInfo plugin (available at <http://www.meteothinker.com>). Therefore, we revise our description in the manuscript.

Throughout the paper authors should clarify their comments about other studies and data availability to show when they are talking about China vs other regions and locations.

Thanks for your suggestion, comments and data availabilities about other studies have been added in the revised manuscript.

Previous studies in China mainly focused on the measurements of VOCs in urban agglomerations such as the Pearl River Delta (PRD) region (Tang et al., 2007; Liu et al., 2008; Cheng et al., 2010; Ling et al., 2011), Yangtze River Delta (YRD) region (An et al., 2014; Li et al., 2016; Shao et al., 2016) and Beijing-Tianjin-Hebei (BTH) region (Li et al., 2015) and key megacities including Beijing (Song et al., 2007; Wang et al., 2010; Yuan et al., 2010), Shanghai (Cai et al., 2010; Wang, 2014), Guangzhou (Zou et al., 2015) and Wuhan (Lyu et al., 2016). These studies found that vehicle emission and solvent usage contributed most to the ambient VOCs in urban areas. A few studies were also conducted in industrial areas (An et al., 2014; Wei et al., 2015; Shao et al., 2016) and petrochemical industrial regions with a lot of VOC emissions (Lin et al., 2004; Wei et al., 2015; Jia et al., 2016; Mo et al., 2017). These studies found

that the VOC sources and compositions are complex due to the different emission and atmospheric processes (Warneke et al., 2014). However, the research conducted in oil and gas area in China is still limited while the VOCs emission characteristics in this type of regions are common around the world (Buzcu-Guven and Fraser, 2008; Simpson et al., 2010; Rutter et al., 2015; Bari et al., 2016). For instance, Leuchner and Rappenglück. (2010) found that natural gas/crude oil sources contributed most to the VOC emissions in Houston. Gilman et al. (2013) found that oil and gas emissions strongly contribute to the propane and butanes in northeast Colorado. Therefore, study concerning VOC emission characteristics studies in oil and gas area in China is very important.

Sections 2.3-2.5 should be re-written to be more concise and then combined. For example, PMF is a model widely used, so the amount of information given on the model is not useful in this paper.

Thanks for your constructive suggestion. Section 2.3-2.5 has been combined to be more concise.

2.3 Data sources and analysis

2.3.1 Meteorological parameters and air pollutants

Other dataset such as the three-hour resolution meteorological parameters (atmospheric pressure (P), temperature (T), relative humidity (RH), wind speed (WS) and direction (WD)) were collected from the Meteomanz (www.meteomanz.com) and are shown in Fig. 2. The boundary layer height (BLH) was computed every three hours each day through the NOAA's READY Archived Meteorological website (<http://www.ready.noaa.gov/READYamet.php>).

The hourly CO, NO₂, O₃, SO₂, ambient inhalable particles (PM₁₀) and fine particles (PM_{2.5}) were measured using an ambient air quality continuous automated monitors (TH-2000 series, Wuhan-Tianhong Instrument Co., Ltd, China) and the data were acquired from the Qingyue Open Environmental Data Center (<https://data.epmap.org>). It should be noted that the NO₂ (NO₂ = NO_x-NO) concentrations were in fact overestimated. This is because some oxidized reactive nitrogen that is converted by the molybdenum during the NO_x measurement while the NO measurement is accurate using the chemiluminescence technic. Therefore, the NO₂ concentrations discussed below are considered greater than the actual values (Dunlea et al., 2007; Zou et al., 2015). According to the ambient air quality standards-II (GB/3095-2012), the main air pollutants were PM₁₀ and PM_{2.5} in winter and NO₂ in autumn (Fig. S2).

2.3.2 VOCs source apportionment and ozone formation potential

Positive matrix factorization (PMF) model has been widely employed for VOCs source apportionment (Buzcu-Guven and Fraser, 2008; Leuchner and Rappenglück, 2010; Liu et al., 2016; Lyu et al., 2016). In this study, the EPA PMF 5.0 (US EPA, 2014) was employed and additional information was given in Appendix A.

The VOC concentrations are not proportional to the ozone formation potential due to their wide ranges of photochemical reactivity with OH radicals (Table 1). Two methods including propylene-equivalent concentrations (Propy-Equiv) and the maximum incremental reactivity (MIR) were adopted to analyze the ozone formation potential of VOCs. More details can be found in the research of Atkinson and Arey. (2003) and Zou et al. (2015).

In the photochemical and diurnal pattern discussion, the authors note that 8-14 is the time when the ratios are reduced because of photochemical removal due to enhancement of ambient temp. Ambient temp is not responsible for photochemical reaction. The increased in reactive radicals such as OH is. This should be corrected throughout this discussion.

Thanks for your correction, we have revised the description.

What are the uncertainties associated with authors calculations and discussion in section 3.5? This is important as the authors want to show such specific contribution sources in a region where the sources are so close to each other. Also, acetylene is a strong marker for combustion, but it has known to be released from some industrial and oil and gas sources too. It is OK to use is as such, but this point should be addressed in the paper.

The uncertainty (expressed by average \pm standard deviation) of each source contribution was calculated based on the bootstrap technics in PMF analysis and was provided (annual contribution) in the revised manuscript. The “acetylene is released from some industrial and oil and gas sources too” is also mentioned in the revised manuscript.

This source was dominantly weighted by ethylene ($95 \pm 3.5\%$), acetylene ($97 \pm 2.6\%$) and moderately influenced by BTEX. These species are key markers of combustion (Fujita, 2001; Watson et al., 2001; Jobson, 2004) or from petrochemical source (Brocco et al., 1997; Song et al., 2007). However, the independent combustion tracers such as CO, NO₂ and PM_{2.5} were well correlated to this source contribution with Pearson correlation coefficients of 0.59, 0.49 and 0.77, respectively (Fig. 12c and Table S3). Therefore, this factor was attributed to combustion source..

The conclusion section should be changed to summary as it is just summarizing the results not adding any conclusions. The conclusions of the paper should relate only to this area. Also, when discussing all VOCs, are the benzene concentrations in this study higher than those in the middle of a high traffic urban area? Using the term VOC to

encompass everything discussed here is not a correct comparison. Isn't BLH a meteorological condition? So, what is the difference between it and the met conditions affecting monthly and daily VOC variations? #2 in conclusions does not add anything and should be removed.

Thanks for your constructive comments and we changed the conclusion into summary. The benzene in this study (1.13 ± 1.62 ppbv) was lower than those measured in urban areas such as Mexico (1.96 ± 0.93 ppbv) (Garzón et al., 2015), Beijing (1.23 ± 0.68 ppbv) (Wang et al., 2010), Shanghai (1.81 ± 0.19 ppbv) (Cai et al., 2010), but was higher than that in Seoul (0.84 ± 0.72 ppbv) (Na and Kim, 2001) and Guangzhou (0.62 ppbv) (Zou et al., 2015). Yes, the BLH also belongs to meteorological condition and the BLH and other meteorological parameters (i.e., wind speed and temperature) both negatively correlated to VOCs variations. So, the meaningless #2 conclusion in original manuscript is removed as the referee suggested.

Reference

- Cai, C., Geng, F., Tie, X., Yu, Q. and An, J.: Characteristics and source apportionment of VOCs measured in Shanghai, China, *Atmos. Environ.*, 44(38), 5005–5014, doi:[10.1016/j.atmosenv.2010.07.059](https://doi.org/10.1016/j.atmosenv.2010.07.059), 2010.
- Garzón, J. P., Huertas, J. I., Magaña, M., Huertas, M. E., Cárdenas, B., Watanabe, T., Maeda, T., Wakamatsu, S. and Blanco, S.: Volatile organic compounds in the atmosphere of Mexico City, *Atmos. Environ.*, 119, 415–429, doi:[10.1016/j.atmosenv.2015.08.014](https://doi.org/10.1016/j.atmosenv.2015.08.014), 2015.
- Na, K. and Kim, Y. P.: Seasonal characteristics of ambient volatile organic compounds in Seoul, Korea, *Atmos. Environ.*, 35, 2603–2614, doi:[10.1016/S1352-2310\(00\)00464-7](https://doi.org/10.1016/S1352-2310(00)00464-7), 2001.
- Wang, B., Shao, M., Lu, S. H., Yuan, B., Zhao, Y., Wang, M., Zhang, S. Q. and Wu, D.: Variation of ambient non-methane hydrocarbons in Beijing city in summer 2008, *Atmos. Chem. Phys.*, 10(13), 5911–5923, doi:[10.5194/acp-10-5911-2010](https://doi.org/10.5194/acp-10-5911-2010), 2010.
- Zou, Y., Deng, X. J., Zhu, D., Gong, D. C., Wang, H., Li, F., Tan, H. B., Deng, T., Mai, B. R., Liu, X. T. and Wang, B. G.: Characteristics of 1 year of observational data of VOCs, NO_x and O₃ at a suburban site in Guangzhou, China, *Atmos. Chem. Phys.*, 15(12), 6625–6636, doi:[10.5194/acp-15-6625-2015](https://doi.org/10.5194/acp-15-6625-2015), 2015.

The figures in this paper are not well prepared. There is too much going on in each figure (sometime irrelevant information). For example, for diurnal pattern figures the addition of day and night color only add information that are not useful.

Thanks for your thoughtful suggestions. The figures in this manuscript have been revised according to the referees' suggestion and are shown at the bottom of this response.

Specific comments:

Page 1, Line 15: The authors do not discuss the atmospheric behaviors of the VOCs in the paper. The closest they come to this is when they discuss the ozone formation potential of the VOCs. Most of the paper is on the VOC concentrations and correlations. The term behaviors should be deleted.

Thanks for your suggestion, the atmospheric behaviors have been deleted.

Page 1, Line 17-18: The authors note that the concentrations of VOCs in this study were 1-50 times higher than those measured in many other urban and industrial regions. This statement is vague. It should either be more specifically addressed (what VOCs, which other studies) or taken out.

Thanks for your suggestion, this sentence was deleted and re-organized. The revised statement is shown as following:

The average concentrations of total VOCs were 297 ± 372 ppbv and the main contributor was alkanes, accounting for 87.5% of the total VOCs.

Page 1, Line 21-22: After Section 3.3 is revised this sentence should be deleted. First, because the correlations were not very strong; second, because correlation (even if present) does not imply causality or influence.

Thanks for your suggestion, the section 3.3 has been revised, and this sentence has been deleted.

Page 1, Line 24: What do the authors mean by asphalt? Is this an asphalt making factory or just asphalt on the roads?

The asphalt means the asphalt making factory emissions and a black oil hill (made of natural asphalt) fugitives in the northwest of the sampling site.

Page 1, Line 25-26: What do the authors mean by “Clear temporal variations differed from one source to another was observed...” temporal variations of what?

In this sentence, we want to express that the diurnal variation of five different VOCs sources derived from the PMF model can be studied due to the high-resolution observation data and different VOCs sources exhibited different diurnal patterns. Therefore, this sentence is revised as following:

The five identified VOC sources exhibited various diurnal variation patterns due to their different emission patterns and the impact of meteorological parameters.

Page 1, Line 28: define CWT

The CWT (concentration weight trajectory) has been defined.

Page 1, Line 28: What do the authors mean by “local emissions”? Are these the emissions from the oil and gas field? From the urban location?

Yes, the local emission means the emission from both the oil and gas field and urban areas. Because in this study, we defined the local area as a circle and more descriptions can be found in the Appendix C.

Page 1, Line 29-30: Even though the data presented here is a good first step to look at the oil and gas emissions in this region, it is far from filling the gaps. Please revise this sentence to reflect what the paper actually does.

Thanks for your suggestion and this sentence has been revised.

Based on the high-resolution observation data, this study clearly described and analyzed the temporal variation of VOC emission characteristics at a typical oil and gas field, which exhibited different atmospheric behaviors compared with that in urban and industrial areas.

Page 2, Line 5-6: The authors are implying that the reason for the detrimental effect of VOCs to human health is their activity as ozone precursors. This is not corrected. It is a part of the picture. VOCs such as benzene are carcinogens and bad for human health, independent of their activity as ozone precursors.

Thanks for your suggestions and we have revised this sentence.

As the key precursors of O₃ formation (Fujita, 2001; Geng et al., 2008; Ran et al., 2009; Lyu et al., 2016), different VOC categories exhibited different ozone formation potential (Carter, 1994; Atkinson and Arey, 2003; Zou et al., 2015). Some VOC species (i.e., benzene) exhibit detrimental effects on human health (Colman Lerner et al., 2012; He et al., 2015) and they have negative impacts on air quality (Vega et al., 2011).

Page 2, Line 7: Indicate the region of discussion because the previous studies in other regions have certainly focused on VOCs from oil and gas.

Yes, we have indicated the regions of the discussion.

Previous studies in China mainly focused on the measurements of VOCs in urban agglomerations such as the Pearl River Delta (PRD) region (Tang et al., 2007; Liu et al., 2008; Cheng et al., 2010; Ling et al., 2011), Yangtze River Delta (YRD) region (An et al., 2014; Li et al., 2016; Shao et al., 2016) and Beijing-Tianjin-Hebei (BTH) region (Li et al., 2015) and key megacities including Beijing (Song et al., 2007; Wang et al., 2010; Yuan et al., 2010), Shanghai (Cai et al., 2010; Wang, 2014), Guangzhou (Zou et al., 2015) and Wuhan (Lyu et al., 2016).

Page 2, Line 15-16: This sentence is not clear and needs revision. What do the authors mean by “depended on processing stages”? Are the authors discussing the processing stages (drilling, fracking, production) or something else?

In this sentence, we want to express that the VOC contributors in industrial and petrochemical areas are complex due to different process and atmospheric processes. The revised sentence is expressed as following:

A few studies were also conducted in industrial areas (An et al., 2014; Wei et al., 2015; Shao et al., 2016) and petrochemical industrial regions with a lot of VOC emissions (Lin et al., 2004; Wei et al., 2015; Jia et al., 2016; Mo

et al., 2017). These studies found that the VOC sources and compositions are complex due to the different emission and atmospheric processes (Warneke et al., 2014)..

Page 2, Line 17-18: Gilman et al found that oil and gas emissions contribute strongly to some VOCs not all VOCs. Please correct this sentence to reflect that.

Thanks for your suggestion and this statement has been revised.

Gilman et al. (2013) found that oil and gas emissions strongly contribute to the propane and butanes in northeast Colorado.

Page 3, Line 9-10: How are the authors claiming that this specific study “contributes to establish the control measures of VOCs at this type of region”? What do they mean by this type of regions?

We conducted the VOCs source apportionment and calculated the contribution of each source to the ozone formation potential (OFP) in section 3.5. We found that despite the NG source contributed most (62.6%) to the ambient air VOCs, it contributed less to the ozone formation. However, the fuel evaporation contributed less to the VOCs (21.6%) but accounted for 41.9% of the OFP. Therefore, more attention should be paid to fuel evaporation due to its high ozone formation potential. That is why we are claiming that this study contributes to establish the control measures of VOCs at this type of region (refers to oil and gas resources rich areas).

Page 3, Line 15-16: Where did the authors get the production and deposit size data? Please cite source
The data source has been cited.

Page 4, Line 26: The authors note that 3-hour met data have been collected but then in Fig 2 they show hourly data? How was this done?

Due to our vague description, the meteorological data are indeed plotted using every three-hour data. Therefore, we modify the figure caption.

Page 4, Line 29: This should be in results not in methods.

Thanks, this sentence has been removed to results and discussions (section 3.3 temporal variation).

Page 10, Line 1-5: The difference is not only due to fuel evaporation. Based on the information presented here there is an urban area nearby and may contribute to the *i/n* pentane ratios. If this is not the case, the authors should add clarification.

We think that the urban sources such as vehicle emission contributed less to the *i*-pentane/*n*-pentane ratios. Firstly, the ratio of *i*-pentane/*n*-pentane in this study (1.03-1.24) was less than those reported emission ratios for vehicle

emission or tunnel study (~2.2–3.8) (Conner et al., 1995; McGaughey et al., 2004). Secondly, the urban area is located the downwind direction of the sampling site (Fig. 1c), which less influences the sampling sites. Thirdly, the PMF analysis in section 3.5 indicated that the pentanes were from the NG and fuel evaporation. Therefore, we revised this part as following:

Additionally, *i*-pentane and *n*-pentane have similar physical and chemical characteristics (i.e., boiling point and reaction rate coefficients with hydroxyl radical), which result in less susceptible of the *i*-pentane / *n*-pentane ratio in source identification (Gilman et al., 2013). The pentanes are always form the NG emission, vehicle emission, liquid gasoline and fuel evaporation with the *i*-pentane/*n*-pentane ratios ranged between 0.82–0.89 (Gilman et al., 2010, 2013), ~2.2–3.8 (Conner et al., 1995; McGaughey et al., 2004), 1.5–3.0, and 1.8–4.6 (Watson et al., 2001), respectively. As shown in Fig. 8b, the slopes of *i*-pentane / *n*-pentane were 1.03–1.24 in this study, suggested that the pentanes were more likely from the mixed sources of NG and fuel evaporation. This assumption was proved by the high loadings of pentanes in NG and fuel evaporation source compositions in section 3.5.5.

Page 10, Line 19-35: This section should be re-written for clarity.

Thanks for your suggestion, we have revised this part as following:

Generally speaking, when the reaction with OH radicals was the only factor controlling the seasonal ratio of longer atmospheric lifetime to shorter lifetime compounds (i.e., benzene / toluene, *m*, *p*-xylene / ethylbenzene), an increasing in ratio value from winter to summer would be expected (Russo et al., 2010). However, the seasonal variation of BTEX ratios in this study was opposite to the general behavior. For example, the benzene / toluene ratio decreased from winter-spring (0.63–0.69) to summer-fall (0.52–0.57) (Fig. 8c) and ethylbenzene / *m*, *p*-xylene ratio also decreased from autumn-winter (0.47–0.69) to spring-summer (0.19–0.37) (Fig. 8d). Same results were also observed both in industry areas (Miller et al., 2012) and urban areas (Ho et al., 2004; Hoque et al., 2008; Russo et al., 2010). The results obtained in this study indicated that there were other factors affecting the seasonal variation such as source emissions. The BTEX mainly originate from vehicle exhaust (Wang et al., 2010), solvent usage (Guo et al., 2004; Yuan et al., 2010) and petrochemical industry (Na and Kim, 2001; Hsieh et al., 2006; Baltrėnas et al., 2011). The ratio of *m*, *p*-xylenes / ethylbenzene here (2.2 ± 1.2) was within the ranges reported at a petrochemical area in southern Taiwan (1.5–2.6) (Hsieh et al., 2006) and the vicinity of a crude oil refinery at the Baltic region (3.0–4.0) (Baltrėnas et al., 2011). Therefore, the BTEX in this area was mainly from the oil refinery emission. The unexpected

low ratios of benzene / toluene and *m, p*-xylene / ethylbenzene in summer was due to the strong oil refinery emission strength and this finding was verified by the seasonal source contribution results in section 3.5.1.

Page 11, Line 10: What is asphaltic?

Due to our vague description, we mean the asphalt and we corrected in the manuscript.

Examples of grammatical errors (these are not all the errors in the paper. The paper should go through a rigorous edit for grammar before publication).

Page 1, Line 13: add for between important and energy

Done

Page 1, Line 14: replace abundant with a grammatically correct adjective

We have replaced abundant with a lot of

The exploring, drilling, transportation and processing in oil and gas regions can release a lot of volatile organic compounds (VOCs).

Page 1, Line 17: revise “set of monitor system”

We have revised

Page 1, Line 25-26: revise for grammar

We have revised

The five identified VOC sources exhibited various diurnal variation patterns due to their different emission patterns and the impact of meteorological parameters.

Page 2, Line 2: revise “volcanos eruption”

Done

Page 2, Line 13: replace intensive with a grammatically correct adjective

We have replaced intensive with a lot of

A few studies were also conducted in industrial areas (An et al., 2014; Wei et al., 2015; Shao et al., 2016) and petrochemical industrial regions with a lot of VOC emissions

Page 3, Line 2: revise “few have concerned the local and regional source...”

We have revised this sentence

A few studies were also conducted in industrial areas (An et al., 2014; Wei et al., 2015; Shao et al., 2016) and petrochemical industrial regions with a lot of VOC emissions

Page 3, Line 3: replace long time with long-term

Done

Page 3, Line 5: Replace researches with grammatically correct term

Done

These practices mainly focus on the atmospheric fine particles (PM_{2.5}), few studies have concerned the local and regional source contributions of VOCs.

Page 3, Line 16: Please correct sentence so that “It” does not refer to 126 petrochemical plants but the area.

Done

This area can be divided into two regions with oil and gas operation and oil refinery at the north direction (Region 1) and petrochemical industry at the south direction (Region 2).

Page 3, Line 23: revise deeply

We have revised this sentence.

The study area is in the hinterland of Eurasia.

Page 3, Line 28: The authors make it sound like there were 56 monitoring sites. I assume this refers to the number of VOCs? Please revise sentence to reflect that.

We have revised this sentence.

From September 2014 to August 2015, 57 ambient VOCs designed as the O₃ precursors by the Photochemical Assessment Monitoring Stations (PAMS) were continuously sampled and measured using an online monitor system (TH-300B, Wuhan-Tianhong Instrument Co., Ltd, China) with two-hour time resolution.

Page 7, Line 13-17: Revise sentences There are much more, which made reading the manuscript very difficult. The authors should have used a technical writer.

We have revised this sentence.

High concentrations of alkanes, ethane and propane in ambient were also reported in other oil and natural gas operation and industrial areas in the US (Páron et al., 2012; Helmig et al., 2014; Warneke et al., 2014). For instance, the average concentrations of ethane and propane were 74 ± 79 ppbv and 33 ± 33 ppbv, respectively in Horse pool and Uintah Basin in the winter of 2012. Despite the highly enhanced VOC levels were due to the temperature

inversion, the VOC levels in Uintah Basin were still higher than those in the regional background areas as the existence of oil and gas exploitation activities (Helmig et al., 2014).

Thanks for your suggestion, we have carefully checked and corrected the grammar in the revised manuscript

Revised figures as the referees suggested.

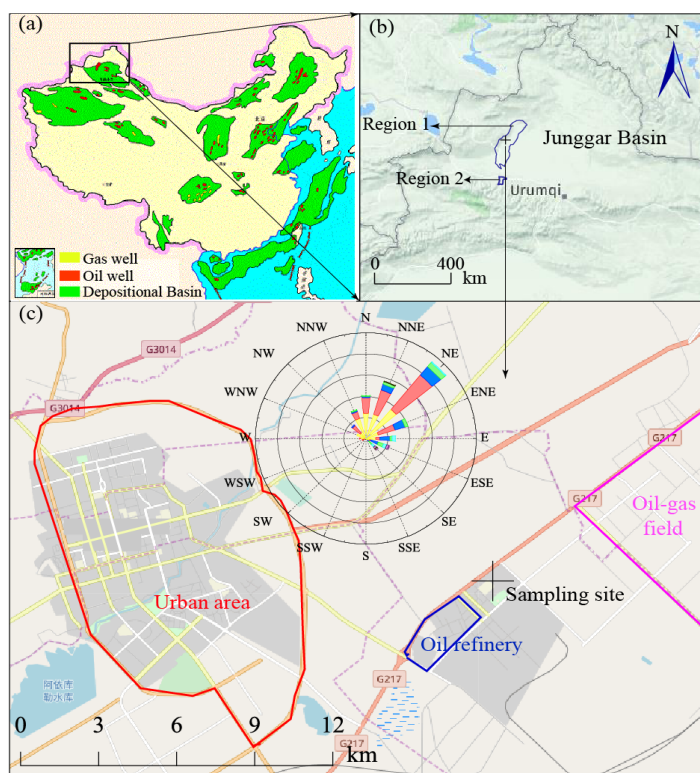


Figure 1. The spatial distribution of oil gas bearing basins in China (a) and the terrain of the study area (b). The sampling site is about 11 km away from the urban area and located in the northeast of an oil refinery plant and southwest of an oil gas field. The northeasterly winds prevailed during the sampling periods (c) (The legend (meaning of the different color) of Fig. 1a is provided. The filled color in Region 1 and 2 (Fig. 1b) is deleted to show the location of the sampling site)

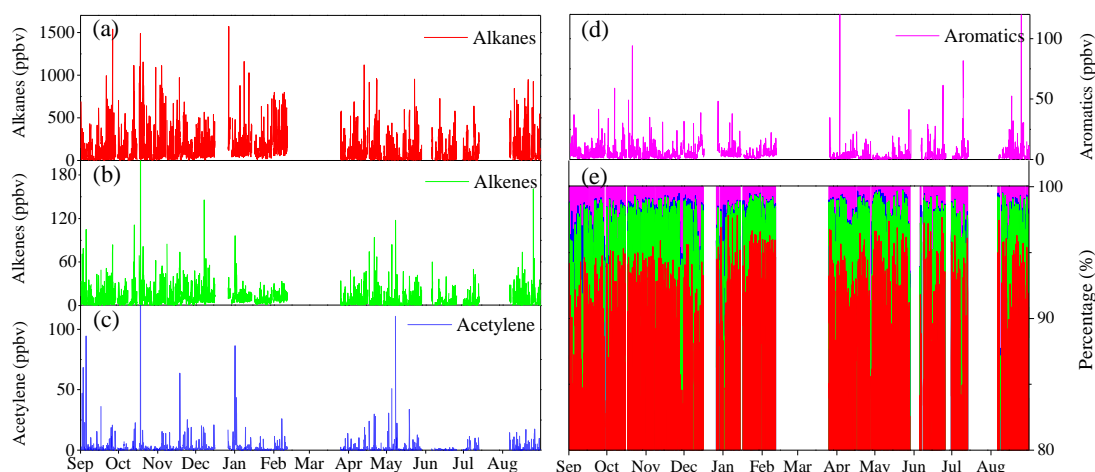
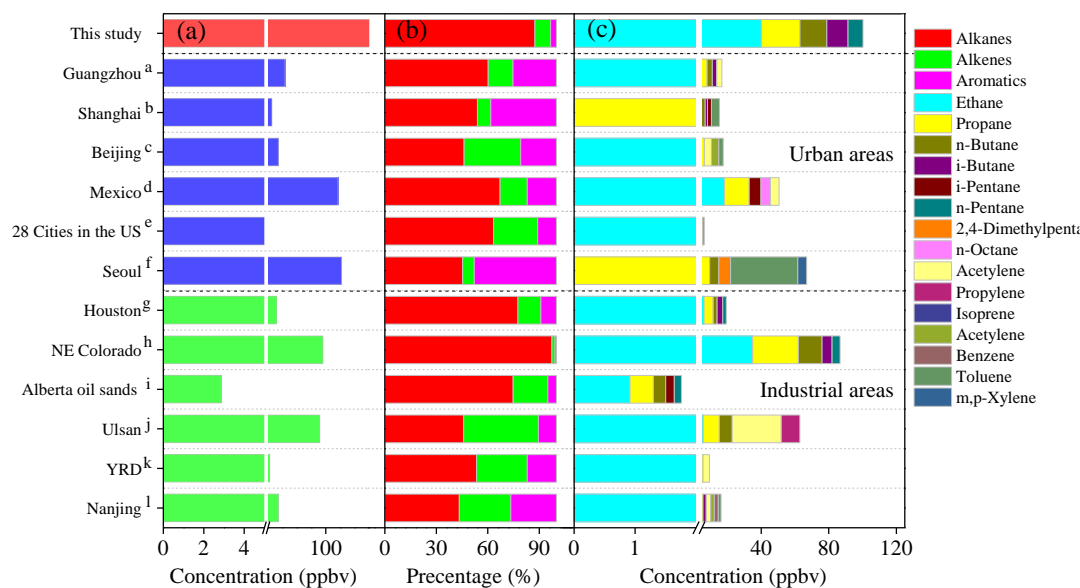


Figure 3. Time series of the hourly concentrations (expressed in ppbv) of four categories of VOCs including alkanes (a), alkenes (b), acetylene (c), aromatics (d), and their fractions (e) during the sampling period.

(There is an error in Fig. 3e that the percentage of aromatics is not corrected and we have corrected it)



^a Zou et al., (2015); ^b Cai et al., (2010); ^c Wang et al., (2010); ^d Garzón et al., (2015); ^e Baker et al., (2008); ^f Na and Kim, (2001); ^g Leuchner and Rappenglück, (2010); ^h Gilman et al., (2013); ⁱ Simpson et al., (2010); ^j Na et al., (2001); ^k An et al., (2014); ^l Shao et al., (2016)

Figure 4. Comparison of the VOC concentrations (a), compositions (b) and the top five VOC species (c) in this study and former studies concerning the VOCs in the ambient of urban and industrial areas.

(In order to give the data sources of the compared areas, we add the superscript in each area and the reference is provided)

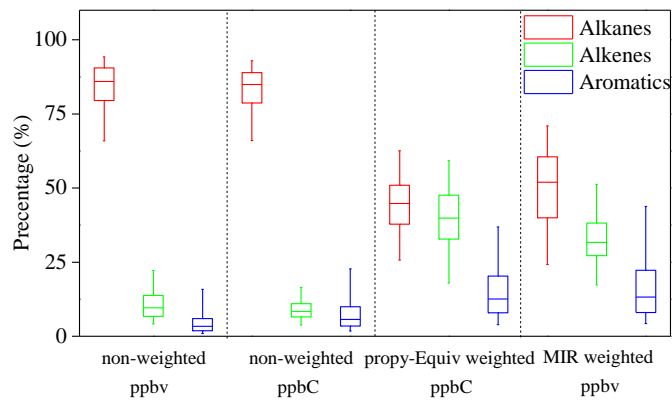


Figure 5. Box and whisker plots of VOC profiles based on different scales during the whole sampling period. Box and Whisker plots are constructed according to 25th-75th and 5th -95th percentile of the calculation results. (The irrelevant color is deleted.)

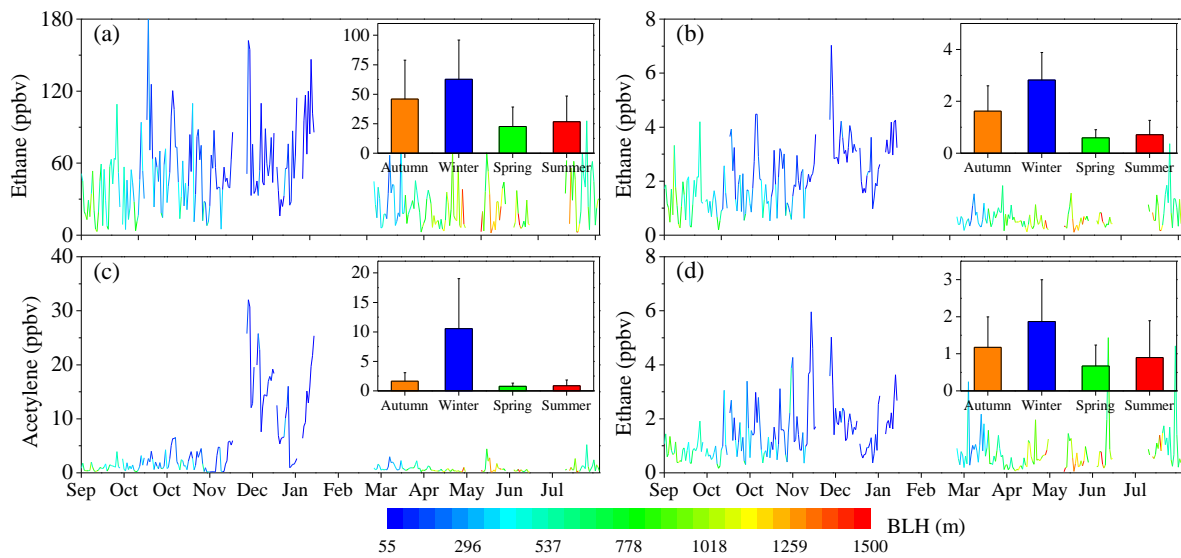


Figure. 6 Seasonal and daily variations of ethane (a), ethylene (b), acetylene (c), and benzene (d) during the sampling period. (The section 3.3 is discussing the temporal variations of different VOC species and Figure. 6 is revised to reflect the seasonal and daily variation.)

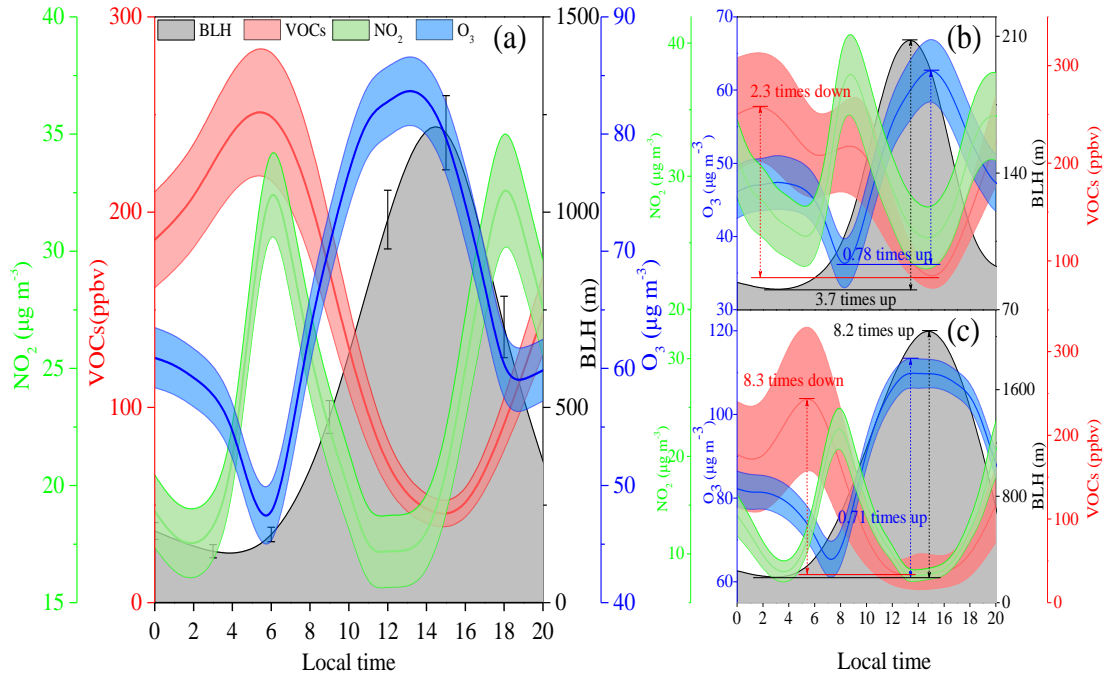


Figure 7. Diurnal variation of boundary layer height (BLH), VOCs, NO₂, and O₃ concentrations in different timescale: annual (a), winter (b) and summer (c). Solid line represents the average value and filled area indicates the 95th confidence intervals of the mean.

(The irrelevant color such as the day and night is deleted. We also add the diurnal variation of NO₂ in Fig. 7b and Fig.7c.)

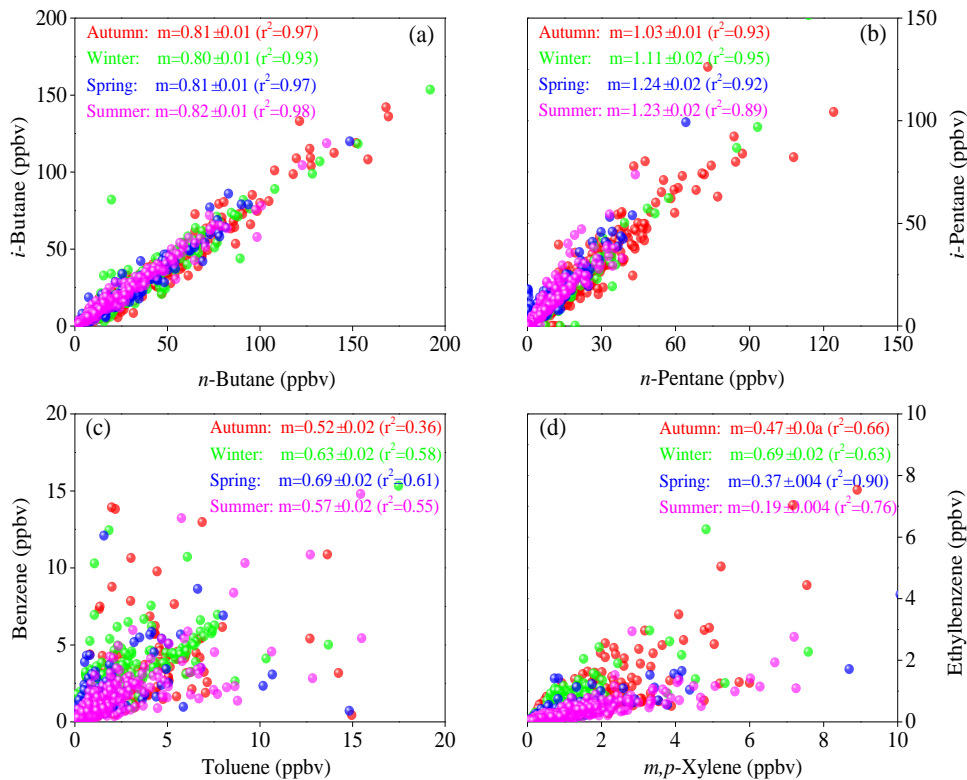


Figure 8. Correlations ($m = \text{slope} \pm \text{standard error}$ (r^2)) between compounds with similar atmospheric lifetimes including *i*-butane/*n*-butane (a) and *i*-pentane/*n*-pentane (b), and compounds with different lifetimes including benzene/toluene (c) and ethylbenzene/*m*, *p*-xylenes (d).

(The x- and y- axis is exchanged (Fig. 8d) to show the ratio of ethylbenzene/*m*, *p*-Xylene (long lifetime compound/short lifetime compound) as discussed in section 3.4)

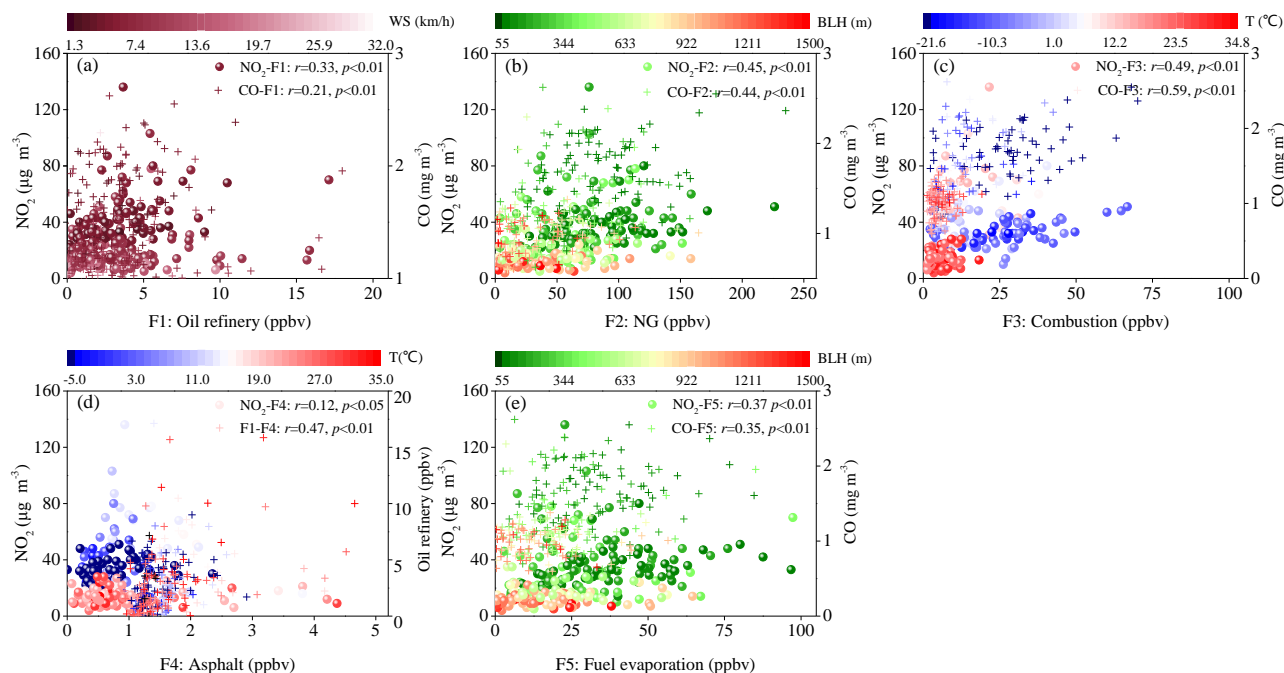


Figure 12. Scatter plots of daily concentrations of trace gas and source contributions including oil refinery (a), NG (b), combustion (c), asphalt (d), and fuel evaporation (e) under different meteorological conditions (wind speed (WS), boundary layer height (BLH) and temperature (T)).

(The F1 (Oil refinery), F2 (NG), F3 (Combustion), F4 (Asphalt).and F5 (Fuel evaporation) were added in x-axis. In addition, the color maps of different meteorological data were unified.)

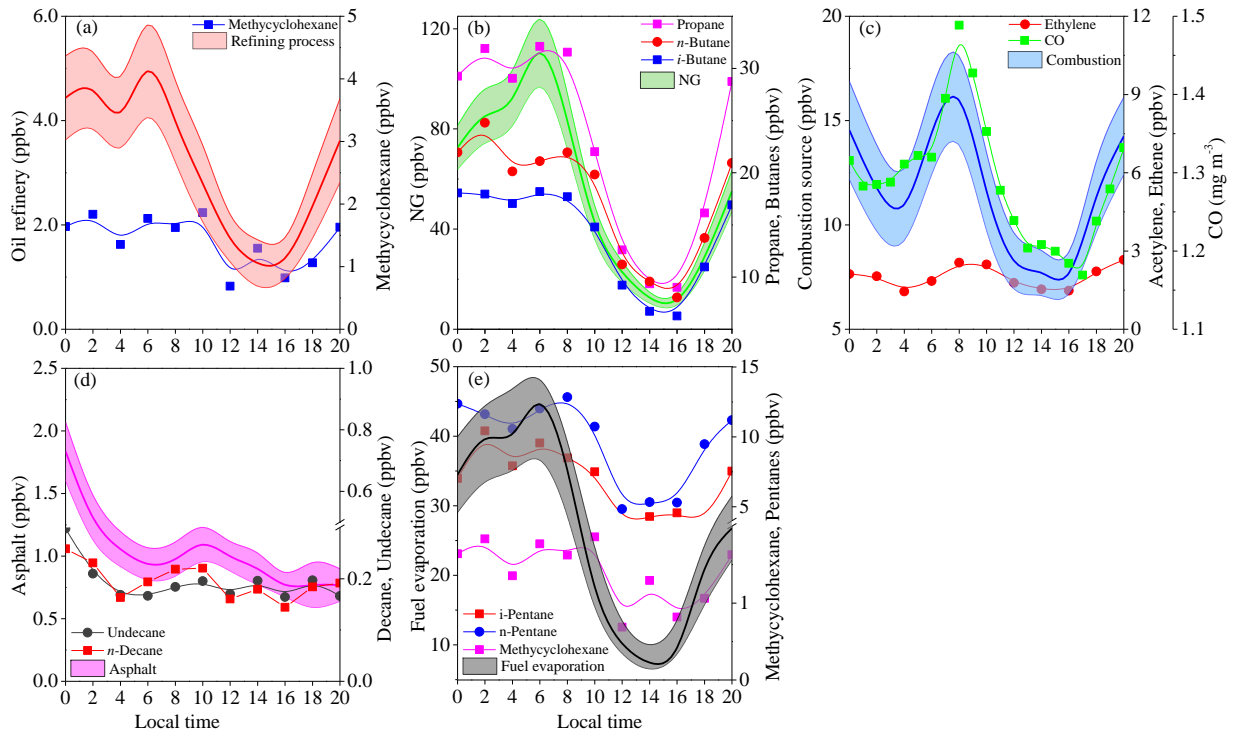


Figure 13. Diurnal variations of the contributions (expressed in ppbv) of five identified sources including oil refining process (a), NG (b), combustion source (c), asphalt (d) and fuel evaporation (e), and specific compounds with high loadings in each source profile. Note that the CO in combustion source was expressed in mg m^{-3} . (The irrelevant color (day and night) and the species that are not well correlated to the source contribution in are deleted. The full name of MCH (methylcyclohexane) is given. In addition, the layout of Fig. 13 is also changed)

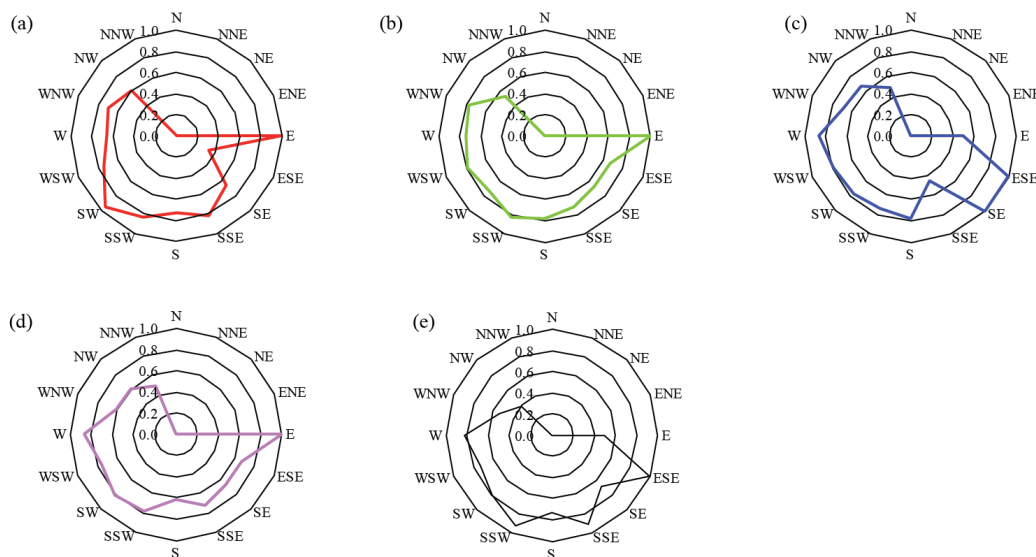


Figure 14. Annual conditional probability function (CPF) plots of five identified VOCs source including oil refinery (a), NG (b), combustion (c), asphalt (d), and fuel evaporation (e). (The irrelevant color is deleted and the layout is changed.)

Response to Referee #2

This paper reported one year VOC measurements in high frequency at oil-gas station area in China. High frequency VOC data enable to show diurnal variations of VOCs in the sampling site and strong influence of meteorological condition for VOC concentrations was elucidated. Using PMF analysis, VOC emission was successfully categorized into five sources. Further, CPF analysis gave more information about the direction of the VOC emission sources. Also, backward trajectory based analysis (PSCF, CWT) were applied.

[General comments]

Similar VOCs measurement and analysis were already demonstrated in urban area, but the detailed VOC observation at oil-gas station area will be important in view point of source area information. Because strong VOC emission sources are close to the measurement site, the analyzed results would be simpler and seems to be reasonable. But I am not sure about the validity of PSCF and CWT analysis in this measurement. When there is a strong source very close to the measurement site (like 2 km from Oil refinery and 6km from Oil-gas field in Fig 1c), the backward trajectories passed the near emission source will be counted as high concentration over its whole trajectory rout. Therefore, the raster analysis (distinguish local and regional area) would be reasonable trial. (But I am afraid that the influence of very close emission sources cannot be excluded, because that 12h radius will be still long and concentration of each grid was estimated from CWT.)

We thank the reviewer for the valuable comments. All of them have been addressed in the revised manuscript. Please see our itemized responses below.

Explanation for the validity of PSCF and CWT

Despite the potential source contribution function (PSCF) method has deficiencies such as the determination of the statistical significance of its outcome is difficult (Stohl, 1996). The PSCF (Polissar et al., 1999; Hsu et al., 2003) and concentration weighted trajectory (CWT) are frequently used to figure out the direction and sources of air pollution at a receptor site. To reduce the uncertainty and increase the confidence of the results, a weighted function is widely used (Wang et al., 2016). Grid cells for which high PSCF values are calculated from the arrival of air parcels at a receptor site with pollutant concentrations higher than a given value. In this study, the 75th percentiles of each source contribution were set as the criterion (Bressi et al., 2014; Wang et al., 2015). The detailed information about the PSCF and CWT calculation can be found in Appendix B.

The PSCF results represent potential source directions rather than locations because PSCF modeling evenly distributes weight along the path of trajectories as the referee mentioned. This even weighting results in a trailing effect so that areas upwind and downwind of the sources are likely to be identified as sources as well (Hsu et al., 2003). Therefore, in this study, we simply define a circle with 12 h radius area as the local areas and the outer areas of this circle is regional. The reasons are listed below:

(1) The duration of *m, p*-xylene decreasing from highest concentrations (at 02:00 LT) to lowest (14:00 LT) was 12 h (section 3.4). The atmospheric lifetime of *m, p*-xylene is about 11.8 h assuming that the OH radical equals to 10^6 rad cm^{-3} . The compounds with atmospheric lifetime longer than *m, p*-xylene can be transported from long distance or accumulated in the local area.

(2) The endpoint of every 2 h backward trajectories in the first 24 h was tested to find the optimum range of “local and nearby” area (Fig. C1). As the backward time increasing from 2 h to 24 h, the area covered by the long air masses increased significantly. Before the first 5 h, the air masses were mainly from the northwest and the east of the sampling site. From 7 h to 12 h, air masses from the northeast, southeast and southwest reached the receptor site and the “shape of local area” formed. After 12 h, the air masses, especially for the trajectories from the west transported for long distance reached the sampling site, indicating the regional conditions.

As the referee mentioned, the 12 h radius to define the local and regional transport was still long that the very close emission sources cannot be excluded. The method used in this study was a trial to give the quantitative information of the local and regional transport despite flaws existed.

Reference

Bressi, M., Sciare, J., Ghersi, V., Mihalopoulos, N., Petit, J.-E., Nicolas, J. B., Moukhtar, S., Rosso, A., Féron, A., Bonnaire, N., Poulakis, E. and Theodosi, C.: Sources and geographical origins of fine aerosols in Paris (France), *Atmos. Chem. Phys.*, 14(16), 8813–8839, doi:10.5194/acp-14-8813-2014, 2014.

Hsu, Y.-K., Holsen, T. M. and Hopke, P. K.: Comparison of hybrid receptor models to locate PCB sources in Chicago, *Atmos. Environ.*, 37(4), 545–562, doi:10.1016/S1352-2310(02)00886-5, 2003.

Stohl, A.: Trajectory statistics-A new method to establish source-receptor relationships of air pollutants and its application to the transport of particulate sulfate in Europe, *Atmos. Environ.*, 30(4), 579–587, doi:10.1016/1352-2310(95)00314-2, 1996.

Wang, L., Liu, Z., Sun, Y., Ji, D. and Wang, Y.: Long-range transport and regional sources of PM_{2.5} in Beijing based on long-term observations from 2005 to 2010, *Atmos. Res.*, 157, 37–48, doi:10.1016/j.atmosres.2014.12.003, 2015.

Wang, Q., Liu, M., Yu, Y. and Li, Y.: Characterization and source apportionment of PM_{2.5}-bound polycyclic aromatic hydrocarbons from Shanghai city, China, *Environ. Pollut.*, 218, 118–128, doi:10.1016/j.envpol.2016.08.037, 2016.

[Detailed comments]

Fig. 1: What is 2 type green area in Fig 1(a)? What is blue area in Fig1(b)? Exact location of the sampling site is difficult to see in Fig1 (b) (because of blue color). Is the sampling site located in Region 1? What is the rose figure in Fig1c? Wind speed or VOC concentration from each direction? If this rose figure shows wind direction, figure caption will be incorrect (“Northwesterly and northeasterly wind prevailed”).

Fig. 1 has been revised. Fig. 1a shows the spatial distribution of oil and gas bearing basins in China in different colors (yellow: gas well, red: oil well, and green: depositional basin). In the Fig. 1b, the sampling site is located in region 1. Fig. 1c shows the wind rose and the prevailing wind.

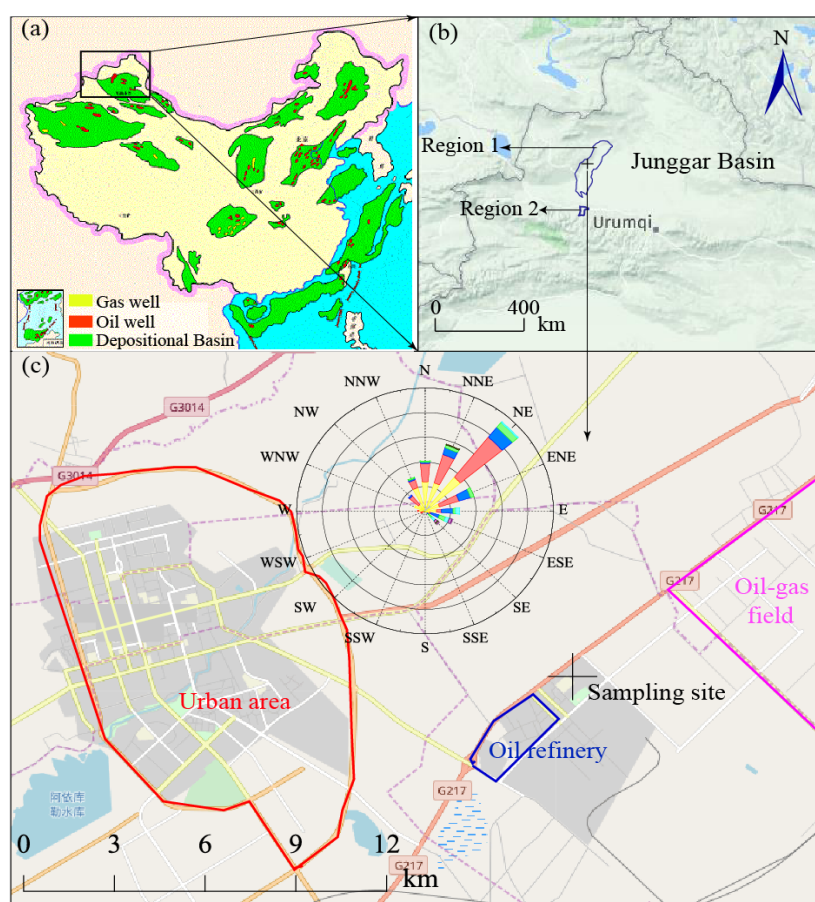


Figure 1. The spatial distribution of oil gas bearing basins in China (a) and the terrain of the study area (b). The sampling site is about 11 km away from the urban area and located in the northeast of an oil refinery plant and southwest of an oil gas field. The northeasterly winds prevailed during the sampling periods (c)

Page4 L3: PLOT column will be used for C₂-C₄ separation in GC. For C₂-C₄ trap, some absorbent (tenax etc) would be used. Please check the explanation about VOC measurement system.

The VOCs analysis method has been checked and some technic errors have been corrected.

Briefly, two-channels were installed to analyze VOCs separately. The water and carbon dioxide in the sampled air was firstly removed at a cold trap maintaining at -80 °C and then concentrated at -150 °C at another cold trap. After the purification and concentration, the VOCs were desorbed by rapid heating to 100 °C. The C₂-C₅ VOCs were separated with a PLOT column (diameter: 0.32 mm, thickness of membrane: 1.5 μm, length: 60 m) and were quantified by the gas chromatograph-flame ionization detector (GC-FID, Agilent 7890). C₅-C₁₂ were separated by a DB-624 column (diameter: 0.25 mm, thickness of membrane: 3 μm and length: 60 m) and were quantified using mass spectrometer detector (MSD, Agilent 5975).

Table 1: Please explain “MDL” (method detection limit). “KOH” will be better to write in small characters.

Thanks for your suggestion and we have revised it.

Fig3: Is the colors in Fig. 3(e) same as Fig. 3(a)-(d)? (In Fig. 3(e), blue (acetylene?) seems larger contribution.)

Thanks for your reminder, the color in Fig. 3(e) is the same as Fig. 3(a)-(d) and we find some errors in Fig. 3e and therefore it has been revised. After correction, the contribution of aromatics (magenta) is greater than acetylene (blue).

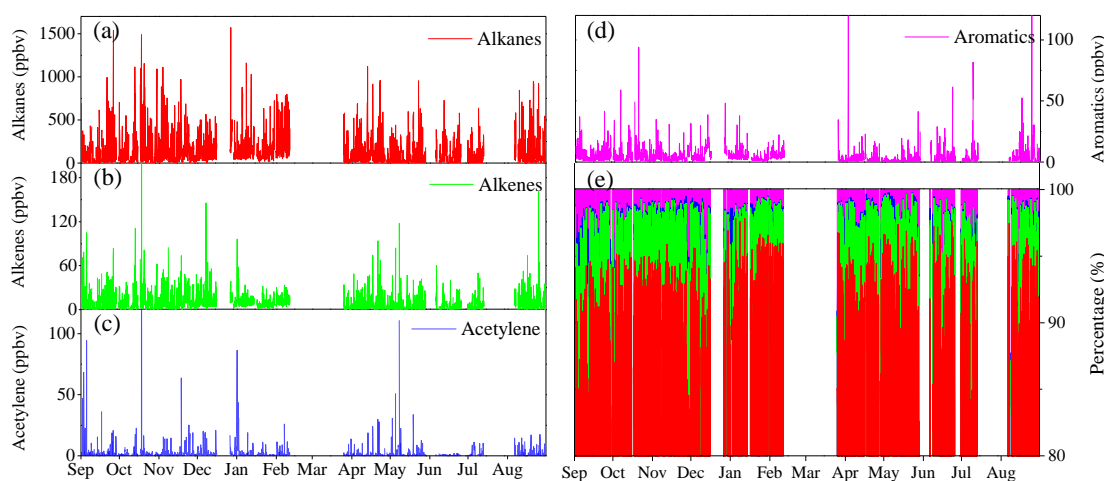


Figure 3. Time series of the hourly concentrations (expressed in ppbv) of four categories of VOCs including alkanes (a), alkenes (b), acetylene (c), aromatics (d), and their fractions (e) during the sampling period.

Fig. 6 and text: Are O₃, BLH etc 24-hour average or only daytime average? There are strong diurnal variations in BLH, O₃ and VOCs, so these plots would be different when you use whole day or only daytime data.

Yes, the O₃, BLH etc. are 24-hour average in the original Fig. 6. In this part, we want to discuss the temporal variation of VOCs in different timescales. For daily variation patterns (Fig. 6), we used the 24-h average values to discuss. Of

course, we agree with the referee’s opinion that the concentrations of O₃, VOC and NO₂ concentrations and BLH would be different during the daytime and nighttime. So, we discussed the diurnal variation of these factors using the 95% confidence interval of gases (VOCs, O₃ and NO₂) and average \pm standard deviation of BLH as shown in Fig. 7. Therefore, we revised the Fig. 6 and Fig. 7 as below:

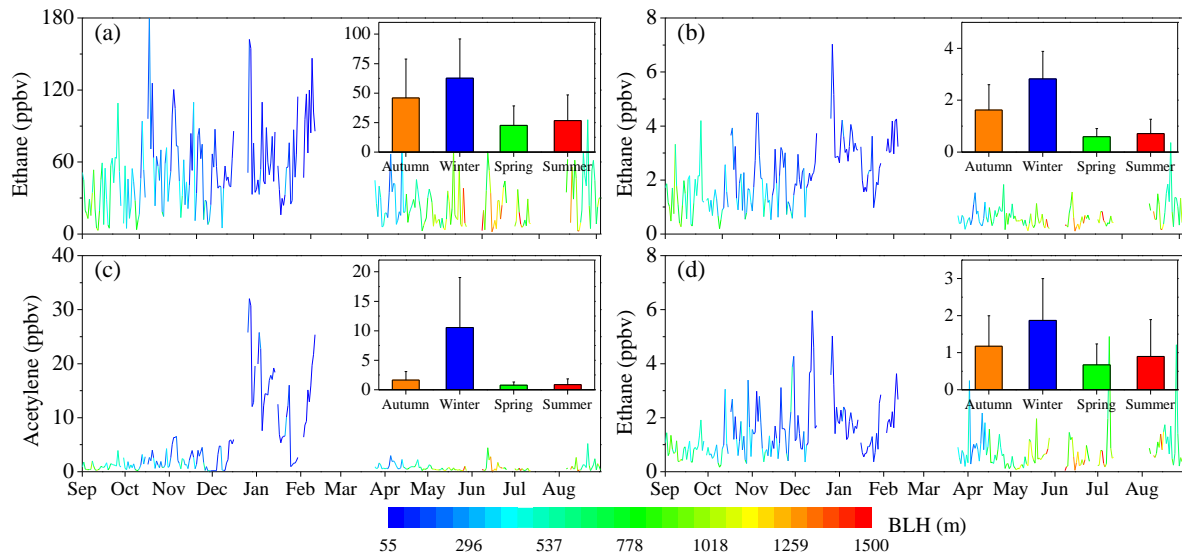


Figure. 6 Seasonal and daily variations of ethane (a), ethylene (b), acetylene (c), and benzene (d) during the sampling period.

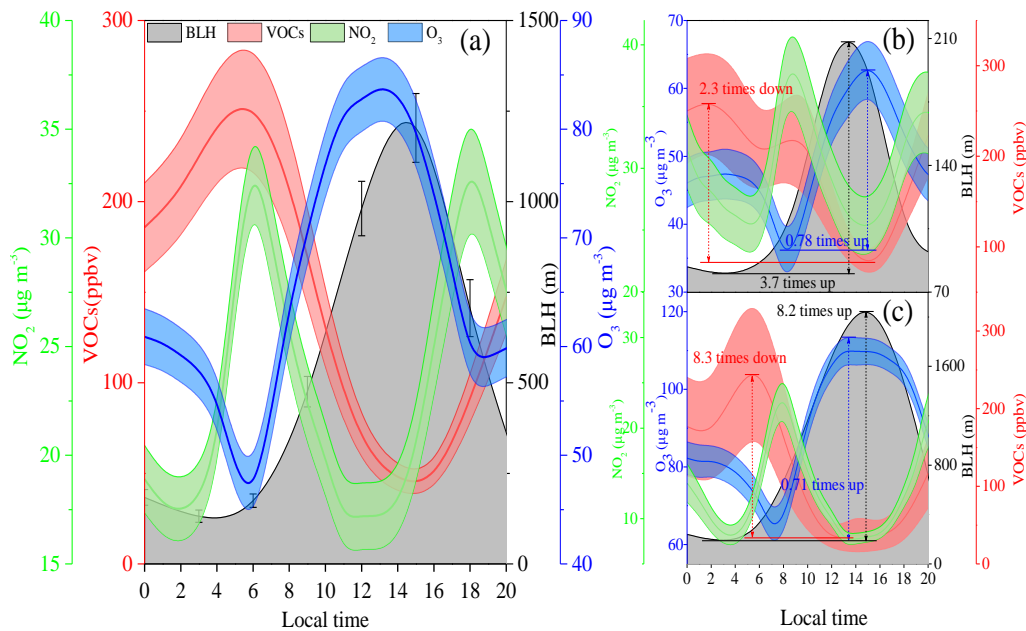


Figure 7. Diurnal variation of boundary layer height (BLH), VOCs, NO₂ and O₃ concentrations in different timescale: annual (a), winter (b) and summer (c). Solid line represents the average value and filled area indicates the 95th confidence intervals of the mean.

Fig12 (d): Is it correct “F1-F4” ? (Is it “CO-F4” ?)

Yes, it is corrected as “F1-F4” in Fig. 12d. To avoid the vague description, the Fig. 12 was revised. For instance, the F1 (Oil refinery), F2 (NG), F3 (Combustion), F4 (Asphalt) and F5 (Fuel evaporation) were added in x-axis. In addition, the color maps of different metrological data were unified.

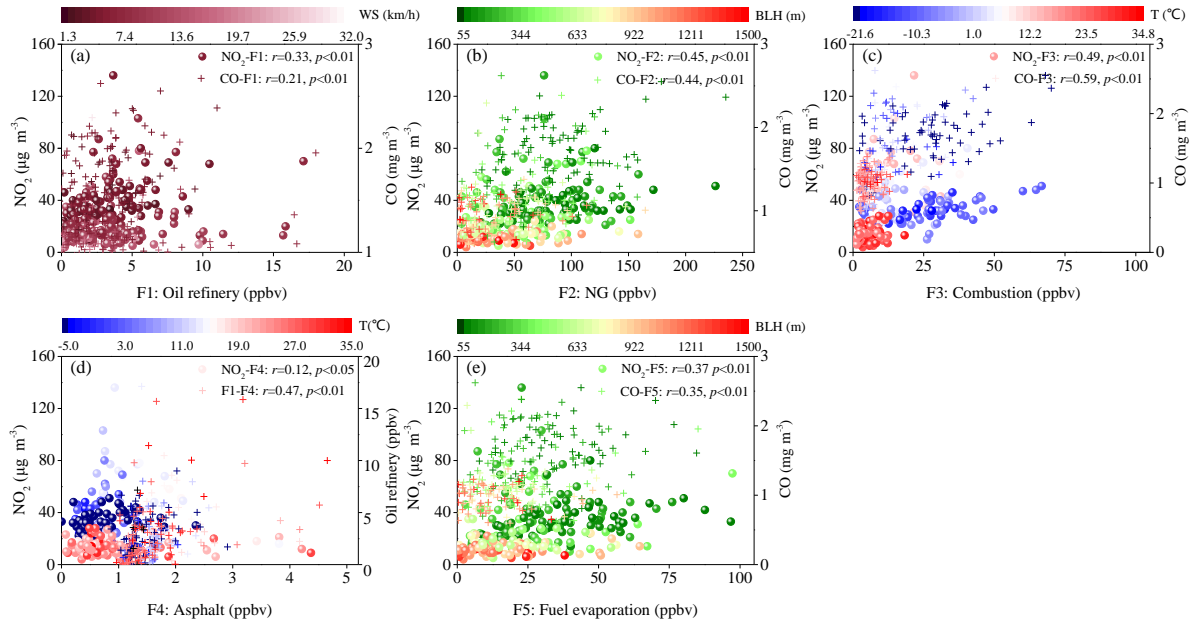


Figure 12. Scatter plots of daily concentrations of trace gas and source contributions including oil refinery (a), NG (b), combustion (c), asphalt (d), and fuel evaporation (e) under different meteorological conditions (wind speed (WS), boundary layer height (BLH) and temperature (T))

Fig13: Please explain MCH and MCP. In the right axis of (a), (b), (e), "/" will be better to show as ",". They are not ratio, but just concentration. “Cyclohexane” etc would be better to show as dot and line.

Thanks for your suggestion. This figure has been revised.

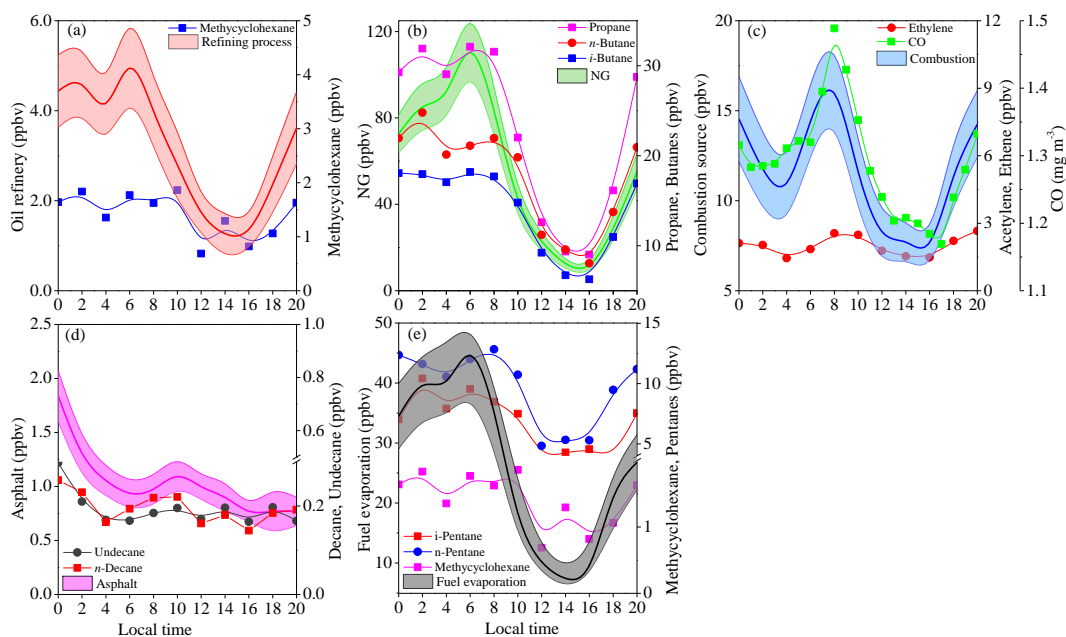


Figure 13. Diurnal variations of the contributions (expressed in ppbv) of five identified sources including oil refining process (a), NG (b), combustion source (c), asphalt (d) and fuel evaporation (e), and specific compounds with high loadings in each source profile. Note that the CO in combustion source was expressed in mg m^{-3}

P12 L24-2: Diurnal pattern of acetylene seems to be different. (Acetylene did not decrease during daytime.)

Yes, we agree with the referee's idea and this expression has been revised.

The diurnal variation of combustion source was in accordance with the diurnal pattern of ethylene and CO with Pearson correlation coefficients as 0.71 ($p < 0.05$) and 0.84 ($p < 0.01$), respectively.

P15 L20-22: "Northeast to Southwest" Is this "Southeast to Southwest"?

Yes, thanks for your correction.

P15 L23-24: Fig.14(b), highest peak is in east direction.

Thanks for your correction, we also find that there were some grids with high PSCF value in the east direction of the sampling site. So, we have revised this sentence as following:

Indeed, high values of CPF, PSCF and CWT were found in the east direction (Fig. 14b, Fig. 15b and Fig. 16b), which indicated that the potential geographic origins of NG.

Response to Referee #3

This paper describes one-year continuous monitoring of VOCs around an oil-gas region in northwest China in order to clarify atmospheric behavior of VOCs in such region. The authors revealed temporal variations such as seasonal and diurnal variations of VOCs around the oil-gas region and analyzed factors of such variations. In addition, they performed source analyses of VOCs and discussed source of VOCs in this region quantitatively.

General comments:

As the authors mentioned, VOCs are main precursors of tropospheric ozone and it is important to clarify atmospheric behavior of VOCs. Examples of VOC observations in oil-gas regions are low, especially; there are few continuous observations of VOCs with high time resolution. The authors supply valuable data and information. In addition, the authors conducted quantitative source analyses of VOCs. I recommend this paper to be published in Atmospheric Chemistry and Physics.

However, I found several dubious points in this paper. The authors should revise appropriately.

The authors would like to thank the reviewer for the detailed comments, which help to improve the manuscript. We have tried to clarify the points raised by the reviewer and to answer all remarks.

Specific comments:

The authors performed several discussions using NO₂. Why do the authors use NO₂ instead of NO_x? I think it is preferable to use NO_x instead of NO₂ (or both NO₂ and NO_x) for many of such discussions. The authors would observe NO and NO₂ because they used a TEI NO_x analyzer based on a chemiluminescence method.

Thanks for your suggestion that using NO_x instead of NO₂ to discuss, however, the NO₂ and other air pollutants data were from the Qingyue Open Environmental Data Center, which only NO₂ is available. So, we had to use the NO₂ to discuss and we will notice this point in our further study.

NO₂ and NO_x concentrations measured by a TEI NO_x analyzer are not accurate because of interferences of descendant species of NO_x such as HNO₃ and PANs. The authors should evaluate such interferences. Especially, organic nitrates could interfere the values of NO₂ concentrations obtained by a TEI NO_x analyzer under high concentrations of large hydrocarbons.

Thanks for your comments. There is a technic error in the manuscript that the NO₂ was actually measured using the automated monitors (TH-2000 series, Wuhan-Tianhong Instrument Co., Ltd, China), which also determine the NO_x using the chemiluminescence technic. Based on the chemiluminescence method, the measured NO concentrations is

accurate. A molybdenum converter was used for NO₂ measurement, and as a result, part of the NO_y (e.g., peroxyacetylnitrate (PAN), HNO₃, and alkyl nitrates) may have been transformed to NO₂ during the sampling. Therefore, a method developed by Lamsal et al. (2008) was used to correct our NO₂ data according to the following formula:

$$CF = \frac{NO_2}{NO_2 + \sum AN + (0.95PAN) + (0.35HNO_3)}$$

where CF is the correct factor, $\sum AN$ is the alkyl nitrates. However, in this study, we do not measure the PAN and HNO₃ and simulate the alkyl nitrates concentrations. Therefore, the NO₂ concentrations discussed in this study were considered greater than the actual values (Dunlea et al., 2007; Zou et al., 2015) and we used the average value of NO₂ concentration to discuss. We will notice this issue in further study.

Reference

Dunlea, E. J., Herndon, S. C., Nelson, D. D., Volkamer, R. M., San Martini, F., Sheehy, P. M., Zahniser, M. S., Shorter, J. H., Wormhoudt, J. C., Lamb, B. K., Allwine, E. J., Gaffney, J. S., Marley, N. A., Grutter, M., Marquez, C., Blanco, S., Cardenas, B., Retama, A., Ramos Villegas, C. R., Kolb, C. E., Molina, L. T. and Molina, M. J.: Evaluation of nitrogen dioxide chemiluminescence monitors in a polluted urban environment, *Atmos. Chem. Phys.*, 7(10), 2691–2704, doi:10.5194/acp-7-2691-2007, 2007.

Lamsal, L. N., Martin, R. V., van Donkelaar, A., Steinbacher, M., Celarier, E. A., Bucsela, E., Dunlea, E. J. and Pinto, J. P.: Ground-level nitrogen dioxide concentrations inferred from the satellite-borne Ozone Monitoring Instrument, *Journal of Geophysical Research*, 113(D16), doi:10.1029/2007JD009235, 2008.

On page 9, lines 6-7, “It should be noted that VOCs: : : as well as BLH.”: I think NO₂ concentrations are controlled solar UV and concentrations of NO and O₃ as well as BLH, but are VOCs controlled concentrations of NO and O₃? (I don’t think so.) The authors should discuss this matter separating VOCs and NO₂.

Thanks for your comment. We have revised this part.

The VOCs had a reverse trend with O₃ ($r = -0.82$, $p < 0.01$). The lower BLH and less photochemical activities resulted in peak values for VOCs and low O₃ concentrations before sunrise (6:00 local time). After sunrise, with the initiation of photochemical oxidation and the increasing of BLH, the concentrations of VOCs decreased while the O₃ increased rapidly. The minimum of VOCs and occurred at about 12:00–14:00 LT was resulted from both dispersion or dilution conditions and photochemical reactions (with highest O₃ concentrations at 14:00 LT) in the afternoon. The diurnal variation of NO₂ was controlled by BLH, O₃ and photochemical reactions (i.e., OH radical) and showed a double peak.

Table 1: The authors should explain r².

Done.

Response to Referee #4

This paper entitled “One year monitoring of volatile organic compounds (VOCs) from an oil-gas station in northwest China” utilized a unique dataset to analyze the differences between the VOC concentrations, compositions, source contributions in an oil-gas station and other urban areas and industrials. The results seem to be interesting with unique characteristics of VOC compositions and sources in this kind of areas. Based on one-year online monitoring of VOC concentrations, the PMF model was successfully employed to source apportionment and the different timescale variations of different source contributions were discussed. The PSCF and CWT method were also employed to investigate the potential geographic origins of VOCs. A new method based on CWT was proposed to attempt to distinguish the local and regional contributions. I suggest this paper can be accepted after minor revision and addressing my questions.

We are very grateful to all important and helpful comments from the referee. The followings are our responses to each comment in detail.

The specific comments are listed as follows:

1. P1 Line 15 the sentence “the ambient VOCs from fifty-six Photochemical Assessment Monitoring Stations (PAMS) VOCs were continuously measured for an entire year (September 2014-August 2015) by a set of on-line monitor system from an oil-gas station in northwest China.” confused me. Pls make it clear.

This sentence has been revised.

To understand the VOC levels, compositions and sources in such region, an oil and gas station in northwest China was chosen as the research site and fifty-seven VOCs designed as the photochemical precursors were continuously measured for an entire year (September 2014–August 2015) using an on-line monitoring system.

2. P1 Line 31: How about replace the keywords “source region and local-regional contribution” to local-regional contribution?

Thanks for your suggestion, and we have revised in the updated manuscript.

3. P2 Line 6: Insert references after “air quality.”

We have added the reference

4. P2 Line 25 Insert references or link.

We have added the link, which the full-text of Air Pollution Prevention Control (APPC) can be found.

5. P4 Line 2~5: Please check and make sure the analysis method is correct.

The VOCs analysis method has been checked and some technic errors have been corrected.

Briefly, two-channels were installed to analyze VOCs separately. The water and carbon dioxide in the sampled air was firstly removed at a cold trap maintaining at $-80\text{ }^{\circ}\text{C}$ and then concentrated at $-150\text{ }^{\circ}\text{C}$ at another cold trap. After the purification and concentration, the VOCs were desorbed by rapid heating to $100\text{ }^{\circ}\text{C}$. The $\text{C}_2\text{--C}_5$ VOCs were separated with a PLOT column (diameter: 0.32 mm, thickness of membrane: $1.5\text{ }\mu\text{m}$, length: 60 m) and were quantified by the gas chromatograph-flame ionization detector (GC-FID, Agilent 7890). $\text{C}_5\text{--C}_{12}$ were separated by a DB-624 column (diameter: 0.25 mm, thickness of membrane: $3\text{ }\mu\text{m}$ and length: 60 m) and were quantified using mass spectrometer detector (MSD, Agilent 5975).

6. P4 Line 8. Technic errors. The PAMS standard gases contain 57 VOC species, including alkane (30), alkene (9), alkene (acetylene), and aromatic (17).

Thanks for your correction and we have revised it.

7. P6 Line 7: The author mentioned that the trajectories were mainly originated from the northwest during the whole sampling period. However, the wind rose (Fig. 1c) indicated the northeasterly winds prevailed in P5 Line 2. How to explain the difference?

The wind rose plot was drawn according the observation data at the sampling site, while the backward trajectory was analyzed using the National Center for Environmental Prediction's Global Data Assimilation System (GDAS) wind field re-analysis. In addition, the wind rose more reflects the instantaneous wind directions, while the back trajectories indicate the long-range transport in large spatial scale. The data source and spatial scale resulted the differences.

8. P7Line 15: You mean $33 \pm 33\text{ppbv}$?

Yes, we have corrected this error.

9. P9 Line 12: The concentrations of O_3 precursors decreased and O_3 increased?

This sentence is confusing and we have revised it in the manuscript. Actually, the O_3 precursors means VOCs and NO_2 in this study and we revised this sentence as below:

After sunrise, with the initiation of photochemical oxidation and the increasing of BLH, the concentrations of VOCs decreased while the O_3 increased rapidly.

10. P9 Line 16~23: When discuss the effects of BLH and photochemical reactions on VOC concentrations in summer and winter. I suggest more statistical method such as ANOVA analysis can be used to test the differences were significant or not.

Thanks for your suggestion. We conducted ANOVA analysis to discuss.

11. P11 Line 18-19 & P12 Line 8~10: The author compared the source contributions in different seasons using the percentage contributions (%) and volume contributions (ppbv) and it's paradoxical using both methods. For instance, in P12 Line 8~10, the percentage contribution in spring was the highest, however, the volume contribution was the lowest among the four seasons. How to explain or avoid?

Thanks for your reminder, we use the relative contribution (%) instead of both relative and absolute contribution (ppbv) to avoid the paradoxical expression.

12. P15 Line 18: Highest CPF values of oil refinery was found in the east direction (Fig. 14a, 14b, and 14d). This sentence confused me.

The CPF plot of this source was corresponding to Fig 14a, not referred to Fig. 14a, 14b, and 14d in the original manuscript. So, we have corrected this sentence.

The highest CPF value of oil refinery was found in east direction of the sampling site (Fig. 14a), which indicated the potential location of this source.

13. P25 Table 1: There are some mistakes such as an extra line under n-decane.

We have corrected this error.

14. P28 Table 3: I am wondering why the average value of four different seasons does not equal to annual value?

The average value of four different seasons does not equal to annual value which is due to the different calculation method. For instance, the local contribution of oil refining source in different seasons was calculated according to the raster analysis of each season, while the annual contributions were calculated according the whole year's CWT analysis. According to the equation 2, the C_{bi} in different seasons was different. So, the average value of four seasons does not equal to the annual contribution.

15. P35 Figure 7 and P41 Figure 13: Due to the time resolution of meteorological parameters, BLH are three hours, while the time resolution of trace gases is one hour as the author mentioned. I suggest that the Pearson correlation can be conducted to give a more statistical reliable relation between VOC concentrations, different source contributions and trace gases.

Thanks for your constructive suggestion, the Pearson correlation between the VOC concentrations and different source contributions and trace gases were conducted. The species which were not well correlated with the corresponding source contributions were deleted. The revised manuscript is shown as following:

3.5.1 Oil refinery

The diurnal pattern of this source contribution was well correlated to the methylcyclohexane ($r = 0.76$, $p < 0.01$) and characterized by a double wave profile with the first peak at 02:00 LT and second peak at 06:00 LT (Fig. 13a).

3.5.2 NG

The diurnal variation of the NG leakage was significantly correlated ($p < 0.01$) with the diurnal pattern of propane *n*-butanes and *i*-butane with Pearson coefficients as 0.94, 0.87 and 0.91, respectively (Fig. 13b), which was also reported by Baudic et al. (2016).

3.5.3 Combustion source

The diurnal variation of combustion source was in accordance with the diurnal pattern of ethylene and CO with Pearson correlation coefficients as 0.71 ($p < 0.05$) and 0.84 ($p < 0.01$), respectively.

3.5.4 Asphalt

The diurnal variation of asphalt was different from other sources and well followed the diurnal patterns of decane ($r = 0.76$, $p < 0.01$) and undecane ($r = 0.86$, $p < 0.01$).

3.5.5 Fuel evaporation

On the contrary, the source contribution followed the diurnal variations of fuel evaporation tracers such as *i*-pentane, *n*-pentane and methylcyclohexane, with Pearson correlation coefficients being 0.86 ($p < 0.01$), 0.87 ($p < 0.01$) and 0.67 ($p < 0.05$), respectively.

One year monitoring of volatile organic compounds (VOCs) from an oil and gas station in northwest China

Huang Zheng^{1,2}, Shaofei Kong^{2,1}, Xinli Xing^{4,2,3}, Yao Mao³, Tianpeng Hu^{4,2}, Yang Ding^{4,2}, Gang Li⁴, Dantong Liu⁵, Shuanglin Li^{1,2}, and Shihua Qi^{1,3}

¹ Department of ~~Atmospheric Sciences~~Environmental Science and Technology, School of Environmental Studies, China University of Geosciences, Wuhan, 430074, China

² Department of Environmental Science and Technology~~Atmospheric Sciences~~, School of Environmental Studies, China University of Geosciences, Wuhan, 430074, China

³ State Key Laboratory of Biogeology and Environmental Geology, China University of Geosciences, Wuhan, 430074, China

⁴ Karamay Environmental Monitoring Center Station, Karamay, 834000, China

⁵ School of Earth and Environmental Sciences, the University of Manchester, M13 9PL, UK

Correspondence to: Shaofei Kong (kongshaofei@cug.edu.cn) or Xinli Xing (xingxinli5300225@163.com)

Abstract. Oil and natural gas are important for energy supply around the world. The exploring, drilling, transportation, and processing in oil-gas oil and gas regions can release abundant-a lot of volatile organic compounds (VOCs). To understand the atmospheric behaviors of VOCs VOC levels, compositions, and sources in such region, an oil and gas station in northwest China was chosen as the study area research site and the fifty-~~six~~-seven VOCs designed as the photochemical precursors by the United State Environmental Protection Agency were continuously measured for an entire year (September 2014 to August 2015) by using an set of on-line monitoring system at an oil-gas station in northwest China. The average concentrations of total VOCs were 297 ± 372 ~~29~~ ppbv, and the main contributor was are alkanes, which concentrations in this study were 1-50 times higher than those measured in many other urban and industrial regions. The VOC compositions were also different from other studies with alkanes contributing accounted accounting for up to 87.5% of the total VOCs in this study. According to the propylene-equivalent concentration and maximum incremental reactivity methods, alkanes were identified as the most important VOC s groups to for the ozone formation potential. The photochemical reaction, meteorological parameters (temperature, relative humidity, pressure, and wind speed) and boundary layer height were found to influence the temporal variations of VOCs at different time scales. The pPositive matrix factorization (PMF) analysis showed that the annual average contributions from natural gas, fuel evaporation, combustion sources, oil refining process, and asphalt (anthropogenic and natural sources) to the total VOCs contributed were 62.6 ± 3.04%, 21.5 ± .99%, 10.9 ± 1.57%, 3.8 ± 0.50% and 1.3 ± 0.69%, respectively, to the total VOCs on the annual average, respectively. The fDue to the the high resolution observation dataset, the diurnal variations of five identified VOCs sources exhibited various diurnal variation patterns due to their different emission patterns and the impact of meteorological parameters. derived from the PMF model were studied and they exhibited different temporal diurnal pattern variations. Clear temporal variations differed from one source to another was observed, due to their differences in source emission strength and the influence of meteorological parameters. Potential source contribution function (PSCF) and contribution weighted trajectory (CWT) models based on backward trajectories indicated that the five identified sources had similar geographic origins. Raster analysis based on CWT analysis indicated that the local emissions

contributed 48.4%–74.6% to the total VOCs. ~~Due to~~Based on the high-resolution observation data, this study clearly described and analyzed ~~contributed to better understand~~the temporal variation of VOC emission characteristics ~~characteristics~~ at a typical ~~in oil-gas~~oil and gas field, which exhibited different atmospheric behaviors compared with that ~~in~~ urban and industrial areas.

This research is a good first step to understand ~~filled the gaps in understanding the VOCs~~ the VOC emission characteristics in the ~~oil-gas~~oil-gas fields ~~region in~~China, where exhibited different source emission behaviors compared with the urban/industrial regions.

Keywords: Volatile organic compounds; ~~oil-gas~~oil-gas oil and gas field; ~~temporal~~spatial-variation; photochemical behavior; source apportionment; ~~source region and~~ local-regional contribution

1 Introduction

Volatile organic compounds (VOCs) are ubiquitous in ambient air and originate from both natural processes (i.e., vegetation emission, ~~volcanos~~volcanic eruption and forest fire) and anthropogenic activities, ~~including such as the~~ fossil fuel combustion, industrial processes and solvent usage (Cai et al., 2010; Leuchner and Rappenglück, 2010; Baudic et al., 2016). As ~~the~~ key precursors of ~~the~~O₃ formation (Fujita, 2001; Geng et al., 2008; Ran et al., 2009; Lyu et al., 2016), ~~different VOCs categories and compounds~~exhibited different ozone formation potentials (Carter, 1994; Atkinson and Arey, 2003; Zou et al., 2015). ~~Some VOCs~~VOCs species (i.e., benzene) ~~also~~exhibit detrimental effects on human health (Colman Lerner et al., 2012; He et al., 2015) and ~~they have negative impacts on~~ air quality (Vega et al., 2011). ~~Till now,~~researches concerning atmospheric VOCs including their emission, atmospheric transformation, health impact and so on ~~is~~are still a hot topic around the world.

Previous studies ~~in China~~mainly focused on ~~the~~measurements of VOCs in urban agglomerations such as the Pearl River Delta (PRD) region (Tang et al., 2007; Liu et al., 2008; Cheng et al., 2010; Ling et al., 2011), Yangtze River Delta (YRD) region (An et al., 2014; Li et al., 2016; Shao et al., 2016) and Beijing-Tianjin-Hebei (BTH) region (Li et al., 2015) and ~~key~~ megacities including Beijing (Song et al., 2007; Wang et al., 2010; Yuan et al., 2010), Shanghai (Cai et al., 2010; Wang, 2014), Guangzhou (Zou et al., 2015) and Wuhan (Lyu et al., 2016). ~~These studies and~~ found that vehicle emission and solvent usage contributed most to the ambient VOCs in urban areas ~~or industrial areas~~ (An et al., 2014; Wei et al., 2015; Shao et al., 2016). ~~A few studies were also conducted in industrial areas~~ (An et al., 2014; Wei et al., 2015; Shao et al., 2016) and petrochemical industrial regions with a lot of VOC emissions (Lin et al., 2004; Wei et al., 2015; Jia et al., 2016; Mo et al., 2017). ~~These studies found that the VOC sources and compositions are complex due to the different emission and atmospheric processes~~ (Warneke et al., 2014). However, ~~the research conducted in oil and gas area in China is still limited while the VOCs emission characteristics in this type of regions are common~~ around the world (Buzcu-Guven and Fraser, 2008; Simpson et al., 2010; Rutter et al., 2015; Bari et al., 2016). For instance, Leuchner and Rappenglück. (2010) found that natural gas/crude oil sources contributed most to the VOCs emissions in Houston. ~~Similar results were reported in the Northeast Colorado due to the oil and natural gas~~

operations (Gilman et al., 2013) found that oil and gas emissions strongly contribute to the propane and butanes in northeast Colorado. Therefore, study concerning VOC emission characteristics studies in oil and gas area in China is very important.

These studies found that vehicle emission and solvent usage contributed most to the ambient VOCs. A few studies were conducted in petrochemical industrial regions with intensive VOC emissions (Lin et al., 2004; Liu et al., 2008a; Wei et al., 2015; Jia et al., 2016; Mo et al., 2017). Studies concerning VOCs at regions of oil-gas exploiting have been reported (Buzcu-Guven and Fraser, 2008; Simpson et al., 2010; Rutter et al., 2015; Bari et al., 2016). The contributors of VOCs at petrochemical regions are quite different from urban regions and are mainly depended on the processing stages (Warneke et al., 2014). Leuchner and Rappenglück (2010) found that natural gas/crude oil sources contributed most to the VOC emissions in Houston. Similar results were reported in the Northeast Colorado due to the oil and natural gas operations (Gilman et al., 2013).

In previous studies, the ambient air was sampled for a few days (weeks) or at a certain season with low time-resolution. The diurnal, monthly and seasonal variations were mostly overlooked, which prevented the understanding of the VOCs' temporal behaviors influenced by the real-time emissions, photochemical reactions, and meteorological parameters condition. Therefore, a long-term monitoring with the a high-time resolution of VOCs is desired (Baudic et al., 2016; Liu et al., 2016). It should be emphasized that in the September of 2013, the VOCs control at petrochemical regions has been listed as one of the main objectives of the Action Plan of Atmospheric Pollution Control released by the central government of China (http://www.gov.cn/zw/gk/2013-09/12/content_2486773.htm), which proposed new requirements to conduct researches in this type of field.

To identify the various-VOC sources, receptor models including chemical mass balance (CMB), positive matrix factorization (PMF) and principal component analysis/absolute principal component scores (PCA/APCS) have been widely used (Guo et al., 2004; Rodolfo Sosa et al., 2009; An et al., 2014; Liu et al., 2016). Meanwhile, dispersion models including conditional probability function (CPF), backward trajectory, potential source contribution function (PSCF) and concentration weighted trajectory (CWT) are also employed to locate the potential source origins (Song et al., 2007; Chan et al., 2011; Liu et al., 2016). Receptor models can only give the source categories and contributions, while the dispersion model can explore the potential geographic source regions. Recently, the combination of these two types of models is developed to figure out the locations of various air pollutant sources (Zhang et al., 2013a; Bressi et al., 2014; Chen et al., 2016). While these practices mainly focus on the atmospheric fine particles (PM_{2.5}), few studies have concerned the local and regional source contributions of VOCs.

In this study, an oil-gas field located in northwest China was chosen as the study area to conduct a long-time-long-term monitoring of VOCs with high-time resolution. The main objectives are to (1) compare VOC concentrations, compositions and ozone formation potential at this oil-gas station with other areas, (2) discuss the relationships between VOC concentrations and meteorological parameters in different time scale, (3) employ PMF model to identify the possible VOC sources by PMF, and (4) identify the local source contributions and regional origins of VOCs based on PMF and dispersion models. This study is the first VOCs research with high-time resolution at the oil-gas and gas fields in China, which provides new information on the temporal distribution variation, photochemical properties and ozone

~~formation potential~~; and local/regional contributions of VOCs and ~~are helpful contributes to to~~ establish ~~the~~ control measures of VOCs at this type of region ~~around the world~~.

2 Materials and methods

2.1 Site description

5 The study area (44.1 ~~---~~ 46.3 °N and 84.7 ~~---~~ 86.0 °E) is located in ~~the~~ northwest China and at the northwestern margin of Junggar Basin, which is an important oil and gas ~~-~~bearing basin (Fig. 1a). The proven deposits of oil and natural gas are 2.41 $\times 10^{-9}$ t and 1.97 $\times 10^{-11}$ m³, respectively ~~in this area~~. There are hundreds of oil and gas wells in this ~~oil-gas~~ ~~oil-gas~~ field with an annual gas deliverability of 1.20 $\times 10^{-10}$ m³ ([Chen, 2015](#)). Additionally, 126 petrochemical plants spread across this area. ~~This area~~It can be divided into two regions with ~~oil-gas~~ ~~oil and gas~~ operation and ~~/~~oil refinery ~~in-at~~ the north direction (Region 1) and petrochemical industry ~~in-at~~ the south direction (Region 2). These two regions are about 150 km in distance (Fig. 1b). Region 1 is abundant in ~~oil-gas~~ ~~oil and gas~~ resources and the main petrochemical factories are oil refineries and natural gas chemical plants. The main products include gasoline, diesel, asphalt, and 1, 3-butadiene ~~and, the~~ ~~The flow charts of~~ chemical process ~~flow charts~~ are shown in Fig. S1. Region 2 is a key petrochemical base, with the production capacity of oil and ethylene being 6 $\times 10^6$ t ~~/yr⁻¹~~ and 2.2 $\times 10^5$ t ~~/yr⁻¹~~, respectively. The sampling site is located on the rooftop of a building (15 m above the ground, 45.6 °N, 85 °E), about 11 km away from the southeast of the urban region. At the northeast of the sampling site, there are hundreds of oil and gas wells (Fig. 1c). The study area is ~~located deeply secluded in~~ ~~-~~ ~~hinterland~~ ~~the hinterland~~ of Eurasia. The typical temperate continental arid desert climate results in high temperature in summer (27.9 °C) and low temperature in winter (~~---~~15.4 °C). The sufficient solar radiation, little precipitation and ~~the~~ low humidity (43 ~~---~~ 56%) result in high evaporation (>3000 mm) in this region.

2.2 Descriptions of instruments and QA/QC

25 From September 2014 to August 2015, ~~57 ambient VOCs designed as the O₃ precursors by the Photochemical Assessment Monitoring Stations (PAMS) in ambient air were~~ continuously sampled and measured using an online monitor system (TH-300B, Wuhan-Tianhong Instrument Co., Ltd, China) with two-hour time resolution ~~online sampling and measurement of fifty-six Photochemical Assessment Monitoring Stations (PAMS) VOCs were conducted at the sampling site.~~ ~~The ambient VOCs were sampled continuously and analyzed automatically at 2 h interval with an online monitor system (TH-300B, Wuhan-Tianhong Instrument Co., Ltd, China).~~ The sampling and analysis procedures were described elsewhere (Lyu et al., 2016). Briefly, two-channels were ~~initialed-installed~~ to sample and analyze VOCs separately. The water and carbon dioxide in the sampled air was ~~firstly~~ removed at a cold trap maintaining at ~~---~~80 °C and then concentrated at ~~---~~150 °C at another cold trap. ~~After the purification and concentration, the VOCs were desorbed by rapid heating to 100 °C. The C₂---~~ ~~C₄~~ ~~C₅~~ VOCs

5 were ~~trapped-separated~~ with a PLOT column (diameter: 0.32 mm, thickness of membrane: ~~5-1.5~~ μm , ~~and~~-length: 60 m) ~~and~~ were quantified by the ~~gas chromatograph-flame ionization detector (GC-FID, Agilent 78920)~~. ~~C₅—C₁₂ were separated by~~ ~~en~~ a DB-624 ~~column~~ (diameter: 0.25 mm, thickness of membrane: 3 μm ; and length: 60 m) and were quantified using mass spectrometer detector (~~GC-MSD, Agilent 5975~~). ~~trapped with an empty capillary column at 150 °C. After the pre-~~ ~~concentration, the VOCs were desorbed by rapid heating to 120 °C. C₂-C₄ VOCs were introduced into a gas chromatograph-~~ ~~flame ionization detector (GC-FID, Agilent 7820) and C₅-C₁₂ VOCs were introduced into a gas chromatograph-mass spectrometer detector (GC-MSD, Agilent 5975) for further analysis.~~

10 The target compounds involved ~~56-57~~ VOC species: alkanes (~~2930~~), alkenes (~~409~~), alkynes (acetylene), and aromatics (~~4617~~). The standard gases from PAMS were used for the equipment calibration and verification through the 5-point method every two weeks (Lyu et al., 2016). The correlation coefficients of the calibration curves usually varied from 0.991 to 0.998. The detection limits were in the range of 0.04 to 0.12 ppbv (Table 1). The missing value was due to power failure or instrument maintenance and was not included in the data analysis.

2.3 Data sources and analysis

PMF receptor model description

15 ~~Positive matrix factorization (PMF) model has been widely employed for VOCs source apportionment (Buceu Guven and Fraser, 2008; Leuchner and Rappenglück, 2010; Liu et al., 2016; Lyu et al., 2016). It decomposes a matrix of X (i × j dimension) into factor contributions matrix G (i × k dimensions) and factor profiles matrix F (k × j dimensions) plus a residue matrix E (i × j dimension):~~

$$x_{ij} = \sum_{k=1}^p g_{ik} f_{kj} + e_{ij} \quad (1)$$

20 where x_{ij} is the concentration of j th VOC species measured in i th sample, g_{ik} represents the contribution of the k th source to the i th sample, f_{kj} represents the mass fraction of the j th compound from the k th source, and e_{ij} is the residual for each sample/species. The purpose of the PMF model is to find the minimum Q value with uncertainty (u_{ij}) introduced into model:

$$Q = \sum_{i=1}^n \sum_{j=1}^m \left[\frac{x_{ij} - \sum_{k=1}^p g_{ik} f_{kj}}{u_{ij}} \right]^2 \quad (2)$$

25 EPA PMF 5.0 (US EPA, 2014) was employed for VOCs source apportionment and more detailed PMF operations were given in Appendix A.

2.4-3.1 Meteorological parameters and air pollutants

Other dataset such as ~~t~~The ~~three3~~-hours resolution meteorological parameters (~~including~~ atmospheric pressure (P), temperature (T), relative humidity (RH), wind speed (WS) and direction (WD)~~—~~) were collected from the Meteomanz

(www.meteomanz.com) are and are shown in Fig. 2. The boundary layer height (BLH) was computed every ~~three~~ 3 hours each day through the NOAA's READY Archived Meteorological website (<http://www.ready.noaa.gov/READYamet.php>).

Significant differences ($p < 0.01$) were found between the meteorological parameters in different seasons (autumn: Sep, Oct and Nov; winter: Dec, Jan and Feb; spring: Mar, Apr and May; summer: Jun, Jul and Aug). During the sampling period, northwesterly and northeasterly winds prevailed (Fig. 1e).

The hourly ~~data of~~ trace gases including CO, NO₂, and O₃, ~~SO₂, ambient airborne inhalable particles~~ particulate matter (PM₁₀) and ~~ambient~~ fine particles (PM_{2.5}) were measured using an ambient air quality continuous automated monitors (TH-2000 series, Wuhan-Tianhong Instrument Co., Ltd, China) and the data were acquired from the Qingyue Open Environmental Data Center (<https://data.epmap.org>). It should be noted that the NO₂ (NO₂ = NO_x - NO) concentrations ~~are~~ were in fact overestimated. This is because some oxidized reactive nitrogen that is converted by the molybdenum during the NO_x measurement while the NO measurement is accurate using the chemiluminescence technic. Therefore, the NO₂ concentrations discussed below are considered greater than the actual values (Dunlea et al., 2007; Zou et al., 2015). ~~were synchronously measured with an enhanced trace level CO analyzer (Model 487TL, Thermo Environmental Instruments (TEI) Inc.), a chemiluminescence trace level NO₂ analyzer (Model 427TL, TEI), and an UV photometric O₃ analyzer (Model 49i, TEI), respectively (Lyu et al., 2016).~~ These three trace gases and hourly dataset of ambient fine particles (PM_{2.5}), airborne particulate matter (PM₁₀) and SO₂ (Model 43i, TEI) were collected from the local environmental monitoring station. According to the ambient air quality standards- II (GB/3095-2012), the main air pollutants were PM₁₀ and PM_{2.5} in winter and NO₂ in autumn (Fig. S2).

2.3.2 VOCs source apportionment and ozone formation potential

Positive matrix factorization (PMF) model has been widely employed for VOCs source apportionment (Buzcu-Guven and Fraser, 2008; Leuchner and Rappenglück, 2010; Liu et al., 2016; Lyu et al., 2016). In this study, the EPA PMF 5.0 (US EPA, 2014) was employed ~~for VOCs source apportionment and more detailed additional PMF operations information~~ ~~was~~ given in Appendix A.

2.5 Ozone formation potential

The VOC concentrations are not proportional to the ozone formation potential due to their wide ranges of photochemical reactivity with OH radicals (Table 1). ~~For example, the rate constant of ethane reacting with OH radicals is $0.27 \times 10^{12} \text{ cm}^3 \text{ molecule}^{-1} \text{ s}^{-1}$ and the rate constant of propylene is $26.3 \times 10^{12} \text{ cm}^3 \text{ molecule}^{-1} \text{ s}^{-1}$ at 298 K.~~ Two methods including propylene-equivalent concentrations (Propy-Equiv) and the maximum incremental reactivity (MIR) were adopted to analyze the ozone formation potential of VOCs. ~~Their calculation equations are expressed as follows~~ More details can be found in the researches² of (Atkinson and Arey, (2003) and; Zou et al., (2015)).

$$C_{j,Propyl-Equiv} = C_{j,C} \times \frac{k_{j,OH}}{k_{Propyl,OH}} \quad (3)$$

$$C_{j,MIR} = MIR_j \times C_{j,ppbv} \times \frac{m_j}{M} \quad (4)$$

where $C_{j,C}$ and $C_{j,ppbv}$ represent the carbon atom concentration (ppbC) and actual concentration by volume (ppbv) for species j , respectively. $k_{j,OH}$, $k_{Propyl,OH}$ and MIR_j denote the chemical reaction rate constant in the free radical reaction of species j , propylene with OH and maximum incremental reactivity for species j , respectively. m_j and M stand for the relative molecular mass of species j and the molecular mass of ozone, respectively. The estimated MIR coefficients and the OH reaction rate constants from former studies are listed in Table 1.

2.2.6.4 Geographic origins of the VOCs

2.2.6.4.1 Conditional probability function (CPF)

The CPF is widely used to locate the direction of sources based on wind direction data (Song et al., 2007). In this study, the directions of various VOC sources were explored based on the G matrix in PMF analysis and wind directions. The CPF is defined as Eq (5):

$$CPF = \frac{m_{\Delta\theta}}{n_{\Delta\theta}} \quad (5)$$

where $m_{\Delta\theta}$ is the number of data from wind sector $\Delta\theta$ (each is 22.5 degree) that exceed the threshold value (75th percentile of each source contribution); $n_{\Delta\theta}$ is the total number of occurrence from the same wind direction. Calm conditions (wind speed < 1 m/s) were excluded from the calculation for its difficulty in defining the wind direction.

2.6.4.2 Backward trajectory analysis

The 48 h backward trajectories at with 2 h intervals (starting from 0:00 to 20:00 local time, LT) were run each day by the TrajStat — plugin of Meteoinfo software (<http://www.meteothinker.com/downloads/index.html>) TrajStat using the Hybrid Single Particle Lagrangian Integrated Trajectory (HYSPLIT) model (Wang et al., 2009; Squizzato and Masiol, 2015). The top start height of the model was set at as 500 m above ground level (Zhao et al., 2015; Liu et al., 2016). The FNL global analysis data produced by the National Center for Environmental Prediction's Global Data Assimilation System (GDAS) wind field re-analysis was introduced into the caTrajStat model calculation. A total of 2743 backward trajectories were ealculated-generated and then were grouped into four clusters according to their geographic sources and histories (Fig. S3). As shown in Fig. S3, the trajectories were mainly originated from the northwest of the sampling site during the whole observation sampling period.

2.6.4.3 Local and regional transport contribution

The potential source contribution function (PSCF) and concentration weighted trajectory (CWT) model are previously used to identify the possible source regions based on the backward trajectory analysis (Cheng et al., 2013; Bressi et al., 2014; Liu

et al., 2016). The PSCF gives the proportion of air pollution trajectory in a given grid and the CWT reflects the concentration levels of trajectories. The geographic domain (31 °–71 °N, 36 °–107 °E) was found to be within the annual range of 48 h backward trajectories. The total number of grids was 11360 with a resolution of 0.5 °×0.5 °. More information about the PSCF and CWT analysis can be found in Appendix B.

5 Local and regional source contributions of the observed VOCs were calculated by raster analysis. In previous studies, the domain was divided into 12 sectors (each was 30 °) to study the regional contributions (Bari et al., 2003; Wang et al., 2015; Wang et al., 2016). However, in this study, the domain was briefly divided into two sections (local and regional), with the sampling site as the original point. The range of local sources was defined as a polar with a radius of 12 h backward trajectories and the range of regional sources was outside of the circle (detailed descriptions can be found in Appendix C). The concentration of each grid was calculated by CWT analysis. By counting and averaging in each section, contributions of local emission and regional transportation were produced. To reduce the effects of background values, the lowest CWT values (C_b) in each section was deduced from the concentrations. The contribution (%) of local source and regional transportation was defined as follows:

$$15 \quad \%C_i = \frac{(C_i - C_{bi}) \times N_i}{\sum_{i=1}^2 (C_i - C_{bi}) \times N_i} \times 100\% \quad (62)$$

where C_i is the mean CWT value in the i th section (local or regional), C_{bi} is the background value of the i th section, N_i is the number of grid with non-zero CWT concentrations in the i th section.

Several factors affect the calculated results of regional and local source contributions, including the radius of the circle and CWT value. In this study, the 12 h backward trajectories were chosen to differentiate the local area from regional area. However, in fact, the longer the backward trajectories were, the lower regional contributions produced. In addition, the PMF model was employed to VOCs source apportionment and the contribution of each identified source was introduced into CWT calculation. However, the negative value of source contribution was inevitably generated despite the application of F-peak in PMF analysis. Therefore, the negative CWT value was excluded in raster analysis and this would affect the results of regional and local source contributions. Overall, although flaws existed in this new method, it gave the a new insight to understand the quantitative contributions of local and regional contribution to the VOCs in the study area.

3 Results and discussions

3.1 VOCs levels and compositions

The statistics of 56 observed VOCs are summarized in Table 1 and the every two hours'ly variations of four VOC categories are shown in Fig. 3. Among the four different VOC groups, the average concentrations of alkanes were highest (129 ± 173 ppbv), followed by alkenes (9.52 ± 14.5 ppbv), aromatic hydrocarbons (4.28 ± 8.24 ppbv) and acetylene (3.03 ± 5.55

ppbv). The top four alkanes species were ethane (39.7 ± 57.3 ppbv), propane (22.6 ± 33.5 ppbv), *n*-butane (15.8 ± 21.4 ppbv) and *i*-butane (12.5 ± 17.5 ppbv). These four species totally accounted for 64.8% of the alkanes. Among the alkenes, 1-pentene, propylene and ethylene were the most abundant species with their average concentrations of 4.47 ± 6.72 ppbv, 1.88 ± 10.2 ppbv and 1.42 ± 1.69 ppbv, respectively. They totally represented 71.8% of the alkenes. 96.7% of the aromatic hydrocarbons were composed by benzene, toluene and *m, p*-xylene, with corresponding average concentrations of 1.13 ± 1.62 ppbv, 1.06 ± 1.91 ppbv and 0.72 ± 1.94 ppbv, respectively. ~~High concentrations of alkanes, ethane and propane in ambient Same findings~~ were also reported in other oil and natural gas operation and industrial ~~areas~~ in the US (Páron et al., 2012; Helmig et al., 2014; Warneke et al., 2014). For instance, the average concentrations of ethane and propane were ~~74 ± 79 ppbv and 33 ± 33 ppbv, respectively~~ ~~in Horse pool and Uintah Basin in the winter of 2012 collected from Horse pool, Uintah Basin.~~ Despite the highly enhanced VOC levels ~~were~~ due to the temperature inversion, the VOC levels in Uintah Basin ~~were~~ still higher ~~than those compared to in the regional background areas because of the existence of oil and gas exploitation activities~~ (Helmig et al., 2014). A distinct chemical signature of collected air samples from the ~~boulder Boulder Atmospheric~~ ~~Observatory in nNortheast Colorado~~ was also found ~~with to show~~ enhanced concentrations of most alkanes (propane, *n*-butane, *i*-pentane and *n*-pentane) (Páron et al., 2012). ~~The comparable VOCs levels and compositions between this study and researches in other oil gas rich areas suggested that VOCs in ambient air was from primary emission from oil and gas development.~~

The VOC concentrations, compositions and the top five species in this study and other areas around the world ~~were~~ also compared and ~~are~~ shown in Fig. 4. The ~~average total~~ VOCs concentrations in this study (297 ± 372 ppbv) were 1—50 times higher than those in urban areas like Beijing (34.5 ppbv), Shanghai (32.4 ppbv), Guangzhou (43.6 ppbv), Seoul (122 ppbv), Mexico (117 ppbv) and 28 cities— in the US (9.91 ppbv) as well as industrial areas, including Houston (31.2 ppbv), northeast Colorado (96.1 ppbv), Alberta oil sands (2.87 ppbv), Ulsan (91.7 ppbv), YRD (22.9 ppbv) and Nanjing (34.5 ppbv) (Fig. 4a). As shown in Fig. 3e and Fig. 4b, the alkanes were the most abundant groups (87.5% on average) during the whole sampling period, which was quite higher than other urban/industrial areas (45.3—67.2%, Fig. 4b). Similar relative high proportions of alkanes were found in Houston (77.1%) (Leuchner and Rappenglück, 2010), Alberta oil sands area (74.8%) (Simpson et al., 2010) and Northeast Colorado (97.4%) (Gilman et al., 2013), which ~~are~~ ~~were~~ all related to oil/ ~~and~~ gas operations. In urban areas, the aromatics accounted for about 10.1—47.9% of the total VOCs, with toluene as one of the most abundant species. Toluene is mainly from solvent usage (Guo et al., 2004; Yuan et al., 2010) or vehicle exhaust emission (Wang et al., 2010) in cities. Another dominant compound in the urban air is propane ($1.45—14.7$ ppbv), which is the main component of liquid petroleum gas/natural gas (LPG/NG) (McCarthy et al., 2013). In industrial areas, alkanes and alkenes contribute most to the total VOCs (43.4—97.4% and 1.8—43.6/30.0%, respectively) with ethane, propane and ethylene as the top species usually (Fig. 4c). They may originate from the incomplete combustion or LPG/NG usage (Durana et al., 2006; Tang et al., 2007; Guo et al., 2011)(Durana et al., 2006; Tang et al., 2007; Guo et al., 2011). To sum up, the concentrations of VOCs in this study were higher than many other regions and cities. The compositions and the top five species of VOCs

exhibited typical characteristics of oil and gas exploring regions, such as Houston (Leuchner and Rappenglück, 2010), North Colorado (Gilman et al., 2013) and Alberta oil sands area (Simpson et al., 2010).

3.2 Contribution of VOCs to ozone formation potential (OFP)

The profiles of different VOCs categories with concentrations expressed in different scales are shown in Fig. 5. The top ten VOCs species to OFP obtained by Propy-Equiv and MIR method are listed in Table S1. Among the top ten compounds calculated by the two methods, six compounds were the same, but differing in their rank order. Considering the kinetic activity, 1-pentene ranked first by Propy-Equiv method. However, the *o*-xylene showed highest OFP based on the MIR method, which may be related with the chemical mechanisms and the impacts of NO_x (Zou et al., 2015). Despite the two methods were different in mechanisms, the proportions of different VOC categories to the OFP were the same. From the non-weighted concentrations by volume and carbon atom, alkanes contributed 83 ± 9% and 82 ± 9%, respectively to the total VOCs concentrations, followed by alkenes (11 ± 6% and 9 ± 4%, respectively) and aromatics (5 ± 6% and 8 ± 7%, respectively). Although the proportions of alkenes and aromatics increased when compared to the values of non-weighted, the alkanes were still dominant, accounting for 45 ± 11% and 50 ± 14%, respectively. In summary, the alkanes had the highest concentrations (for both volume and carbon atom) and largest proportions to the OFP weighted by Propy-Equiv and MIR method. The results of this study were different from previous researches. For example, the alkanes with the highest concentrations (both for volume and carbon atom) contributed less to OFP, while alkenes and aromatics with less concentrations contributed most to the OFP in Guangzhou (73% and 83%, respectively) (Zou et al., 2015) and Tianjin (about 28—40% and 32—42%) (Liu et al., 2016) as well as a petrochemical industrialized city (48—49% and 37—49%, respectively) (Jia et al., 2016).

3.3 Temporal variations

~~The temporal variation of VOC concentrations is controlled by several factors such as the meteorological parameters, photochemical reactions and emission sources. Due to the lack of information on source emission strengths, we analyzed the effects of the other two factors on VOC concentrations. The effects of meteorological conditions on VOCs were assessed by Pearson correlation analysis (Fig. S4). The photochemical removal of VOCs was evaluated by analyzing the relationship between the VOCs concentrations and other trace gases (i.e., NO₂ and O₃) (Fig. 6). Temporal variation of selected parameters and VOCs were analyzed in different timescales.~~

~~Fig. 6 shows the temporal variations of ethane, ethylene, acetylene and benzene in different timescales. Though differences existed, the selected compounds broadly represent the respective alkanes, alkenes, alkynes and aromatics (Lyu et al., 2016). Significant differences were found between the meteorological parameters in different seasons ($p < 0.01$) and the highest concentrations of these species in winter were observed. The seasonal variation of VOCs is controlled by meteorological conditions, photochemical activities and source emissions. The highest values in winter was due to inhibited photochemical~~

activities under suppressed dispersion conditions (averaged BLH as 121 ± 71.7 m, wind speed as 1.20 ± 0.76 m s⁻¹) and low temperature (-11.8 ± 5.00 °C). For instance, all these species were negatively correlated with BLH, exhibiting higher VOC levels under lower BLH (Fig. 6). The wind speed and temperature were also found negatively correlated with VOC concentrations and ethylene showed the highest negative correlation coefficient with these parameters (Table S2). The less photochemical reactions can result in the high concentrations in winter, which was proved by negative correlation between VOCs and O₃ (Table S2). Additional sources (i.e., combustion) may be also present, in view of the obvious increase of acetylene (Fig. 6c) from summer (0.87 ± 1.00 ppbv) to winter (10.5 ± 8.51 ppbv). Conversely, the high temperature, wind speed and BLH favor the dilution and dispersion of ambient VOCs and the photochemical depletion in summer. The daily concentrations of VOCs were found negatively correlated with temperature and wind speed, with r being -0.29 ($p < 0.01$) and -0.39 ($p < 0.01$), respectively. This finding was consistent with previous study (Lyu et al., 2016; Marčulaitienė et al., 2017). High VOC levels in low temperature are due to more frequent stagnant conditions in cold seasons and proved by the negative correlation between VOCs and BLH ($r = -0.45$, $p < 0.01$) in this study. Higher wind speed indicates better dispersion conditions and thus resulting in lower VOC concentrations. Positive correlations between the VOCs and relative humidity ($r = 0.35$, $p < 0.01$) and atmospheric pressure ($r = 0.19$, $p < 0.01$) were found, which was in line with former studies (Maré et al., 2015; Marčulaitienė et al., 2017).

At 99% confidence interval, the monthly VOC concentrations were positively correlated with NO₂ ($r = 0.63$, $p < 0.01$) (Fig. 6a) and the VOCs were negatively correlated with O₃ ($r = -0.60$, $p < 0.01$) (Fig. 6b). Similarly, significant correlations were also found between the daily NO₂, O₃ and VOCs, as shown in Fig. 6c and Fig. 6d. It should be noted that VOCs and NO₂ concentrations were controlled by solar UV, concentrations of NO and O₃ as well as BLH. For example, the BLH in May, June and July was higher than 900 m, which may explain the lowest NO₂ and VOC concentrations during the sampling period. The diurnal variations of VOCs concentrations and trace gases (NO₂ and O₃) related to photochemical reaction are shown in Fig. 7, had a pronounced diurnal variation, which is summarized graphically by annual average value in Fig. 7a. The VOCs had a reverse trend with O₃ ($r = -0.82$, $p < 0.01$). The lower BLH and less photochemical activities resulted in the peak values for the precursors of O₃ including VOCs and NO₂ and low O₃ concentrations before sunrise (6:00 local time). After sunrise, with the initiation of photochemical oxidation and the increasing of BLH, the concentrations of O₃ precursors decreased while the VOCs decreased and O₃ increased rapidly. The minimum of VOCs and NO₂ occurred at about 12:00–14:00 LT was resulted from both dispersion or dilution conditions and photochemical reactions (with highest O₃ concentrations at 14:00 LT) in the afternoon. The diurnal variation of NO₂ was controlled by BLH, O₃ and photochemical reactions (i.e., OH radical) and showed a double peak. The similar diurnal patterns of different atmospheric lifetime compounds including ethane, ethylene, acetylene and benzene (the most abundant contributors to its categories) were also found (Fig. S45). To better understand the effects of BLH and photochemical reactions on VOCs, the diurnal variations of VOCs, BLH and O₃ in winter and summer were analyzed (Fig. 7b, c). VOC concentrations in winter ($213.79.9 \pm 97.713.2$ to $263.59.3$ ppbv) were significantly higher than those in summer ($130.28.2 \pm 9.58$ to 261 ± 10073.9 ppbv). However, the VOCs in summer and winter decreased by 8.3 times and 2.3 times, respectively, from maximum to minimum. This was due to the BLH

increased by 8.2 times in summer while ~~the~~ BLH in winter only increased by 2.3 times. The effects of photochemical reactions on VOCs in two seasons were comparable, which was explained by similar O₃ increment in winter (0.78 times up) and summer (0.71 times up). Therefore, we can conclude that the role of BLH variation was more important than ~~the~~ photochemical reaction for the diurnal variation of VOCs.

5 ~~Overall, the monthly and daily variations of VOCs were influenced by meteorological conditions and photochemical reactions while the diurnal pattern of VOCs was more influenced by BLH.~~

3.4 Ambient ratios: sources and photochemical removal

Ambient ratios for VOC species holding similar reaction rates with OH radicals can reflect the source features, as these compounds are equally affected by the photochemical processing and the new emission inputs (Russo et al., 2010; Baltrėnas et al., 2011; Miller et al., 2012). For example, *n*-butane and *i*-butane have similar reaction rates with the OH radicals, with the differences less than <10% and the ratios of these pair species indicated different sources. The butanes are associated with NG, LPG, vehicle emission and biomass burning and the ratios of *i*-butane/*n*-butane varied according to sources (i.e., 0.2—0.3 for vehicle, 0.46 for LPG and 0.6—1.0 for NG) (Buzcu and Fraser, 2006; Russo et al., 2010). In this study, the slope of *i*-butane/*n*-butane (0.80—0.82, Fig. 8a) was within the range of reported emissions from natural gas. ~~Additionally, *i*-pentane and *n*-pentane have similar physical and chemical characteristics (i.e., boiling point and reaction rate coefficients with hydroxyl radical), which result in less susceptible of the *i*-pentane / *n*-pentane ratio in source identification —the ratio of *i* pentane / *n* pentane is less be susceptible to perturbations and can be used to source identification~~ (Gilman et al., 2013). ~~The pentanes are always form the NG emission, vehicle emission, liquid gasoline —and fuel evaporation with the *i*-pentane/*n*-pentane ratios ranged between 0.82—0.89 (Gilman et al., 2010, 2013), ~2.2—3.8 (Conner et al., 1995; McGaughey et al., 2004), 1.5—3.0 (Zhang et al., 2013b), and 1.8—4.6 (Watson et al., 2001), respectively. As shown in Fig. 8b, the slopes of *i*-pentane / *n*-pentane were 1.03—1.24 in this study, suggested that the pentanes were more likely form from the mixed sources of NG and fuel evaporation. This assumption was proved by the high loadings of pentanes in NG and fuel evaporation source compositions in section 3.5.5. Additionally, the slope of *i* pentane and *n* pentane was in the range of 1.03–1.24 (Fig. 8b), which was larger than those related to oil and natural gas operations (0.82–0.89) (Gilman et al., 2010, 2013), but less than those measured for liquid gasoline and fuel evaporation (>1.5) (Conner et al., 1995; McGaughey et al., 2004; Watson et al., 2001; Zhang et al., 2013b). The ratios of *i* pentane/*n* pentane indicated that the VOCs originated from the mixed sources of NG and fuel evaporation in this study.~~

Information on the photochemical removal process can be obtained by comparing the ambient ratios of aromatics due to their differences in atmospheric lifetimes. For example, the atmospheric lifetimes of benzene (9.4 days), toluene (1.9 days) and ethylbenzene (1.6 days) are relative longer than *m*-xylene (11.8 h) and *p*-xylene (19.4 h) (Monod et al., 2001). The commonly used ratios are benzene/*t*oluene, *m*, *p*-xylene/*e*thylbenzene, benzene/*e*thylbenzene, and toluene/*e*thylbenzene. The diurnal variations of these compounds and ratios are shown in Fig. 9. A continuous decreasing of these compounds and ratios were

observed from 08:00 to 14:00 LT, indicating the increased photochemical removal processes due to the increase in reactive radicals (i.e., hydroxyl radical)~~enhancement of ambient temperature~~. The diurnal patterns of benzene/_ethylbenzene and toluene/_ethylbenzene in this study (Fig. 9b, d) were opposite to ~~that those~~ observed in Dallas, which was mainly influenced by vehicle emission (Qin et al., 2007). After 14:00 LT, the increasing of the ratios and aromatic concentrations were due to the weakening of photochemical activities. The unusual high concentrations of ethylbenzene and *m, p*-xylene were observed at about 02:00 LT (Fig. 9c), which might be related to new emissions. This assumption was verified by a small peak occurred at 02:00 LT in the diurnal ~~distribution~~ profile of oil refinery source (see section 3.5.1). After 12 h dispersion, dilution and photochemical reaction, the concentrations of these two compounds reached its minimum values at about 14:00 LT.

Generally speaking, when the reaction with OH radicals was the only factor controlling the temporal/seasonal ratio of variation of VOC concentrations, an increase of the concentration ratios for longer atmospheric lifetime toover shorter lifetime compounds (i.e., benzene / toluene, *m, p*-xylene / ethylbenzene), an increasing in ratio value from winter to summer from lower ambient temperature to higher temperature would be expected (Russo et al., 2010). ~~The diurnal variation of benzene, toluene, ethylbenzene, and xylene (BTEX) obeyed the rule as discussed above, However,~~ the seasonal variation of BTEX ratios in this study was opposite to the general behavior~~at~~ exceptionally. For example, the benzene /_toluene ratio ~~decreased~~increased from winter—spring (0.63—0.69) summer fall (0.5–0.6) to summer—fall (0.52—0.57) winter spring (0.6–0.7) periods (Fig. 8c) and ethylbenzene *m, p*-xylene/ *m, p*-xyleneethylbenzene ratio also decreased from autumn—winter (0.47—0.69) to spring—summer (0.192–0.374) to autumn winter (0.9–1.4) periods (Fig. 8d). ~~The s~~Same results were also observed both in industry areas (Miller et al., 2012) and urban areas (Ho et al., 2004; Hoque et al., 2008; Russo et al., 2010). The results obtained in this study indicated that there were other factors affecting the seasonal variation, such as source emissions. The BTEX mainly originate from vehicle exhaust (Wang et al., 2010), solvent usage (Guo et al., 2004; Yuan et al., 2010) and petrochemical industry (Na and Kim, 2001; Hsieh et al., 2006; Baltrėnas et al., 2011). ~~As discussed above, the emission from vehicles was not obvious from the diurnal variation of BTEX and the solvent usage was negligible in the study area.~~ The ratios of *m, p*-xylenes/_ethylbenzene in this study here (2.2 ± 1.2) were within the ranges reported at a petrochemical area in southern Taiwan (1.5—2.6) (Hsieh et al., 2006) and the vicinity of a crude oil refinery at the Baltic region (3.0—4.0) (Baltrėnas et al., 2011). Therefore, the BTEX in this area was mainly from the oil refinery emission. The unexpected low ratios of benzene / toluene and *m, p*-xylene / ethylbenzene in summer was due to the strong oil refinery emission strength and this highest *m, p*-xylenes/ethylbenzene ratio in summer can also be related to the highest contribution of oil refinery. This finding was verified by the seasonal source contribution results in section 3.5.1.

3.5 Source apportionment: temporal variation and contribution to OFP

Five sources including oil refining process, NG, combustion source, asphalt and fuel evaporation were identified by the PMF analysis and their source profiles and daily contributions are shown in Fig. 10. The monthly, seasonal and annual contributions were calculated and shown in Fig. 11. The relationships between daily source contributions and meteorological parameters

and trace gases were analyzed by scatter plots (Fig. 12). The source apportionment of this high-resolution dataset provided a unique opportunity to discuss the diurnal variation of different sources as shown in Fig. 13.

3.5.1 Oil refining

5 The emissions from the refining process are complex due to the diversities of VOC species, which depend on the production processes (Vega et al., 2011; Mo et al., 2015). The crude oil is composed of $\geq C_5$ alkanes, cycloalkanes, aromatics, and ~~asphaltics asphaltics (Simpson et al., 2010) and these. These matters y~~ are supplied as the raw materials ~~to for~~ various oil refining processes ~~(Simpson et al., 2010)~~. High fractions of C_5 — C_9 alkanes including hexane ($32 \pm 6.2\%$), cyclohexane ($40 \pm 7.9\%$), methylcyclohexane ($47 \pm 6.9\%$), *n*-octane ($56 \pm 4.2\%$), *n*-nonane ($58 \pm 2.9\%$), and aromatics (i.e., $22 \pm 3.0\%$ for benzene, $39 \pm 5.4\%$ for toluene and $45 \pm 7.3\%$ for xylenes) presented in this factor (Fig. 10a), which was similar to the chemical compositions measured from the oil refinery (Liu et al., 2008; Dumanoglu et al., 2014). The calculated daily source contributions from PMF model were well correlated with the ~~corresponding species of~~ high loadings species in its source profiles. For example, the methylcyclohexane showed significant correlation with this source contribution (Fig. S56a), suggesting that the tracers of oil refinery were well produced by the PMF model. The main products from oil refinery are gasoline, diesel, lube, and kerosene in this area, consistent with the factor derived here.

15 The annual contribution of oil refining source was relatively stable throughout the year ($3.8 \pm 0.50\%$, 3.2 ppbv). The highest relative contribution was found in summer (5.3% , 2.0 ppbv) and the lowest in winter (2.4% , 2.9 ppbv) (Figure 11b). The Pearson analysis between the daily source contributions and wind speed disclosed a middle statistically negative correlation ($r = -0.12$, $p < 0.05$). However, no statistically significant correlations between the daily source contribution and other meteorological parameters were found (Table S32), even for the BLH. On the contrary, statistically significant positive correlations between this source and trace gases (NO_2 and CO) were found, with r being 0.33 and 0.21, respectively (Fig. 12a). These trace gases were are associated with oil refinery emission (Cetin et al., 2003). Therefore, the daily variation of oil refinery source in this study was more controlled by oil refining emission strength and less influenced by meteorological conditions.

25 The diurnal pattern of this source contribution was ~~similar with the variation well correlated to the~~ of methylcyclohexane ($r = 0.76$, $p < 0.01$) and cyclohexane and characterized by a double wave profile with a the first peak at 02:00 LT and second peak at 06:00 LT (Fig. 13a). A small peak occurred at 02:00 was due to the increasing of ethylbenzene and *m*, *p*-xylene (Fig. 9) and the second peak occurred at 06:00 LT resulted from the low BLH. After sunrise, the contribution continuously decreased owing to the increasing of BLH and photochemical reactions and the minimum value occurred at 14:00 LT.

3.5.2 Natural gas

30 Ethane and propane are the most abundant non-methane hydrocarbon compounds in the composition of natural gas (Xiao et al., 2008; McCarthy et al., 2013). The ratios of *i*-butane / *n*-butane indicated the butanes were from the natural gas (section

3.43). ~~In-By~~ the PMF analysis, a NG source was identified through the high weights on ethane ($81 \pm 2.4\%$), propane ($85 \pm 5.3\%$), *n*-butane ($62 \pm 7.5\%$), and *i*-butane ($54 \pm 6.4\%$). As an important oil and gas resources base in China, the export amount of natural gas from this region was $4.4 \times 10^{-9} \text{ m}^3$ and the loss rate was 1.4% in 2014 (Chen, 2015). The leakage from the exploiting, storing, transporting and processing cannot be ignored, suggesting that it was reasonable to attribute this factor to natural gas source.

The annual contribution of the NG leakage source was 53 ppbv, accounting for $62.6 \pm 3.04\%$ of the total VOCs averagely. The highest contribution presented in spring (65.2% , 38.9 ppbv), followed by summer (63.6% , 43.4 ppbv), autumn (63.0% , 56.7 ppbv), and winter (60.4% , 73.1 ppbv). The daily variation of this source was influenced by meteorological parameters such as the BLH ($r = -0.42$, $p < 0.01$) (Table S32). The significant positive correlations between NO₂ and CO and the source contribution were also found with Pearson coefficients being 0.45 and 0.44, respectively (Fig. 12b), indicating that the daily variation of NG source was influenced by ~~metrological~~ meteorological conditions and photochemical activities. The diurnal variation of the NG leakage was significantly correlated ($p < 0.01$) with the source mostly followed the diurnal pattern of ethane, propane and *n*-butanes and *i*-butane with Pearson coefficients being 0.94, 0.87 and 0.91, respectively (Fig. 13b), which was also reported by Baudic et al. (2016). The diurnal behaviors of this source were characterized by a nighttime high and mid-afternoon low pattern, which can be interpreted as the diurnal pattern evolution of BLH development BLH (Bon et al., 2011; Baudic et al., 2016).

3.5.3 Combustion source

~~This source e-combustion source~~ was dominantly weighted by ethylene ($95 \pm 3.5\%$), acetylene ($97 \pm 2.6\%$) and moderately influenced by BTEX. These species are key markers of combustion (Fujita, 2001; Watson et al., 2001; Jobson, 2004) or from petrochemical source (Brocco et al., 1997; Song et al., 2007). However, Known as the independent combustion tracers such as the CO, NO₂, and PM_{2.5} were well correlated to with this source contribution, with Pearson correlation coefficients being of 0.59, 0.49 and 0.77, respectively (Fig. 12c and Table S32). Therefore, this factor was attributed to combustion source. This source e-source contribution of this factor exhibited obvious seasonal differences with highest contribution in winter (14.9% , 18.1 ppbv) and lowest contribution in summer (6.9% , 4.7 ppbv). This seasonal difference was due to the temperature change and was proved by a the significant negative correlation with the ambient temperature ($r = -0.57$, $p < 0.01$). The diurnal variation of combustion source was in accordance with the diurnal pattern of ethylene, acetylene, and CO with Pearson correlation coefficients being -0.71 ($p < 0.05$) and 0.84 ($p < 0.01$), respectively. It was characterized by a double peak profile with an initial increasing from 03:00 to 08:00 LT and a second increasing at nighttime (20:00—024:00 LT) (Fig. 13c). The increase in the morning was related to the low BLH. Different from other researches, no increasing trend of this source was found during 07:00—10:00 LT in this study here, while combustion source was reported to be increasing at the rush-hour period (Gaimoz et al., 2011; Baudic et al., 2016). On the contrary, the decreasing trends were found for independent combustion tracers (CO and NO₂) during this period (Fig. 7a). In another rush-hour of 18:00—20:00 LT, the enhancement of

combustion source contributions and CO from 16:00 LT (Fig. 11c) may be related with the reduction of BLH. The reduction of NO₂ from 18:00 LT (Fig. 7a) were also observed, which indicated that the diurnal variation of combustion source was less affected by vehicle exhaust in ~~this the present~~ study.

3.5.4 Asphalt

Asphalt released predominantly C₈—C₁₁ alkanes including *n*-octane, *n*-nonane, *n*-decane and *n*-undecane, totally contributed to over 50% of VOC emissions from asphalt application (Brown et al., 2007; Liu et al., 2008; Deygout, 2011), with *n*-undecane along accounting for 17% (Liu et al., 2008). Benzene, toluene and xylenes are also enriched for asphalt VOC emissions (Chong et al., 2014). High loadings of C₉—C₁₂ VOCs including *n*-nonane, *n*-decane, *n*-undecane, and *n*-dodecane were found in this factor, averaged as 46%, 64%, 72%, and 85%, respectively. The annual processing capacity of heavy oil in this area was 9.0 × 10⁻⁶ t and the fugitive emission was inevitable. ~~Therefore, this factor was attributed to asphalt.~~

The annual contribution of ~~asphalt this source~~ was the lowest among the five sources and only contributed 1.3 ± 0.69% to the total VOCs. The daily contributions of this source and temperature had a statistically reliable positive correlation ($r = 0.19$, $p < 0.01$). The seasonal variation of this source was influenced by temperature with the highest contributions occurred in autumn (2.1%) and the lowest in winter (0.5%). However, the influence of BLH on ~~this the contribution of asphalt source contribution~~ was not significant ($r = 0.04$, $p > 0.05$). The correlations between this source and O₃ was found insignificant ($r = 0.001$, $p > 0.05$). However, significant positive correlation between ~~asphalt this source~~ and oil refinery source was ~~observed found~~ ($r = 0.47$, $p < 0.01$) (Fig. 12d), indicating they shared the same origin, ~~which should be s~~ (oil refining processes ~~in current study~~). The diurnal variation of ~~asphalt this source~~ was different from ~~the other sources and well followed the diurnal patterns of decane (r = 0.76, p < 0.01) and undecane (r = 0.86, p < 0.01)s~~. It continuously decreased from 2:00 to 6:00 LT, slowly increased from 6:00 to 10:00 LT and subsequently decreased (Fig. 13d). A minimum source contribution occurred when the BLH was low in the morning, which was contrary to the other sources. ~~In addition, no significant correlation between this source and O₃ (r = -0.02, p > 0.05) was found. An increasing for n dodecane from 06:00 to 18:00 LT was observed, implying less impact of photochemical removal and increasing of the BLH.~~ Therefore, the temporal variation of ~~asphalt this source~~ was less controlled by BLH and photochemical reaction, but was more influenced by the emission strength.

3.5.5 Fuel evaporation

The gasoline evaporation profile holds high proportions of *i*-pentane, *trans*-2-pentene, *cis*-2-pentene, benzene, and toluene (Liu et al., 2008; Zhang et al., 2013b). The *i*-pentane is a key tracer of gasoline evaporation due to its high abundance (Gentner et al., 2009; Zhang et al., 2013b). The ratios of *i*-pentane to *n*-pentane is useful to identify the potential sources including NG (0.82—0.89), liquid gasoline (1.5—3.0), fuel evaporation (1.8—4.6), and vehicle emission (2.2—3.8) (Harley et al., 2001; McGaughey et al., 2004; Russo et al., 2010; Gilman et al., 2013). As discussed above, the ratios of *i*-pentane to *n*-pentane indicated a mixed source in this region. From ~~the~~ PMF modeling results, high loadings on *i*-pentane and *n*-pentane

were present in ~~this the~~ factor profile, which accounted for $85 \pm 5.3\%$ and $71 \pm 6.4\%$ of total species, respectively. Additionally, this factor was influenced by hexane ($60 \pm 5.6\%$), cyclohexane ($45 \pm 10\%$), methylcyclohexane ($52 \pm 7.5\%$), benzene ($23 \pm 3.0\%$), and toluene ($19 \pm 4.0\%$), which were related to diesel fuel evaporation (Liu et al., 2008). As shown in Fig. S1, the products of oil refinery included the gasoline and diesel, with the annual productions of 9.5×10^5 t and 1.9×10^5 t, respectively (Chen, 2015). Therefore, this factor represented the fuel evaporation.

The fuel evaporation is ~~fugitive and~~ controlled by temperature, leading to higher contributions in summer. The highest contribution was found in summer (~~as 22.9%~~) in this study. ~~The same~~ results were also observed previously (Baudic et al., 2016; Liu et al., 2016). A significant correlation between the contributions of NG and fuel evaporation was ~~observed found~~ ($r = 0.65$, $p < 0.01$), indicating ~~this two contributions of the two types of~~ sources were influenced by ~~the~~ similar factors. The diurnal distribution pattern of fuel evaporation source was different from former studies in urban area (with an increasing trend from 7:00 to 10:00 LT due to the morning rush ~~hour traffic~~) (Baudic et al., 2016). ~~On the contrary, the source contribution followed the diurnal variations of fuel evaporation tracers such as *i*-pentane, *n*-pentane and methycyclohexane, with Pearson correlation coefficients being 0.86 ($p < 0.01$), 0.87 ($p < 0.01$) and 0.67 ($p < 0.05$), respectively.~~

3.5.6 Contribution to OFP

The contributions of five identified VOC sources to OFP were also evaluated using F matrix and MIR method (~~Eq. 4~~). The fuel evaporation showed ~~the~~ highest contribution (41.9%, 41.6 ppbv), followed by NG (29.6%, 29.4 ppbv), combustion (14.2%, 14.1 ppbv), oil refinery (11.3%, 11.2 ppbv) and asphalt (3.0%, 3.0 ppbv). Therefore, more attention should be paid to ~~the~~ fuel evaporation due to its high ozone formation potential. It should be noted that the source contributions to OFP were calculated by 20 selected VOC species in PMF model ~~analysing~~ and the actual contributions to OFP were higher than the results.

3.6 Source contributions compared with previous studies

The source apportionment results showed that the dominant source in this study was the natural gas source, contributing ~~62.6 ± 3.04%~~ 63% to the total VOCs on the annual average, followed by fuel evaporation ($21.5 \pm 2.992\%$), combustion source ($10.9 \pm 1.574\%$), oil refinery ($3.80 \pm 0.50\%$), and asphalt emission ($1.30 \pm 0.69\%$). Each identified PMF factor exhibited obvious temporal variations due to ~~the~~ emission strength, photochemical reaction and meteorological ~~parameters conditions~~. The source apportionment results in this study were compared with formers based on long- ~~time series term~~ monitoring (Table 2).

The contributors to VOCs in urban areas were complex with at least five different sources, including fuel evaporation, LPG/NG, industrial emission, vehicle emission, and solvent usage (Table 2). While the number of VOC sources apportioned in industrial areas was less compared to the cities. For example, only three sources including vehicle emission (58.3%), solvent usage (22.2%), and industrial activities (19.5%) were apportioned by principle component analysis-multiple linear regression (PCA-MLR) in Lanzhou, a petrochemical industrialized city in northwest China (Jia et al., 2016). Same results ~~were was~~ also found in Houston that only fuel evaporation, industrial emission, and vehicle emission were identified (Leuchner and Rappenglück,

2010). In these studies, the vehicle emission was an important source both in urban and industrial areas and contributed about 11—58.3% to the total VOCs (Table 2). However, the vehicle emission source was not identified in this study due to several reasons. Firstly, despite there was similarity between the source profiles of combustion or fuel evaporation in this study and the vehicle emission (l.e.e.g., high loadings on acetylene, ethylene, BTEX, butanes, and pentanes), the temporal variations of these species did not show a distinct increasing during the traffic rush-hour. In fact, the identified combustion source in this study represented the characteristics of coal burning and torch burning in oil refinery (to eliminate the hazardous gases). Secondly, differences existed in sampling location and vehicle amounts. In previous urban studies, the sampling location was in megacities with huge vehicle flows. For example, in the research of Wuhan (Lyu et al., 2016), the sampling site located in the city center and the car population ownership was 2.2×10^6 in by the end of 2015. While the sampling location in this study here was about 11 km away from the urban areas and the car ownership was only 1.1×10^5 . Therefore, the factor with higher loadings of these species was not likely to be contributed by vehicle emission in this study.

LPG and NG sources are usually apportioned both in urban and industrial areas. These sources contribute 10%—32% to the total VOCs and are mainly from household or industrial fugitive emission. However, in this study, the NG source was mainly from the NG exploitation and NG chemical industry due to its abundance in this area and accounted for $62.6 \pm 3.04\%$ on average to VOCs, —which was higher than many other areas as summarized in Table 2.

Solvent usage also accounts for a large proportion of total VOCs in urban areas (4.7—36.4%). In this study, a similar source related to asphalt was identified with heavy weights on C_9 — C_{12} compounds. The solvent usage in urban areas is usually from painting or coating. However, the asphalt in this study originated from oil refinery (Fig. S1) and fugitive emission from a black oil hill located in at the northwest of the sampling site. Due to its high boiling point, the seasonal contribution of asphalt was distinct with highest contribution in July (7.2%) and lowest contribution in January (1.4%). Despite the source contribution of asphalt was low, it was unique in this study.

3.7 Geographic origins of VOCs sources: local vs. regional contributions

The possible geographic origins of five identified VOC sources were explored by CPF, PSCF and CWT as shown in Fig. 14, Fig. 15 and Fig. 16, respectively. These methods aimed at providing insights on the potential geographic origins of VOCs sources but did not claim to be precise at the cell level or pixel level.

The highest CPF values of oil refinery was found in the east direction of the sampling site (Fig. 14a, 14b and 14d), which indicated the potential location of this source. However, in fact, the oil refineries are mainly located in the southwest of the sampling site (Fig. 1c) and high CPF value (0.95) was also found in southwest direction. Therefore, the CPF results was able to reflect the location of the oil refineries well. Similarly, high probabilities and concentrations of oil refinery were also found from the northeast-southeast to southwest area of the sampling site according to the PSCF (Fig. 15a) and CWT plots (Fig. 16a). As shown in Fig. 1a and 1b, the sampling site is located in the west of the Junggar Basin, which is the second largest oil-gas oil and gas basin of in China. Indeed, high values of CPF, PSCF and CWT were found in the east direction (Fig. 14b,

Fig. 15b and Fig. 16b), which indicated that the potential geographic origins of NG. However, the CPF and PSCF analysis of NG source did not exhibit high probabilities from east direction of the sampling site (Fig. 14b, Fig. 15b), while high CWT values of this source occurred in east direction (Fig. 16b). Given the fact that the NG source was composed by long atmospheric lifetime species (i.e., ethane, propane and butanes), the high probabilities and concentrations of this factor were likely resulted from aged air masses from each direction. The combustion source showed high potentials from ESE to SE directions according to the CPF, PSCF, and CWT plots. There were no high values in the northwest direction of sampling site, where the urban area locates. This also indicated that the combustion from vehicle emission was insignificant in this study. For asphalt source, highest CPF value was found in the east direction while the PSCF and CWT plots showed high values in the northeast direction. As discussed above, the asphalt source in this study were from the natural source (black oil hill in the northwest of sampling site) and oil refinery (southwest direction). The CPF, PSCF, and CWT results indicated that these methods failed to locate the natural source of asphalt. The potential geographic origins of fuel evaporation were widespread from ESE to W directions, which was similar to the oil refinery source.

Differences Diversities of geographic origins were also found in different seasons (Fig. S67–S134). The potential source areas of the five sources spread from northeast to southwest in autumn. In winter, both PSCF and CWT methods indicated that the VOC sources were probably from the southeast and southwest. In spring, VOCs were mainly from long-range transport from west. However, high probabilities and contributions existed around the sampling site. In summer, high potentials and contributions were from the west to the southeast direction. Overall, the five sources exhibited different local source areas proved by the CPF plots on the annual scale. Similar regional distributions of these sources were found on the seasonal scale. To quantify the contributions of local emission and long-range transport to the sampling site, raster analysis based on CWT was used and the results are summarized in Table 3. Annually, except for the combustion source, the identified VOC sources were mainly from the local emission, with contributions of 53.6% for oil refining, 54.5% for NG, 50.5% for asphalt and 50.6% for fuel evaporation, respectively. The seasonal patterns were same with the annual pattern, exhibiting higher contributions from local contributions areas and the differences only existed in the proportions. The highest local contributions of oil refining (69.4%) and combustion (69.2%) were observed in summer, while the local sources contributed most to the NG (74.6%), asphalt (65.4%) and fuel evaporation (68.3%) in autumn.

4 Conclusions Summary

Based on one-year continuously online monitoring of VOCs in an oil-gas field, and on the use of PMF receptor model, back trajectory, PSCF, and CWT dispersion models, this study allowed for (i) compared the comparison of the VOC levels and compositions with other studies, (ii) the temporal variation of the total VOCs at different time scale (seasonal, monthly and diurnal), identify (iii) the VOCs source apportionment of VOCs, and (iv) the exploration of explored the potential geographic origins of five identified VOC sources. The main findings are summarized as follows:

1. The total VOC concentrations in this study were not only higher than those in urban areas, but also higher than those measured in petrochemical areas. Alkanes contributed most to the total ~~The VOCs compositions in this study were similar to those observed in petrochemical areas such as Uintah Basin and Northeast Colorado, with the alkanes contributed most (accounting for 87.5% and; 128 ± 82.4 ppbv on average) to the total VOCs,~~ followed by alkenes (6.81% and; 9.1 ± 5.6 ppbv), aromatic hydrocarbons (3.37% and; 4.8 ± 6.5 ppbv), and acetylene (2.32% and; 3.1 ± 5.1 ppbv).

~~2. The monthly and daily variations of the total VOCs were influenced by meteorological conditions and photochemical reactions while the diurnal pattern of VOCs was more impacted by boundary layer height.~~

~~3.2.~~ Five sources with local characteristics were identified. The NG contributed most to the VOCs (62.6 ± 3.04 %), followed by fuel evaporation (21.5 ± 2.99 %), combustion source (10.9 ± 1.57 %), oil refining (3.80 ± 0.50 %), and asphalt (1.30 ± 0.69 %).

The NG and fuel evaporation source contributions showed positive correlation with each other and shared the same diurnal variation pattern, exhibiting a single peak profile. The diurnal pattern variation of oil refining and combustion source exhibited similar double wave with peaks occurred 06:00–08:00 LT. Different from other sources, the diurnal profile of asphalt exhibited a decreasing trend from nighttime to its minimum before sunrise (06:00 LT).

~~4.3.~~ The geographic origins of five VOC sources were the same during the whole period. The differences existed in the seasonal variations of them. For instance, VOCs were mainly from northeast and southwest in autumn, while ~~it~~they originated from southeast and southwest in winter. The raster analysis indicated that the VOCs in this study were mainly from local emission with contributions ~~ranged~~ ranging from 48.4% to 74.6% in different seasons.

In summary, this study found that the VOC concentrations, compositions, ozone formation potential, and sources were different from ~~other~~ those in urban and industrial areas and similar to ~~oil-gas~~ oil-gas rich areas. It will be helpful for the VOCs control in these type of regions around the world.

Data availability

The VOC concentrations during the whole sampling period are available on request from Shaofei Kong (kongshaofei@cug.edu.cn).

Acknowledgements. This study was financially supported by the Key Program of Ministry of Science and Technology of the People's Republic of China (2016YFA0602002; 2017YFC0212602). The research was also supported by the Fundamental Research Funds for the Central Universities, China University of Geosciences, Wuhan. The authors are grateful to the local Environmental Monitoring Center Station for their sampling works ~~in sampling campaign~~. We thank Qingyue Open Environmental Data Center (<https://data.epmap.org>) for providing air quality data.

Reference

- An, J., Zhu, B., Wang, H., Li, Y., Lin, X. and Yang, H.: Characteristics and source apportionment of VOCs measured in an industrial area of Nanjing, Yangtze River Delta, China, *Atmos. Environ.*, 97, 206–214, doi:10.1016/j.atmosenv.2014.08.021, 2014.
- 5 Atkinson, R. and Arey, J.: Atmospheric Degradation of Volatile Organic Compounds, *Chem. Rev.*, 103(12), 4605–4638, doi:10.1021/cr0206420, 2003.
- [Baker, A. K., Beyersdorf, A. J., Doezema, L. A., Katzenstein, A., Meinardi, S., Simpson, I. J., Blake, D. R. and Sherwood Rowland, F.: Measurements of nonmethane hydrocarbons in 28 United States cities, *Atmos. Environ.*, 42\(1\), 170–182, doi:10.1016/j.atmosenv.2007.09.007, 2008.](#)
- 10 Baltrėnas, P., Baltrėnaitė, E., Šerevičienė, V. and Pereira, P.: Atmospheric BTEX concentrations in the vicinity of the crude oil refinery of the Baltic region, *Environ. Monit. Assess.*, 182(1–4), 115–127, doi:10.1007/s10661-010-1862-0, 2011.
- Bari, A., Dutkiewicz, V. A., Judd, C. D., Wilson, L. R., Luttinger, D. and Husain, L.: Regional sources of particulate sulfate, SO₂, PM_{2.5}, HCl, and HNO₃, in New York, NY, *Atmos. Environ.*, 37(20), 2837–2844, doi:10.1016/S1352-2310(03)00200-0, 2003.
- 15 Bari, M. A., Kindzierski, W. B. and Spink, D.: Twelve-year trends in ambient concentrations of volatile organic compounds in a community of the Alberta Oil Sands Region, Canada, *Environ. Int.*, 91, 40–50, doi:10.1016/j.envint.2016.02.015, 2016.
- Baudic, A., Gros, V., Sauvage, S., Locoge, N., Sanchez, O., Sarda-Estève, R., Kalogridis, C., Petit, J.-E., Bonnaire, N., Baisné, D., Favez, O., Albinet, A., Sciare, J. and Bonsang, B.: Seasonal variability and source apportionment of volatile organic compounds (VOCs) in the Paris megacity (France), *Atmos. Chem. Phys.*, 16(18), 11961–11989, doi:10.5194/acp-16-11961-2016, 2016.
- 20 Bon, D. M., Ulbrich, I. M., de Gouw, J. A., Warneke, C., Kuster, W. C., Alexander, M. L., Baker, A., Beyersdorf, A. J., Blake, D., Fall, R., Jimenez, J. L., Herndon, S. C., Huey, L. G., Knighton, W. B., Ortega, J., Springston, S. and Vargas, O.: Measurements of volatile organic compounds at a suburban ground site (T1) in Mexico City during the MILAGRO 2006 campaign: measurement comparison, emission ratios, and source attribution, *Atmos. Chem. Phys.*, 11(6), 2399–2421, doi:10.5194/acp-11-2399-2011, 2011.
- 25 Bressi, M., Sciare, J., Ghersi, V., Mihalopoulos, N., Petit, J.-E., Nicolas, J. B., Moukhtar, S., Rosso, A., Féron, A., Bonnaire, N., Poulakis, E. and Theodosi, C.: Sources and geographical origins of fine aerosols in Paris (France), *Atmos. Chem. Phys.*, 14(16), 8813–8839, doi:10.5194/acp-14-8813-2014, 2014.
- 30 [Brocco, D., Fratarcangeli, R., Lepore, L., Petricca, M. and Ventrone, I.: Determination of aromatic hydrocarbons in urban air of Rome, *Atmos. Environ.*, 31\(4\), 557–566, doi:10.1016/S1352-2310\(96\)00226-9, 1997.](#)

- Brown, S. G., Frankel, A. and Hafner, H. R.: Source apportionment of VOCs in the Los Angeles area using positive matrix factorization, *Atmos. Environ.*, 41(2), 227–237, doi:10.1016/j.atmosenv.2006.08.021, 2007.
- Buzcu, B. and Fraser, M. P.: Source identification and apportionment of volatile organic compounds in Houston, TX, *Atmos. Environ.*, 40(13), 2385–2400, doi:10.1016/j.atmosenv.2005.12.020, 2006.
- 5 Buzcu-Guven, B. and Fraser, M. P.: Comparison of VOC emissions inventory data with source apportionment results for Houston, TX, *Atmos. Environ.*, 42(20), 5032–5043, doi:10.1016/j.atmosenv.2008.02.025, 2008.
- Cai, C., Geng, F., Tie, X., Yu, Q. and An, J.: Characteristics and source apportionment of VOCs measured in Shanghai, China, *Atmos. Environ.*, 44(38), 5005–5014, doi:10.1016/j.atmosenv.2010.07.059, 2010.
- Callén, M. S., Iturmendi, A. and López, J. M.: Source apportionment of atmospheric PM_{2.5}-bound polycyclic aromatic hydrocarbons by a PMF receptor model. Assessment of potential risk for human health, *Environ. Pollut.*, 195, 167–177, doi:10.1016/j.envpol.2014.08.025, 2014.
- Carter, W. P. L.: Development of Ozone Reactivity Scales for Volatile Organic Compounds, *Air Waste*, 44(7), 881–899, doi:10.1080/1073161X.1994.10467290, 1994.
- 15 Cetin, E., Odabasi, M. and Seyfioglu, R.: Ambient volatile organic compound (VOC) concentrations around a petrochemical complex and a petroleum refinery, *Sci. Total Environ.*, 312(1), 103–112, doi:10.1016/S0048-9697(03)00197-9, 2003.
- Chan, Y., Hawas, O., Hawker, D., Vowles, P., Cohen, D. D., Stelcer, E., Simpson, R., Golding, G. and Christensen, E.: Using multiple type composition data and wind data in PMF analysis to apportion and locate sources of air pollutants, *Atmos. Environ.*, 45(2), 439–449, doi:10.1016/j.atmosenv.2010.09.060, 2011.
- 20 Chen, Y.-C., Chiang, H.-C., Hsu, C.-Y., Yang, T.-T., Lin, T.-Y., Chen, M.-J., Chen, N.-T. and Wu, Y.-S.: Ambient PM_{2.5}-bound polycyclic aromatic hydrocarbons (PAHs) in Changhua County, central Taiwan: Seasonal variation, source apportionment and cancer risk assessment, *Environ. Pollut.*, 218, 372–382, doi:10.1016/j.envpol.2016.07.016, 2016.
- Cheng, H., Guo, H., Saunders, S. M., Lam, S. H. M., Jiang, F., Wang, X., Simpson, I. J., Blake, D. R., Louie, P. K. K. and Wang, T. J.: Assessing photochemical ozone formation in the Pearl River Delta with a photochemical trajectory model, *Atmos. Environ.*, 44(34), 4199–4208, doi:10.1016/j.atmosenv.2010.07.019, 2010.
- 25 Cheng, I., Zhang, L., Blanchard, P., Dalziel, J. and Tordon, R.: Concentration-weighted trajectory approach to identifying potential sources of speciated atmospheric mercury at an urban coastal site in Nova Scotia, Canada, *Atmos. Chem. Phys.*, 13(12), 6031–6048, doi:10.5194/acp-13-6031-2013, 2013.
- Chong, D., Wang, Y., Guo, H. and Lu, Y.: Volatile Organic Compounds Generated in Asphalt Pavement Construction and Their Health Effects on Workers, *J. Constr. Eng. Manag.*, 140(2), 4013051, doi:10.1061/(ASCE)CO.1943-7862.0000801, 2014.
- 30 Colman Lerner, J. E., Sanchez, E. Y., Sambeth, J. E. and Porta, A. A.: Characterization and health risk assessment of VOCs in occupational environments in Buenos Aires, Argentina, *Atmos. Environ.*, 55, 440–447, doi:10.1016/j.atmosenv.2012.03.041, 2012.

- Conner, T. L., Lonneman, W. A. and Seila, R. L.: Transportation-Related Volatile Hydrocarbon Source Profiles Measured in Atlanta, *J. Air Waste Manag. Assoc.*, 45(5), 383–394, doi:10.1080/10473289.1995.10467370, 1995.
- Deygout, F.: Volatile emissions from hot bitumen storage tanks, *Environ. Prog. Sustain. Energy*, 30(1), 102–112, doi:10.1002/ep.10444, 2011.
- 5 Dumanoglu, Y., Kara, M., Altiok, H., Odabasi, M., Elbir, T. and Bayram, A.: Spatial and seasonal variation and source apportionment of volatile organic compounds (VOCs) in a heavily industrialized region, *Atmos. Environ.*, 98, 168–178, doi:10.1016/j.atmosenv.2014.08.048, 2014.
- [Dunlea, E. J., Herndon, S. C., Nelson, D. D., Volkamer, R. M., San Martini, F., Sheehy, P. M., Zahniser, M. S., Shorter, J. H., Wormhoudt, J. C., Lamb, B. K., Allwine, E. J., Gaffney, J. S., Marley, N. A., Grutter, M., Marquez, C., Blanco, S., Cardenas, B., Retama, A., Ramos Villegas, C. R., Kolb, C. E., Molina, L. T. and Molina, M. J.: Evaluation of nitrogen dioxide chemiluminescence monitors in a polluted urban environment, *Atmos. Chem. Phys.*, 7\(10\), 2691–2704, doi:10.5194/acp-7-2691-2007, 2007.](#)
- 10
- Durana, N., Navazo, M., G óñez, M. C., Alonso, L., Garc á, J. A., Ilardia, J. L., Gangoiti, G. and Iza, J.: Long term hourly measurement of 62 non-methane hydrocarbons in an urban area: Main results and contribution of non-traffic sources, *Atmos. Environ.*, 40(16), 2860–2872, doi:10.1016/j.atmosenv.2006.01.005, 2006.
- 15
- Fujita, E. M.: Hydrocarbon source apportionment for the 1996 Paso del Norte Ozone Study, *Sci. Total Environ.*, 276(1–3), 171–184, doi:10.1016/S0048-9697(01)00778-1, 2001.
- Gaimoz, C., Sauvage, S., Gros, V., Herrmann, F., Williams, J., Locoge, N., Perrussel, O., Bonsang, B., d’Argouges, O., Sarda-Est ève, R. and Sciare, J.: Volatile organic compounds sources in Paris in spring 2007. Part II: source apportionment using positive matrix factorisation, *Environ. Chem.*, 8(1), 91, doi:10.1071/EN10067, 2011.
- 20
- [Garz ón, J. P., Huertas, J. I., Magaña, M., Huertas, M. E., C árdenas, B., Watanabe, T., Maeda, T., Wakamatsu, S. and Blanco, S.: Volatile organic compounds in the atmosphere of Mexico City, *Atmos. Environ.*, 119, 415–429, doi:10.1016/j.atmosenv.2015.08.014, 2015.](#)
- Geng, F., Tie, X., Xu, J., Zhou, G., Peng, L., Gao, W., Tang, X. and Zhao, C.: Characterizations of ozone, NO_x, and VOCs measured in Shanghai, China, *Atmos. Environ.*, 42(29), 6873–6883, doi:10.1016/j.atmosenv.2008.05.045, 2008.
- 25
- Gentner, D. R., Harley, R. A., Miller, A. M. and Goldstein, A. H.: Diurnal and Seasonal Variability of Gasoline-Related Volatile Organic Compound Emissions in Riverside, California, *Environ. Sci. Technol.*, 43(12), 4247–4252, doi:10.1021/es9006228, 2009.
- Gilman, J. B., Burkhardt, J. F., Lerner, B. M., Williams, E. J., Kuster, W. C., Goldan, P. D., Murphy, P. C., Warneke, C., Fowler, C., Montzka, S. A., Miller, B. R., Miller, L., Oltmans, S. J., Ryerson, T. B., Cooper, O. R., Stohl, A. and de Gouw, J. A.: Ozone variability and halogen oxidation within the Arctic and sub-Arctic springtime boundary layer, *Atmos. Chem. Phys.*, 10(21), 10223–10236, doi:10.5194/acp-10-10223-2010, 2010.
- 30

- Gilman, J. B., Lerner, B. M., Kuster, W. C. and de Gouw, J. A.: Source Signature of Volatile Organic Compounds from Oil and Natural Gas Operations in Northeastern Colorado, *Environ. Sci. Technol.*, 47(3), 1297–1305, doi:10.1021/es304119a, 2013.
- 5 Guo, H., Wang, T. and Louie, P. K. K.: Source apportionment of ambient non-methane hydrocarbons in Hong Kong: Application of a principal component analysis/absolute principal component scores (PCA/APCS) receptor model, *Environ. Pollut.*, 129(3), 489–498, doi:10.1016/j.envpol.2003.11.006, 2004.
- Guo, H., Zou, S. C., Tsai, W. Y., Chan, L. Y. and Blake, D. R.: Emission characteristics of nonmethane hydrocarbons from private cars and taxis at different driving speeds in Hong Kong, *Atmos. Environ.*, 45(16), 2711–2721, doi:10.1016/j.atmosenv.2011.02.053, 2011.
- 10 Harley, R. A., McKeen, S. A., Pearson, J., Rodgers, M. O. and Lonneman, W. A.: Analysis of motor vehicle emissions during the Nashville/Middle Tennessee Ozone Study, *J. Geophys. Res. Atmos.*, 106(D4), 3559–3567, doi:10.1029/2000JD900677, 2001.
- He, Z., Li, G., Chen, J., Huang, Y., An, T. and Zhang, C.: Pollution characteristics and health risk assessment of volatile organic compounds emitted from different plastic solid waste recycling workshops, *Environ. Int.*, 77, 85–94, doi:10.1016/j.envint.2015.01.004, 2015.
- 15 Helmig, D., Thompson, C. R., Evans, J., Boylan, P., Hueber, J. and Park, J.-H.: Highly Elevated Atmospheric Levels of Volatile Organic Compounds in the Uintah Basin, Utah, *Environ. Sci. Technol.*, 48(9), 4707–4715, doi:10.1021/es405046r, 2014.
- Ho, K. F., Lee, S. C., Guo, H. and Tsai, W. Y.: Seasonal and diurnal variations of volatile organic compounds (VOCs) in the atmosphere of Hong Kong, *Sci. Total Environ.*, 322(1–3), 155–166, doi:10.1016/j.scitotenv.2003.10.004, 2004.
- 20 Hoque, R. R., Khillare, P. S., Agarwal, T., Shridhar, V. and Balachandran, S.: Spatial and temporal variation of BTEX in the urban atmosphere of Delhi, India, *Sci. Total Environ.*, 392(1), 30–40, doi:10.1016/j.scitotenv.2007.08.036, 2008.
- Hsieh, L., Yang, H. and Chen, H.: Ambient BTEX and MTBE in the neighborhoods of different industrial parks in Southern Taiwan, *J. Hazard. Mater.*, 128(2–3), 106–115, doi:10.1016/j.jhazmat.2005.08.001, 2006.
- 25 Jia, C., Mao, X., Huang, T., Liang, X., Wang, Y., Shen, Y., Jiang, W., Wang, H., Bai, Z., Ma, M., Yu, Z., Ma, J. and Gao, H.: Non-methane hydrocarbons (NMHCs) and their contribution to ozone formation potential in a petrochemical industrialized city, Northwest China, *Atmos. Res.*, 169, 225–236, doi:10.1016/j.atmosres.2015.10.006, 2016.
- Jobson, B. T.: Hydrocarbon source signatures in Houston, Texas: Influence of the petrochemical industry, *J. Geophys. Res.*, 109(D24), doi:10.1029/2004JD004887, 2004.
- 30 Leuchner, M. and Rappenglück, B.: VOC source–receptor relationships in Houston during TexAQS-II, *Atmos. Environ.*, 44(33), 4056–4067, doi:10.1016/j.atmosenv.2009.02.029, 2010.
- Li, L., Xie, S., Zeng, L., Wu, R. and Li, J.: Characteristics of volatile organic compounds and their role in ground-level ozone formation in the Beijing-Tianjin-Hebei region, China, *Atmos. Environ.*, 113, 247–254, doi:10.1016/j.atmosenv.2015.05.021, 2015.

- Li, L., An, J. Y., Shi, Y. Y., Zhou, M., Yan, R. S., Huang, C., Wang, H. L., Lou, S. R., Wang, Q., Lu, Q. and Wu, J.: Source apportionment of surface ozone in the Yangtze River Delta, China in the summer of 2013, *Atmos. Environ.*, 144, 194–207, doi:10.1016/j.atmosenv.2016.08.076, 2016.
- Lin, T., Sree, U., Tseng, C., Chiu, K., Wu, C. and Lo, J.: Volatile organic compound concentrations in ambient air of Kaohsiung petroleum refinery in Taiwan, *Atmos. Environ.*, 38(25), 4111–4122, doi:10.1016/j.atmosenv.2004.04.025, 2004.
- Ling, Z., Guo, H., Cheng, H. and Yu, Y. F.: Sources of ambient volatile organic compounds and their contributions to photochemical ozone formation at a site in the Pearl River Delta, southern China, *Environ. Pollut.*, 159(10), 2310–2319, doi:10.1016/j.envpol.2011.05.001, 2011.
- Liu, B., Liang, D., Yang, J., Dai, Q., Bi, X., Feng, Y., Yuan, J., Xiao, Z., Zhang, Y. and Xu, H.: Characterization and source apportionment of volatile organic compounds based on 1-year of observational data in Tianjin, China, *Environ. Pollut.*, 218, 757–769, doi:10.1016/j.envpol.2016.07.072, 2016.
- ~~Liu, P., Yao, Y., Tsai, J., Hsu, Y., Chang, L. and Chang, K.: Source impacts by volatile organic compounds in an industrial city of southern Taiwan, *Sci. Total Environ.*, 398(1–3), 154–163, doi:10.1016/j.scitotenv.2008.02.053, 2008a.~~
- Liu, Y., Shao, M., Fu, L., Lu, S., Zeng, L. and Tang, D.: Source profiles of volatile organic compounds (VOCs) measured in China: Part I, *Atmos. Environ.*, 42(25), 6247–6260, doi:10.1016/j.atmosenv.2008.01.070, 2008b.
- Lyu, X., Chen, N., Guo, H., Zhang, W., Wang, N., Wang, Y. and Liu, M.: Ambient volatile organic compounds and their effect on ozone production in Wuhan, central China, *Sci. Total Environ.*, 541, 200–209, doi:10.1016/j.scitotenv.2015.09.093, 2016.
- ~~Maré, M., Bielawska, M., Wardeneki, W., Namieśnik, J. and Zabiegała, B.: The influence of meteorological conditions and anthropogenic activities on the seasonal fluctuations of BTEX in the urban air of the Hanseatic city of Gdansk, Poland, *Environ. Sci. Pollut. Res.*, 22(15), 11940–11954, doi:10.1007/s11356-015-4484-9, 2015.~~
- ~~Marčiulaitienė, E., Šerevičienė, V., Baltrėnas, P. and Baltrėnaitė, E.: The characteristics of BTEX concentration in various types of environment in the Baltic Sea Region, Lithuania, *Environ. Sci. Pollut. Res.*, 24(4), 4162–4173, doi:10.1007/s11356-016-8204-x, 2017.~~
- McCarthy, M. C., Aklilu, Y.-A., Brown, S. G. and Lyder, D. A.: Source apportionment of volatile organic compounds measured in Edmonton, Alberta, *Atmos. Environ.*, 81, 504–516, doi:10.1016/j.atmosenv.2013.09.016, 2013.
- McGaughey, G. R., Desai, N. R., Allen, D. T., Seila, R. L., Lonneman, W. A., Fraser, M. P., Harley, R. A., Pollack, A. K., Ivy, J. M. and Price, J. H.: Analysis of motor vehicle emissions in a Houston tunnel during the Texas Air Quality Study 2000, *Atmos. Environ.*, 38(20), 3363–3372, doi:10.1016/j.atmosenv.2004.03.006, 2004.
- Miller, L., Xu, X., Grgicak-Mannion, A., Brook, J. and Wheeler, A.: Multi-season, multi-year concentrations and correlations amongst the BTEX group of VOCs in an urbanized industrial city, *Atmos. Environ.*, 61, 305–315, doi:10.1016/j.atmosenv.2012.07.041, 2012.

- Mo, Z., Shao, M., Lu, S., Qu, H., Zhou, M., Sun, J. and Gou, B.: Process-specific emission characteristics of volatile organic compounds (VOCs) from petrochemical facilities in the Yangtze River Delta, China, *Sci. Total Environ.*, 533, 422–431, doi:10.1016/j.scitotenv.2015.06.089, 2015.
- Mo, Z., Shao, M., Lu, S., Niu, H., Zhou, M. and Sun, J.: Characterization of non-methane hydrocarbons and their sources in an industrialized coastal city, Yangtze River Delta, China, *Sci. Total Environ.*, 593–594, 641–653, doi:10.1016/j.scitotenv.2017.03.123, 2017.
- Monod, A., Sive, B. C., Avino, P., Chen, T., Blake, D. R. and Sherwood Rowland, F.: Monoaromatic compounds in ambient air of various cities: a focus on correlations between the xylenes and ethylbenzene, *Atmos. Environ.*, 35(1), 135–149, doi:10.1016/S1352-2310(00)00274-0, 2001.
- Na, K. and Kim, Y.: Seasonal characteristics of ambient volatile organic compounds in Seoul, Korea, *Atmos. Environ.*, 35, 2603–2614, doi:10.1016/S1352-2310(00)00464-7, 2001.
- Péron, G., Frost, G., Miller, B. R., Hirsch, A. I., Montzka, S. A., Karion, A., Trainer, M., Sweeney, C., Andrews, A. E., Miller, L., Kofler, J., Bar-Ilan, A., Dlugokencky, E. J., Patrick, L., Moore, C. T., Ryerson, T. B., Siso, C., Kolodzey, W., Lang, P. M., Conway, T., Novelli, P., Masarie, K., Hall, B., Guenther, D., Kitzis, D., Miller, J., Welsh, D., Wolfe, D., Neff, W. and Tans, P.: Hydrocarbon emissions characterization in the Colorado Front Range: A pilot study, *J. Geophys. Res. Atmos.*, 117(D4), doi:10.1029/2011JD016360, 2012.
- Qin, Y., Walk, T., Gary, R., Yao, X. and Elles, S.: C₂–C₁₀ nonmethane hydrocarbons measured in Dallas, USA—Seasonal trends and diurnal characteristics, *Atmos. Environ.*, 41(28), 6018–6032, doi:10.1016/j.atmosenv.2007.03.008, 2007.
- Ran, L., Zhao, C., Geng, F., Tie, X., Tang, X., Peng, L., Zhou, G., Yu, Q., Xu, J. and Guenther, A.: Ozone photochemical production in urban Shanghai, China: Analysis based on ground level observations, *J. Geophys. Res.*, 114(D15), doi:10.1029/2008JD010752, 2009.
- Rodolfo Sosa, E., Humberto Bravo, A., Violeta Mugica, A., Pablo Sanchez, A., Emma Bueno, L. and Krupa, S.: Levels and source apportionment of volatile organic compounds in southwestern area of Mexico City, *Environ. Pollut.*, 157(3), 1038–1044, doi:10.1016/j.envpol.2008.09.051, 2009.
- Russo, R. S., Zhou, Y., White, M. L., Mao, H., Talbot, R. and Sive, B. C.: Multi-year (2004-2008) record of nonmethane hydrocarbons and halocarbons in New England: seasonal variations and regional sources, *Atmos. Chem. Phys.*, 10(10), 4909–4929, doi:10.5194/acp-10-4909-2010, 2010.
- Rutter, A. P., Griffin, R. J., Cevik, B. K., Shakya, K. M., Gong, L., Kim, S., Flynn, J. H. and Lefer, B. L.: Sources of air pollution in a region of oil and gas exploration downwind of a large city, *Atmos. Environ.*, 120, 89–99, doi:10.1016/j.atmosenv.2015.08.073, 2015.
- Shao, P., An, J., Xin, J., Wu, F., Wang, J., Ji, D. and Wang, Y.: Source apportionment of VOCs and the contribution to photochemical ozone formation during summer in the typical industrial area in the Yangtze River Delta, China, *Atmos. Res.*, 176–177, 64–74, doi:10.1016/j.atmosres.2016.02.015, 2016.

- Simpson, I. J., Blake, N. J., Barletta, B., Diskin, G. S., Fuelberg, H. E., Gorham, K., Huey, L. G., Meinardi, S., Rowland, F. S., Vay, S. A., Weinheimer, A. J., Yang, M. and Blake, D. R.: Characterization of trace gases measured over Alberta oil sands mining operations: 76 speciated C₂–C₁₀ volatile organic compounds (VOCs), CO₂, CH₄, CO, NO, NO₂, NO_y, O₃ and SO₂, *Atmos. Chem. Phys.*, 10(23), 11931–11954, doi:10.5194/acp-10-11931-2010, 2010.
- 5 Song, Y., Shao, M., Liu, Y., Lu, S., Kuster, W., Goldan, P. and Xie, S.: Source Apportionment of Ambient Volatile Organic Compounds in Beijing, *Environ. Sci. Technol.*, 41(12), 4348–4353, doi:10.1021/es0625982, 2007.
- Squizzato, S. and Masiol, M.: Application of meteorology-based methods to determine local and external contributions to particulate matter pollution: A case study in Venice (Italy), *Atmos. Environ.*, 119, 69–81, doi:10.1016/j.atmosenv.2015.08.026, 2015.
- 10 Tang, J., Chan, L., Chan, C., Li, Y., Chang, C., Liu, S., Wu, D. and Li, Y.: Characteristics and diurnal variations of NMHCs at urban, suburban, and rural sites in the Pearl River Delta and a remote site in South China, *Atmos. Environ.*, 41(38), 8620–8632, doi:10.1016/j.atmosenv.2007.07.029, 2007.
- US EPA: Positive Matrix Factorization Model for environmental data analyses, [online] Available from: <https://www.epa.gov/air-research/positive-matrix-factorization-model-environmental-data-analyses> (Accessed 20
- 15 September 2016), 2014.
- Vega, E., Sánchez-Reyna, G., Mora-Perdomo, V., Iglesias, G. S., Arriaga, J. L., Limón-Sánchez, T., Escalona-Segura, S. and Gonzalez-Avalos, E.: Air quality assessment in a highly industrialized area of Mexico: Concentrations and sources of volatile organic compounds, *Fuel*, 90(12), 3509–3520, doi:10.1016/j.fuel.2011.03.050, 2011.
- Wang, B., Shao, M., Lu, S., Yuan, B., Zhao, Y., Wang, M., Zhang, S. and Wu, D.: Variation of ambient non-methane
- 20 hydrocarbons in Beijing city in summer 2008, *Atmos. Chem. Phys.*, 10(13), 5911–5923, doi:10.5194/acp-10-5911-2010, 2010.
- Wang, H.: Source Profiles and Chemical Reactivity of Volatile Organic Compounds from Solvent Use in Shanghai, China, *Aerosol Air Qual. Res.*, doi:10.4209/aaqr.2013.03.0064, 2014.
- Wang, L., Liu, Z., Sun, Y., Ji, D. and Wang, Y.: Long-range transport and regional sources of PM_{2.5} in Beijing based on
- 25 long-term observations from 2005 to 2010, *Atmos. Res.*, 157, 37–48, doi:10.1016/j.atmosres.2014.12.003, 2015.
- Wang, Q., Liu, M., Yu, Y. and Li, Y.: Characterization and source apportionment of PM_{2.5}-bound polycyclic aromatic hydrocarbons from Shanghai city, China, *Environ. Pollut.*, 218, 118–128, doi:10.1016/j.envpol.2016.08.037, 2016.
- Wang, Y., Zhang, X. and Draxler, R. R.: TrajStat: GIS-based software that uses various trajectory statistical analysis methods to identify potential sources from long-term air pollution measurement data, *Environ. Model. Softw.*, 24(8),
- 30 938–939, doi:10.1016/j.envsoft.2009.01.004, 2009.
- Warneke, C., Geiger, F., Edwards, P. M., Dube, W., Páron, G., Kofler, J., Zahn, A., Brown, S. S., Graus, M., Gilman, J. B., Lerner, B. M., Peischl, J., Ryerson, T. B., de Gouw, J. A. and Roberts, J. M.: Volatile organic compound emissions from the oil and natural gas industry in the Uintah Basin, Utah: oil and gas well pad emissions compared to ambient air composition, *Atmos Chem Phys*, 14(20), 10977–10988, doi:10.5194/acp-14-10977-2014, 2014.

- Watson, J. G., Chow, J. C. and Fujita, E. M.: Review of volatile organic compound source apportionment by chemical mass balance, *Atmos. Environ.*, 35(9), 1567–1584, doi:10.1016/S1352-2310(00)00461-1, 2001.
- Wei, W., Lv, Z., Cheng, S., Wang, L., Ji, D., Zhou, Y., Han, L. and Wang, L.: Characterizing ozone pollution in a petrochemical industrial area in Beijing, China: a case study using a chemical reaction model, *Environ. Monit. Assess.*, 187(6), 377, doi:10.1007/s10661-015-4620-5, 2015.
- 5 Xiao, Y., Logan, J. A., Jacob, D. J., Hudman, R. C., Yantosca, R. and Blake, D. R.: Global budget of ethane and regional constraints on U.S. sources, *J. Geophys. Res.*, 113(D21), doi:10.1029/2007JD009415, 2008.
- [Yu, C. H., Zhu, X. and Fan, Z.: Spatial/Temporal Variations and Source Apportionment of VOCs Monitored at Community Scale in an Urban Area. edited by Y. Zhang, PLoS ONE, 9\(4\), e95734, doi:10.1371/journal.pone.0095734, 2014.](#)
- 10 Yuan, B., Shao, M., Lu, S. and Wang, B.: Source profiles of volatile organic compounds associated with solvent use in Beijing, China, *Atmos. Environ.*, 44(15), 1919–1926, doi:10.1016/j.atmosenv.2010.02.014, 2010.
- Zhang, R., Jing, J., Tao, J., Hsu, S.-C., Wang, G., Cao, J., Lee, C. S. L., Zhu, L., Chen, Z., Zhao, Y. and Shen, Z.: Chemical characterization and source apportionment of PM_{2.5} in Beijing: seasonal perspective, *Atmos. Chem. Phys.*, 13(14), 7053–7074, doi:10.5194/acp-13-7053-2013, 2013a.
- 15 Zhang, Y., Wang, X., Zhang, Z., Lü S., Shao, M., Lee, F. S. C. and Yu, J.: Species profiles and normalized reactivity of volatile organic compounds from gasoline evaporation in China, *Atmos. Environ.*, 79, 110–118, doi:10.1016/j.atmosenv.2013.06.029, 2013b.
- Zhao, M., Huang, Z., Qiao, T., Zhang, Y., Xiu, G. and Yu, J.: Chemical characterization, the transport pathways and potential sources of PM_{2.5} in Shanghai: Seasonal variations, *Atmos. Res.*, 158–159, 66–78, doi:10.1016/j.atmosres.2015.02.003, 2015.
- 20 Zou, Y., Deng, X. J., Zhu, D., Gong, D. C., Wang, H., Li, F., Tan, H. B., Deng, T., Mai, B. R., Liu, X. T. and Wang, B. G.: Characteristics of 1 year of observational data of VOCs, NO_x and O₃ at a suburban site in Guangzhou, China, *Atmos. Chem. Phys.*, 15(12), 6625–6636, doi:10.5194/acp-15-6625-2015, 2015.

Table 1. Concentrations (mean \pm standard deviation) during the sampling period and the photochemical properties of VOCs during the sampling period.

Species	r^2 ^a	MDL _b	MIR ^{ac}	$\frac{k_{OH}}{k_{OH}^{ref}}$ ($\times 10^{12}$) ^{dh}	ppbv	ppbC
Alkanes					129 \pm 173	387 \pm 439
Ethane ^{ee}	0.997	0.05	0.25	0.25	39.7 \pm 57.3	53.2 \pm 76.7
Propane	0.999	0.021	0.48	1.09	22.6 \pm 33.5	44.5 \pm 65.7
<i>i</i>-Butane	0.994	0.012	1.21	2.12	12.5 \pm 17.5	32.3 \pm 45.2
<i>n</i>-Butane	0.994	0.03	1.02	2.36	15.8 \pm 21.4	40.8 \pm 55.5
Cyclopentane	0.997	0.026	2.4	4.97	8.64 \pm 16.0	26.7 \pm 50.1
<i>i</i>-Pentane	0.998	0.012	1.38	3.6	8.96 \pm 13.3	28.8 \pm 42.7
<i>n</i>-Pentane	0.984	0.026	1.04	3.94	8.81 \pm 12.4	28.3 \pm 39.7
2,2-Dimethylbutane	0.998	0.007	0.82	2.23	0.24 \pm 0.60	0.92 \pm 2.30
2,3-Dimethylbutane	0.999	0.005	1.07	5.78	1.81 \pm 2.91	6.94 \pm 11.2
2-Methylpentane	0.984	0.005	1.5	5.2	3.36 \pm 5.96	12.9 \pm 22.9
3-Methylpentane	0.998	0.007	1.5	5.2	1.40 \pm 2.77	5.38 \pm 10.6
<i>n</i>-Hexane	0.997	0.016	0.98	5.2	3.08 \pm 4.88	11.8 \pm 18.7
2,4-Dimethylpentane	0.999	0.005	1.5	4.77	0.13 \pm 0.56	0.56 \pm 2.49
Methylcyclopentane	0.999	0.008	2.8	—	1.28 \pm 3.30	4.81 \pm 12.4
2-Methylhexane	0.996	0.008	1.08	—	0.57 \pm 1.19	2.56 \pm 5.31
Cyclohexane	0.997	0.004	1.28	6.97	1.23 \pm 2.03	4.61 \pm 7.61
2,3-Dimethylpentane	0.997	0.016	1.31	—	0.85 \pm 1.37	3.79 \pm 6.11
3-Methylhexane	0.995	0.006	1.4	—	0.77 \pm 1.39	3.42 \pm 6.21
2,2,4-Trimethylpentane	0.994	0.003	0.93	3.34	0.05 \pm 0.42	0.23 \pm 2.14
<i>n</i> -Heptane	0.994	0.007	0.81	6.76	4.07 \pm 30.5	18.2 \pm 136
Methylcyclohexane	0.995	0.008	1.8	9.64	1.43 \pm 2.47	7.28 \pm 12.6
2,3,4-Trimethylpentane	0.994	0.008	1.6	6.6	0.06 \pm 0.48	0.32 \pm 2.42
2-Methylheptane	0.99	0.008	0.96	—	0.87 \pm 1.41	4.43 \pm 7.20
3-Methylheptane	0.991	0.009	0.99	—	0.20 \pm 0.53	1.03 \pm 2.71
<i>n</i>-Octane	0.989	0.121	0.6	8.11	0.97 \pm 1.28	4.93 \pm 6.51
<i>n</i>-Nonane	0.998	0.021	0.54	9.7	0.29 \pm 0.59	1.68 \pm 3.37
<i>n</i>-Decane	0.995	0.03	0.46	11	0.23 \pm 0.32	1.44 \pm 2.05
<i>n</i>-Undecane	0.992	0.02	0.42	12.3	0.19 \pm 0.24	1.29 \pm 1.66
<i>n</i>-Dodecane	0.993	0.01	0.38	13.2	39.7 \pm 57.3	53.2 \pm 76.7
Alkenes					9.52 \pm 14.5	30.6 \pm 41.7
Ethylene	0.997	0.003	7.4	8.52	1.42 \pm 1.69	1.78 \pm 2.11
Propylene	0.998	0.025	9.4	26.3	1.88 \pm 10.2	3.53 \pm 19.1
<i>trans</i> -2-butene	0.997	0.031	10	64	0.60 \pm 1.34	1.50 \pm 3.34
1-Butene	0.994	0.03	8.9	31.4	0.63 \pm 1.04	1.58 \pm 2.59
<i>cis</i> -2-butene	0.999	0.023	10	56.4	0.70 \pm 2.06	1.75 \pm 5.15
1-Pentene	0.993	0.03	6.2	31.4	4.47 \pm 6.72	14.0 \pm 21.0
<i>trans</i> -2-Pentene	0.998	0.009	8.8	67	0.19 \pm 0.67	0.60 \pm 2.11
Isoprene	0.998	0.008	9.1	101	0.20 \pm 0.75	0.62 \pm 2.28
<i>cis</i> -2-Pentene	0.998	0.015	8.8	65	0.09 \pm 0.25	0.28 \pm 0.80
1-Hexene	0.984	0.008	4.4	37	1.36 \pm 2.74	5.09 \pm 10.3
Acetylene	0.998	0.048	0.5		3.03 \pm 5.55	3.52 \pm 6.44
Aromatics					4.28 \pm 8.24	22.2 \pm 25.3
Benzene	0.997	0.007	0.42	1.22	1.13 \pm 1.62	3.95 \pm 5.66
Toluene	0.995	0.005	2.7	5.63	1.06 \pm 1.91	4.34 \pm 7.84

Ethylbenzene	0.992	0.003	2.7	7	0.30 ± 2.40	1.41 ± 11.4
<i>m, p</i>-Xylene	0.986	0.002	7.4	18.7	0.72 ± 1.94	3.42 ± 9.19
<i>o</i>-Xylene	0.989	0.003	6.5	13.6	0.20 ± 0.59	0.95 ± 2.79
Styrene	0.991	0.013	2.2	58	0.40 ± 2.60	1.87 ± 12.1
<i>iso</i> -Propylbenzene	0.986	0.02	2.2	6.3	0.06 ± 0.24	0.32 ± 1.28
<i>n</i> -Propylbenzene	0.986	0.016	2.1	5.8	0.05 ± 0.16	0.29 ± 0.85
<i>m</i> -ethyltoluene	0.989	0.02	—	18.6	0.09 ± 0.20	0.49 ± 1.06
<i>p</i> -ethyltoluene	0.992	0.02	—	11.8	0.08 ± 0.18	0.44 ± 0.98
1,3,5-Trimethylbenzene	0.989	0.004	10.1	56.7	0.09 ± 0.18	0.47 ± 0.96
<i>o</i> -ethyltoluene	0.999	0.02	—	11.9	0.07 ± 0.18	0.35 ± 0.95
1,2,4-Trimethylbenzene	0.991	0.003	8.8	32.5	0.14 ± 0.25	0.74 ± 1.34
1,2,3-Trimethylbenzene	0.993	0.002	8.9	32.7	0.09 ± 0.16	0.46 ± 0.85
<i>m</i> -diethylbenzene	0.991	0.02	—	—	0.07 ± 0.08	0.40 ± 0.50
<i>p</i> -diethylbenzene	0.993	0.03	—	—	0.10 ± 0.10	0.57 ± 0.61

^a [Correlation coefficients of calibration curves](#)

^b [Method detection limit](#)

^{a,c} Units: g O₃/g VOCs (Carter, 1994).

^{b,d} Units: ×10⁻¹² cm³ molecule⁻¹ s⁻¹ (Atkinson and Arey, 2003)

^{e-c} Species in bold were used in source apportionment

Table 2 Comparison of VOCs source apportionment results with formers

Area	Sampling period	Model	Sources							
			Fuel evaporation	LPG/NG	Industrial emission	Vehicle emission	Solvent usage	Coal biomass	Stationery or +mobile	Biogenic others
Tianjing, urban ^a	Nov. 2014—Oct. 2015	PMF	8.7	18.6	19.9	39.1	4.7	10.6		9.0
Wuhan, urban ^b	Feb. 2013—Oct. 2014	PMF		19.8 ±0.9	14.4 ±0.9	27.8 ±0.9	16.2 ±0.4	21.8 ±0.9		
Lanzhou, downtown ^c	Jan.—Dec. 2013	PCA—MLR			19.5	58.3	22.2			
Paris, urban ^d	Jan. 2010—Dec. 2010	PMF	5	16		23	26	13		17
Nanjing, industrial area ^e	Mar. 2011—Feb. 2012	PCA/APCS	15—48		15—23	29—50	6—15			1—4 15—23
Hong Kong, urban ^f	Jan. 2001—Dec. 2001	PCA/APCS		11—19.4	5.2—9	38.9—48	32—36.4			0.1
Paterson, urban ^g	Nov. 2005—Dec. 2006	PMF			16	31	19		12	22
Houston, industrial area ^h	Aug. 2006—Sep. 2006	PMF	20—37		39—58	11—16				
Los Angeles, urban ⁱ	2001—2003 (Jul.—Sep.)	PMF	47—58	13	15	22—24				1—3
This study	Sep. 2014—Aug. 2015	PMF	21.5 ±2.99	62.6 ±3.04	3.8 ±0.50			10.9 ±1.57		1.3 ±0.69

^a Liu et al., (2016);^b Lyu et al., (2016);^c Jia et al., (2016);^d Baudic et al., (2016);^e An et al., (2014);^f Guo et al., (2007);^g Yu et al., (2014);^h Leuchner and Rappenglück, (2010);ⁱ Brown et al., (2007)

Table 3 Contributions (%) of local sources and regional transport of five sources in different seasons.

Seasons	Oil refining		NG		Combustion source		Asphalt		Fuel evaporation	
	Local	Regional	Local	Regional	Local	Regional	Local	Regional	Local	Regional
Autumn	64.5	35.5	74.6	25.4	68.6	31.4	65.4	34.6	68.3	31.7
Winter	60.1	39.9	60.0	40.0	58.5	41.5	60.3	39.7	59.0	41.0
Spring	66.5	33.5	66.0	34.0	59.7	40.3	64.0	36.0	60.0	40.0
Summer	69.4	30.6	71.9	28.1	69.2	30.8	62.7	37.3	65.9	34.1
Annual	53.6	46.4	54.5	45.5	48.8	51.2	50.5	49.5	50.6	49.4

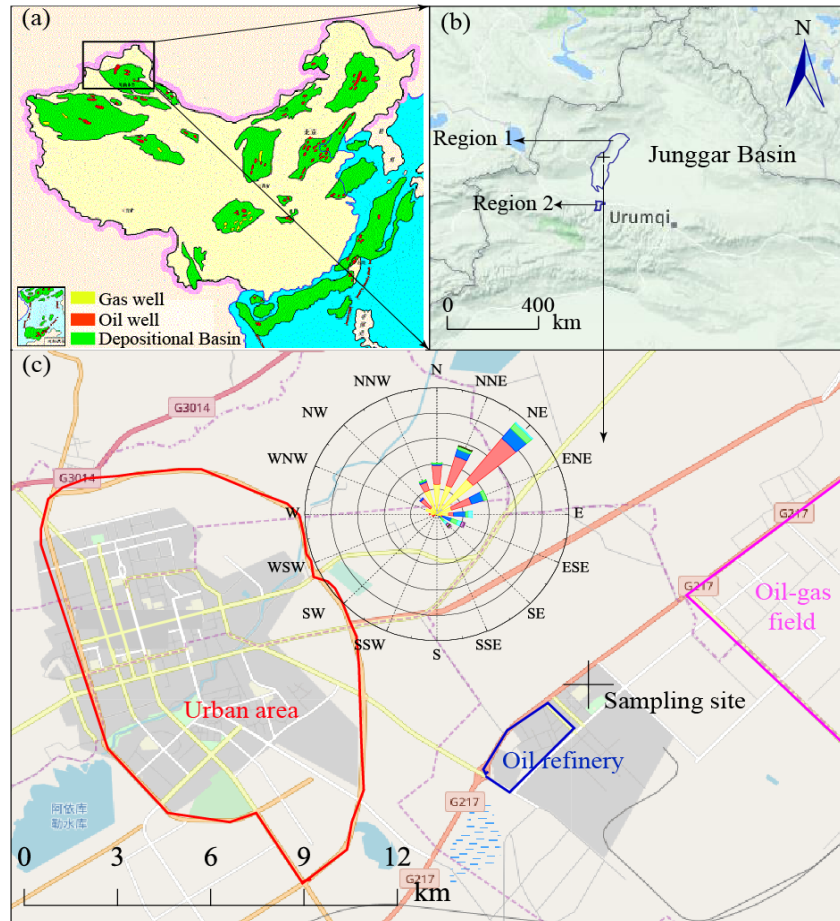


Figure 1. The spatial distribution of ~~oil-gas~~ oil-gas and ~~gas~~ gas bearing basins in China (a) and the terrain of the study area (b). The sampling site is about 11 km away from the urban area and located in the northeast of an oil refinery plant and southwest of an ~~oil-gas~~ oil-gas and ~~gas~~ gas field. The northeasterly winds prevailed during the sampling periods (c). ~~Northwesterly and northeasterly winds prevailed during the sampling periods.~~

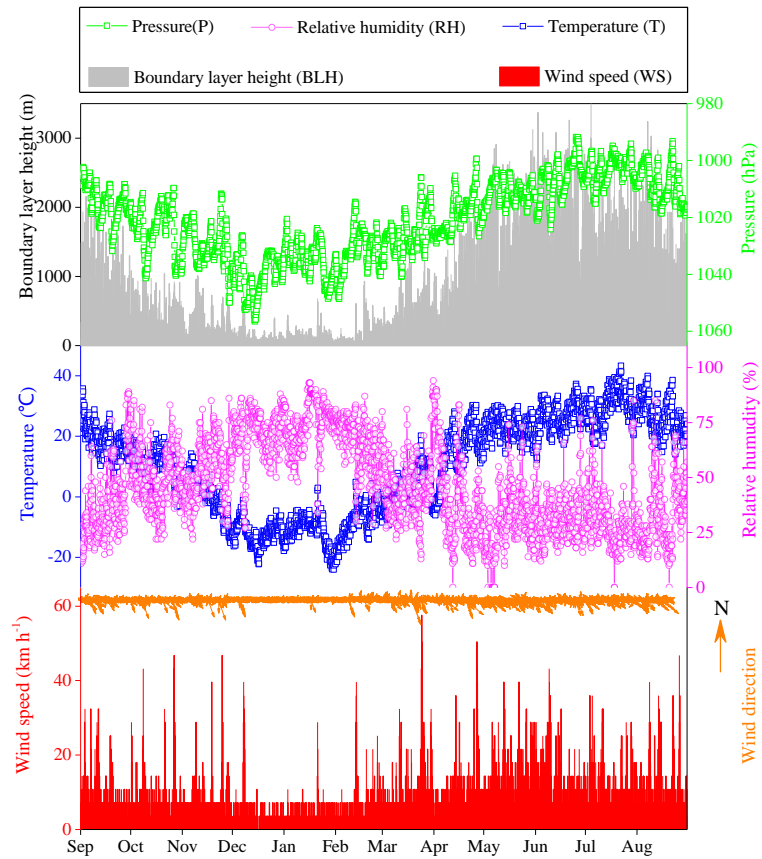


Figure 2. Hourly variations of Every three-hour meteorological parameters at the observation site from September 2014 to August 2015.

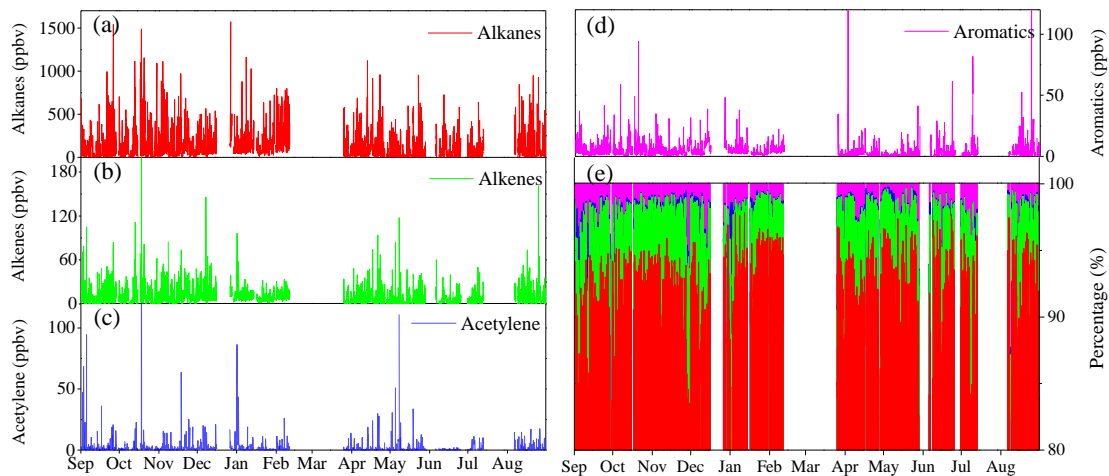


Figure 3. Time series of ~~the every two hours~~ concentrations (expressed in ppbv) ~~for the of~~ four ~~of~~ VOCs categories ~~of~~ VOCs including alkanes (a), alkenes (b), acetylene (c), aromatics (d), and their fractions (e) during the sampling period. _

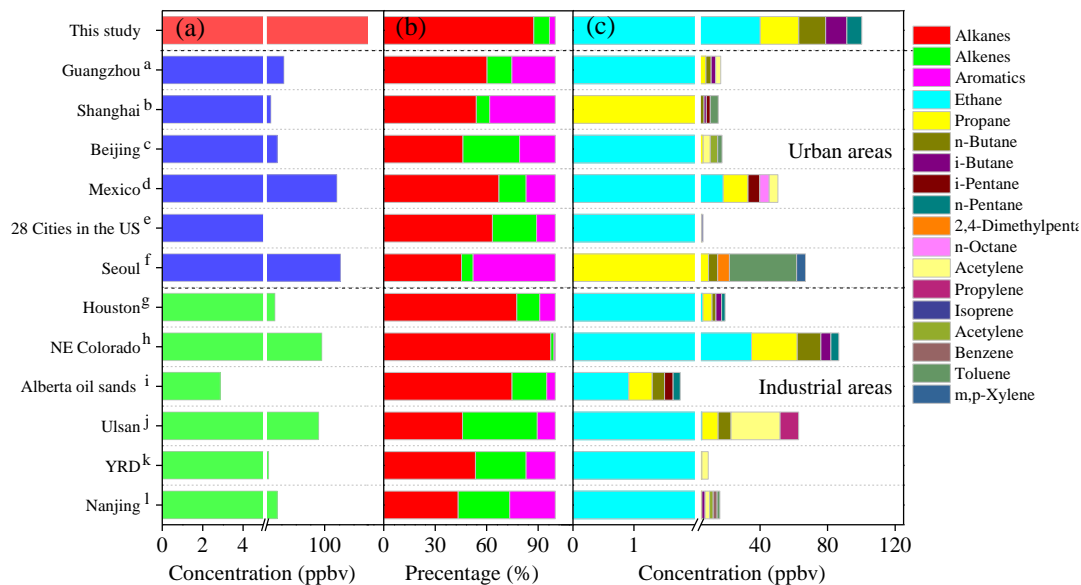


Figure 4. Comparison of the VOCs concentrations (a), compositions (b) and the top five VOCs species (c) in this study ~~and~~ with former studies concerning the VOCs in ~~the~~ the ambient air of urban and industrial areas.

^a Zou et al. (2015); ^b Cai et al. (2010); ^c Wang et al. (2010); ^d Garzón et al. (2015); ^e Baker et al. (2008); ^f Na and Kim, (2001); ^g Leuchner and Rappenglück, (2010); ^h Gilman et al. (2013); ⁱ Simpson et al. (2010); ^j Na et al. (2001); ^k An et al. (2014); ^l Shao et al. (2016)

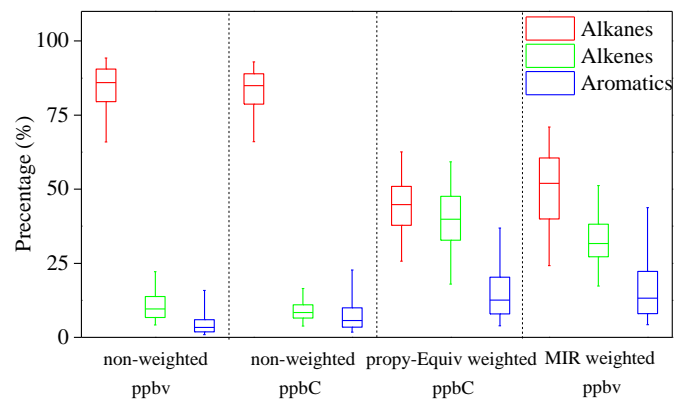


Figure 5. Box and whisker plots of VOCs profiles based on different scales during the whole sampling period. Box and Whisker plots are constructed according to 25th—75th and 5th—95th percentile of the calculation results.

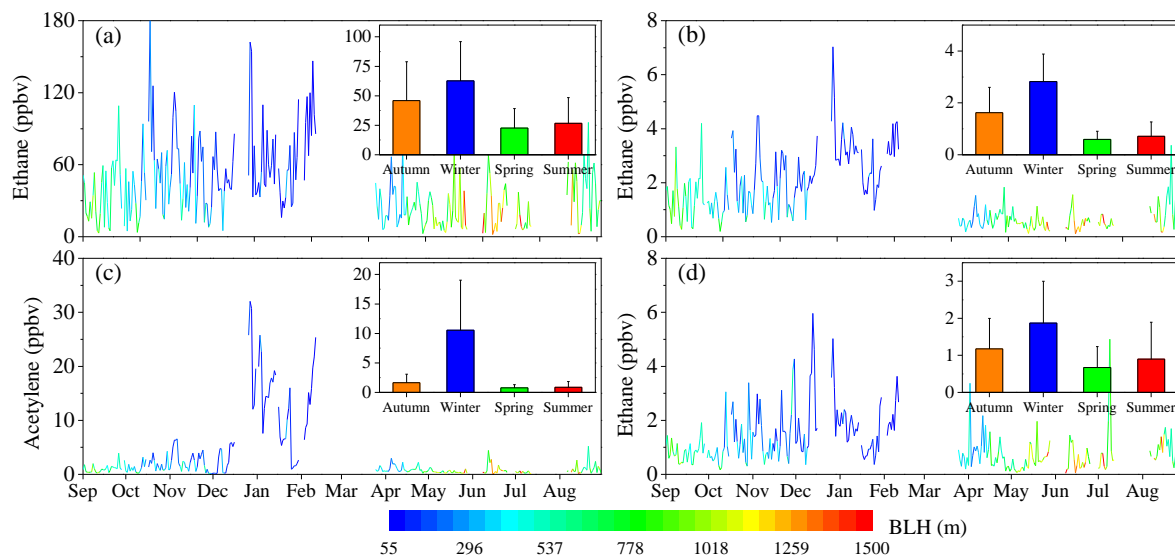


Figure 6 Seasonal and daily variations of ethane (a), ethylene (b), acetylene (c), and benzene (d) during the sampling period. **Figure 6.** Scatter plots of VOCs, NO_2 and O_3 under different boundary layer height (BLH) at monthly (a and b) and daily timescale (c and d).

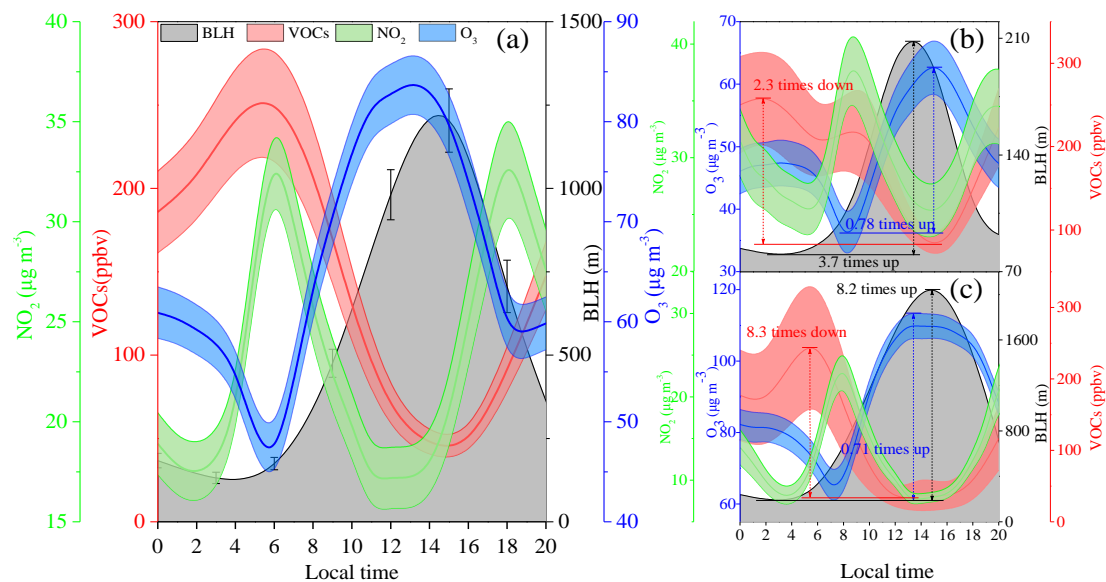


Figure 7. Diurnal variation of boundary layer height (BLH), VOCs, NO₂, and O₃ concentrations in different timescale: annual (a), winter (b) and summer (c). Solid line represents the average value and filled area indicates the 95th confidence intervals of the mean.

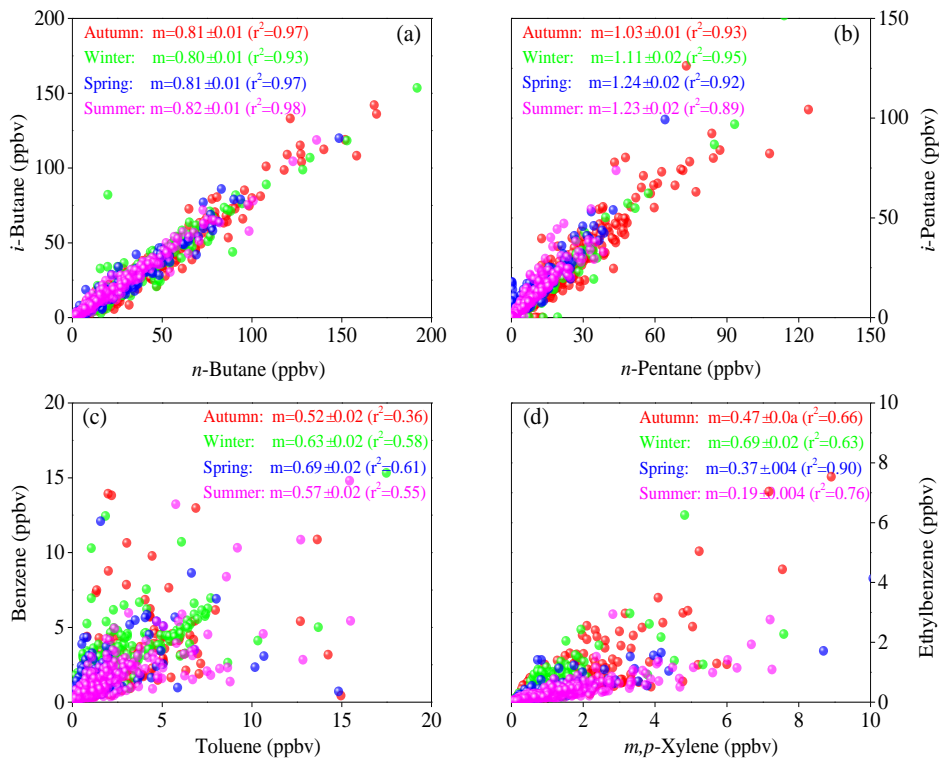


Figure 8. Correlations ($m = \text{slope} \pm \text{standard error}$ (r^2)) between compounds with similar atmospheric lifetimes including *i*-butane/*n*-butane (a) and *i*-pentane/*n*-pentane (b), and compounds with different lifetimes including benzene/toluene (c) and *m,p*-xylenes/ethylbenzene/*m,p*-xylenes (d).

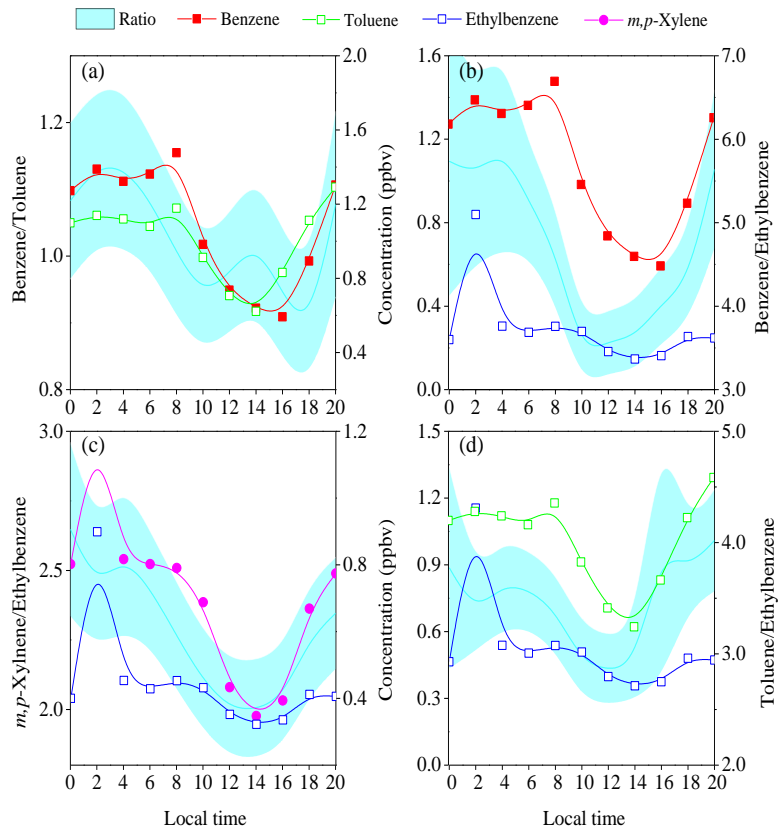


Figure 9. Diurnal variations of benzene, toluene, ethylbenzene, and *m,p*-xylene and their ratios: benzene/toluene (a), benzene/ethylbenzene (b), *m,p*-xylene/ethylbenzene (c), and toluene/ethylbenzene (d).

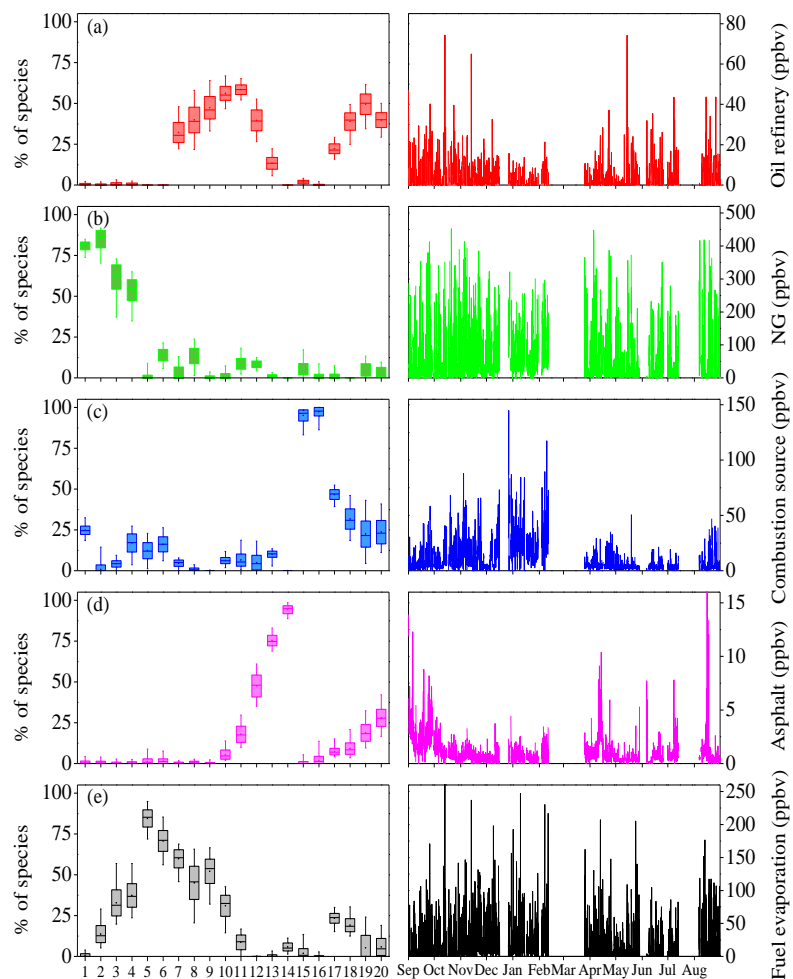


Figure 10. Source profiles of five factors resolved by PMF modeling including oil refinery (a), NG (b), combustion source (c), asphalt (d) and fuel evaporation (e), and their corresponding hourly source contributions. Box and whisker plots are constructed according to the 5th-95th percentiles of the F-peak bootstrap runs ($n = 100$).

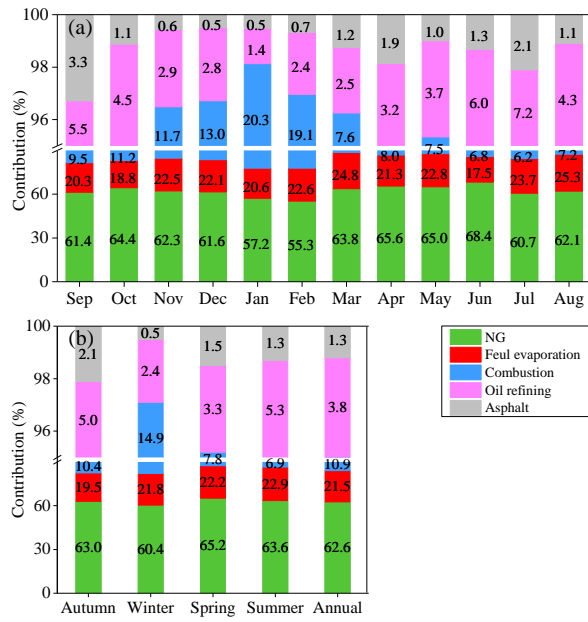


Figure 11. Variations of monthly averaged (a) and seasonal averaged (b) contributions of five identified VOC_s sources (expressed in %).

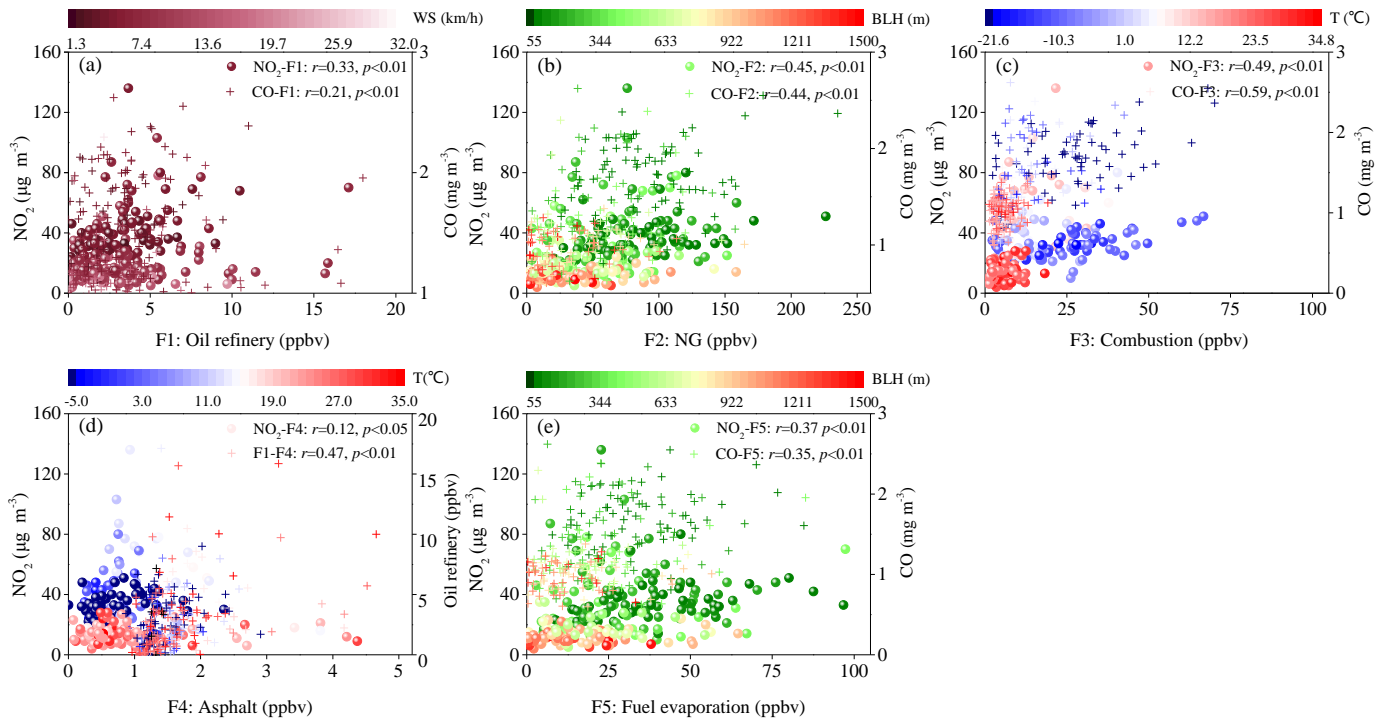


Figure 12. Scatter plots of daily concentrations of trace gas and source contributions including oil refinery (a), NG (b), combustion (c), asphalt (d), and fuel evaporation (e) under different meteorological conditions (wind speed (WS), boundary layer height (BLH) and temperature (T)).

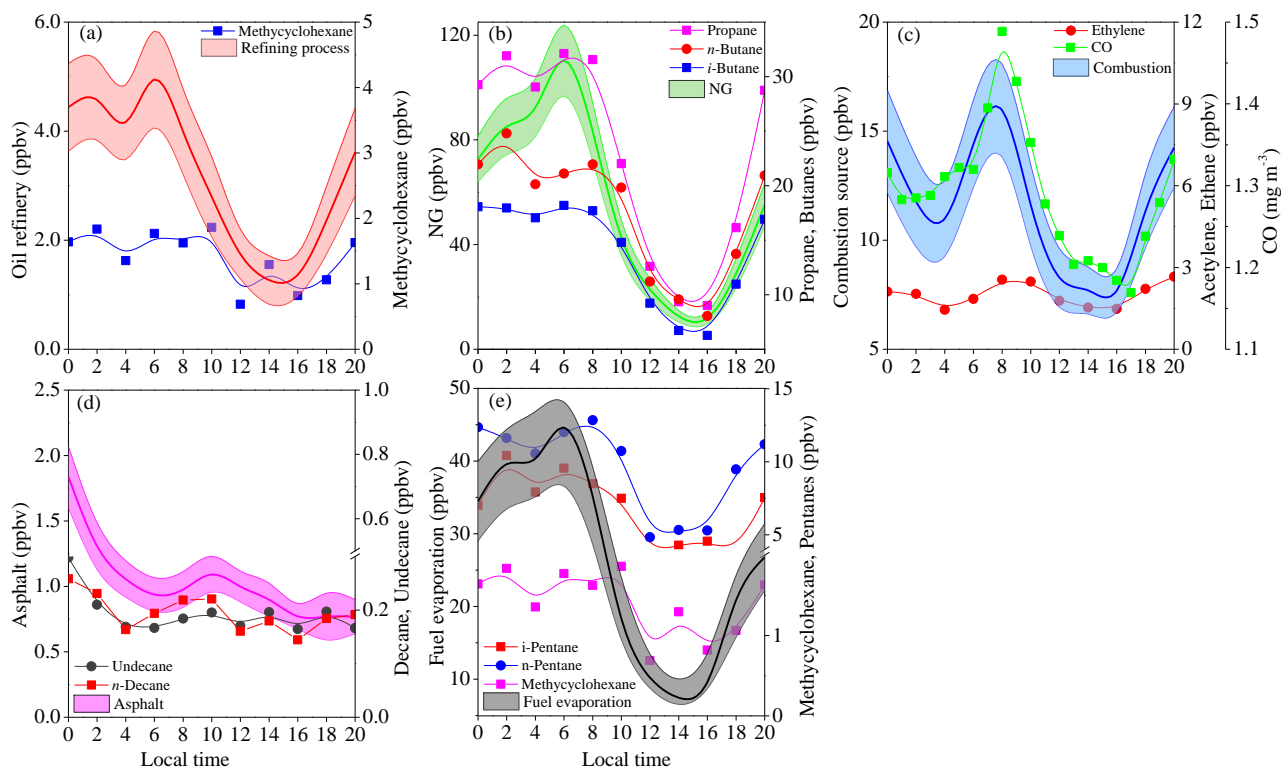


Figure 13. Diurnal variations of the contributions (expressed in ppbv) of five identified sources including oil refining process (a), NG (b), combustion source (c), asphalt (d) and fuel evaporation (e), and specific compounds with high loadings in each source profile. Note that the CO in combustion source was expressed in mg m^{-3} .

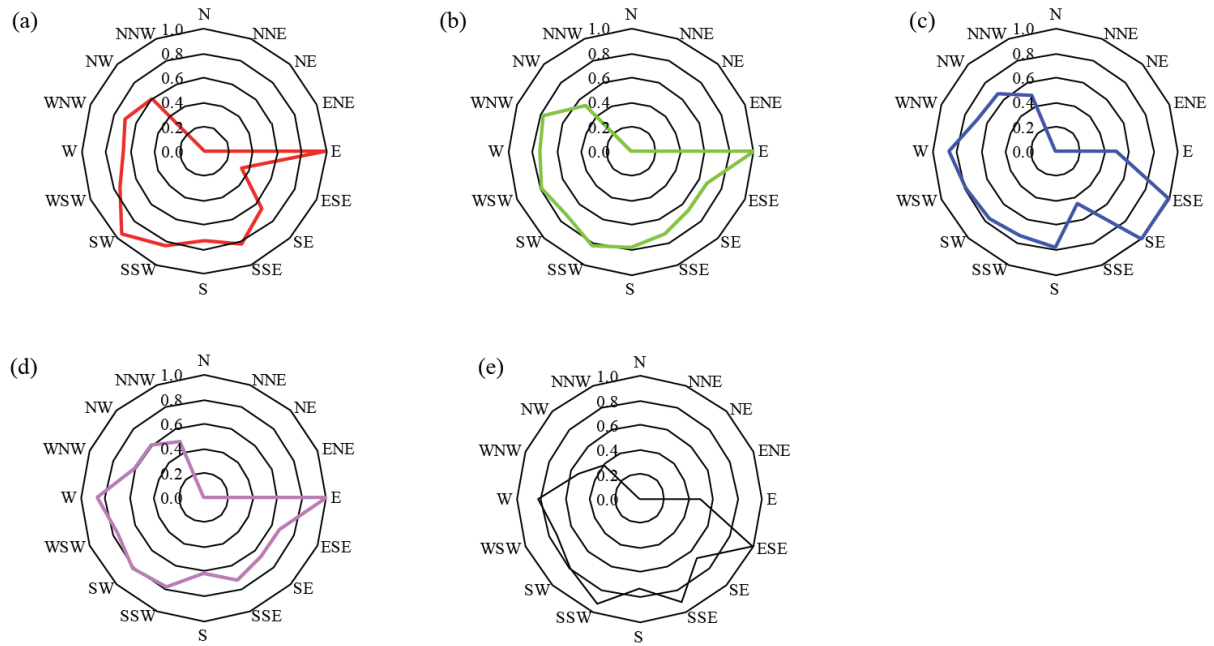


Figure 14. Annual conditional probability function (CPF) plots of five identified VOCs source including oil refinery (a), NG (b), combustion (c), asphalt (d); and fuel evaporation (e).

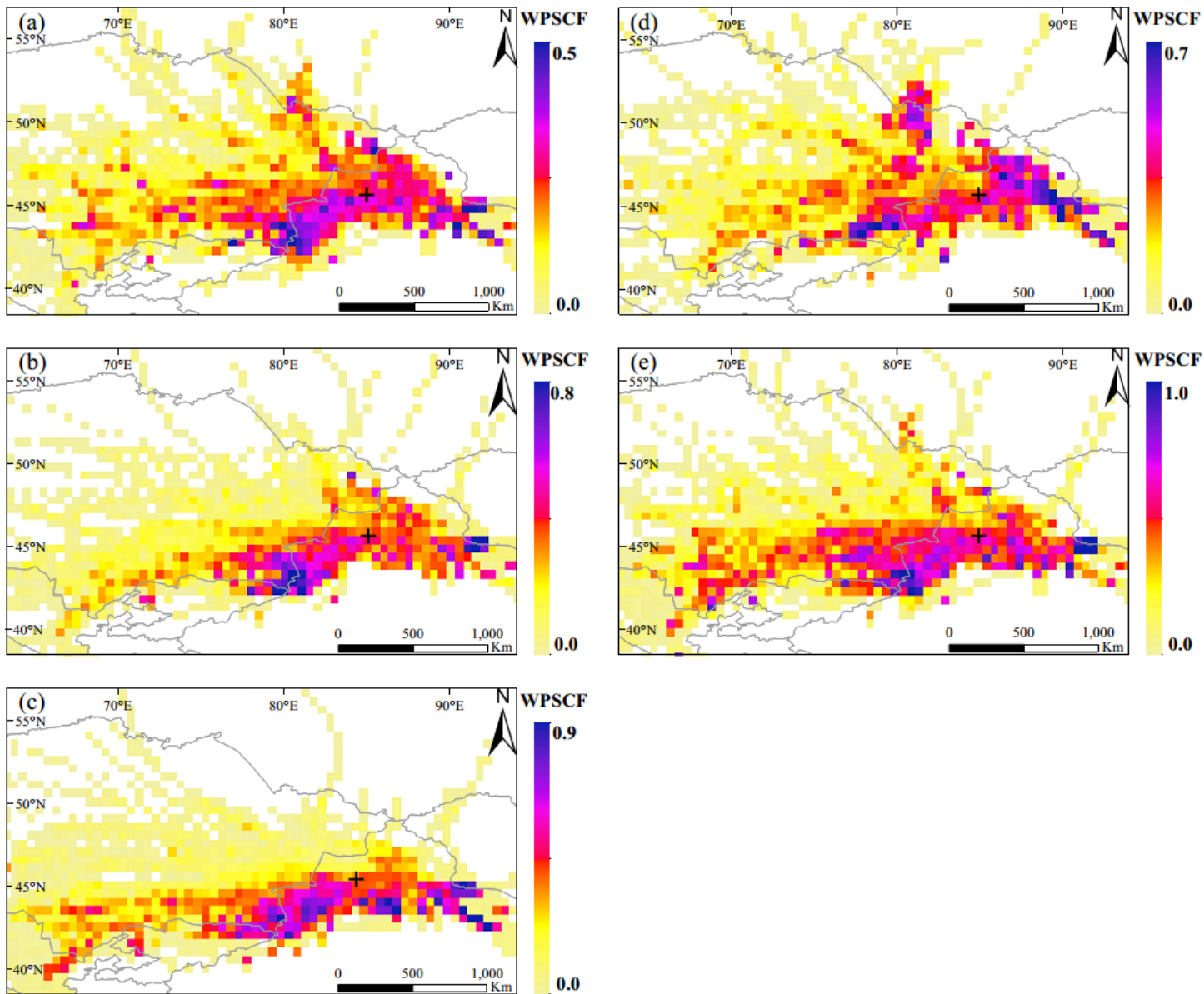


Figure 15. Annual weight potential source contribution function (WPSCF) maps for five identified sources derived from PMF analysis including oil refining (a), NG (b), combustion source (c), asphalt (d), and fuel evaporation (e). The black cross represents the sampling site.

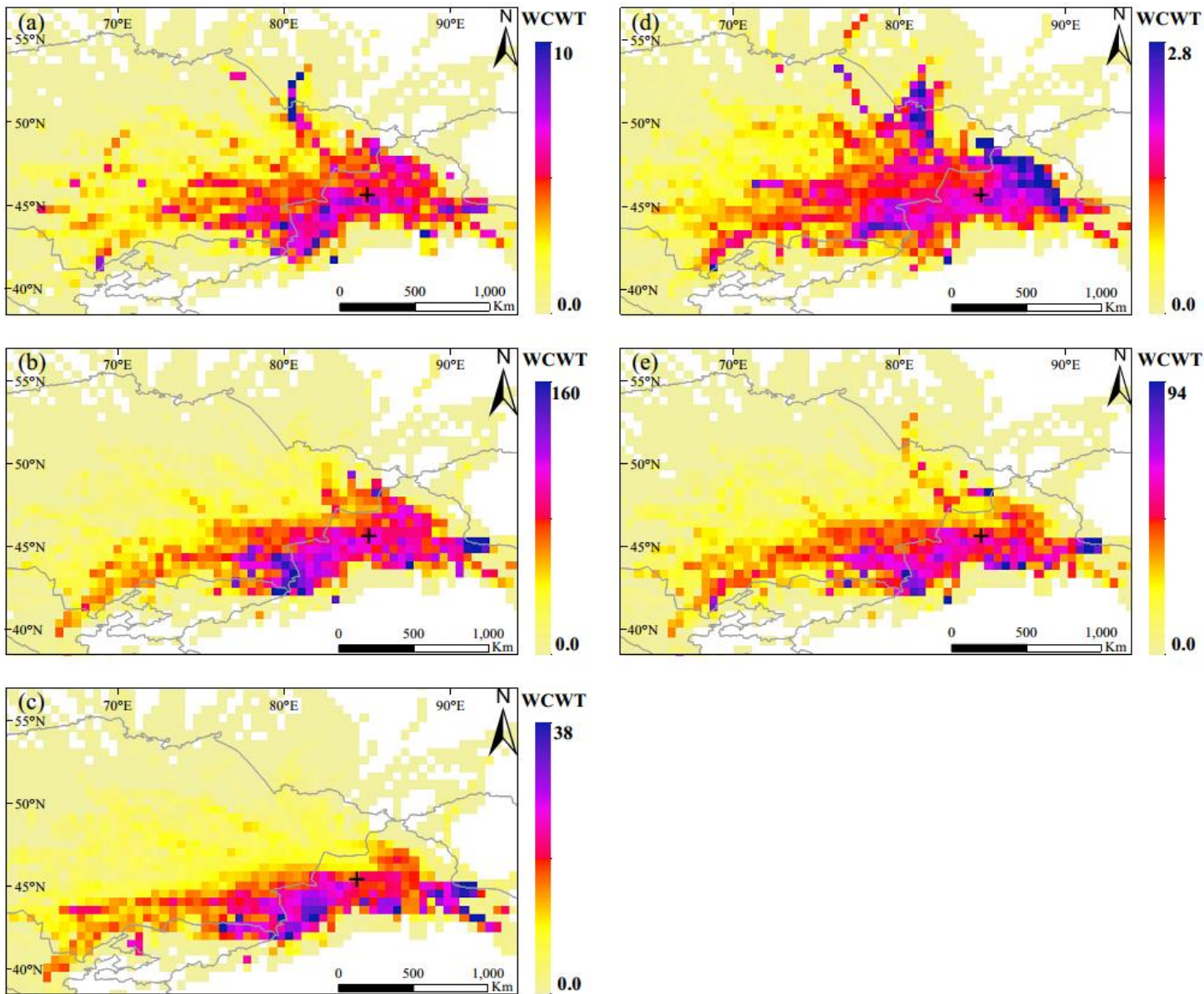


Figure 16. Annual weight concentration weighted trajectory (WCWT) maps for five identified sources derived from PMF analysis including oil refining (a), NG (b), combustion source (c), asphalt (d), and fuel evaporation (e). The black cross represents the sampling site.

Appendix A Detail operation of positive matrix factorization (PMF) in source apportionment of VOCs dataset.

A1 Data preparation

Two files including species concentrations and uncertainty file are required to be introduced into the EPA PMF 5.0 model. The concentrations file is a i (number of samples) \times j dimension (number of species) matrix (\mathbf{X} matrix) of number of samples (column) plus the number of species (row), i.e., 2743 \times 20 in this study. There are two types of uncertainty files: sample-specific and equation-based. The sample-specific uncertainty file is also a matrix with the same dimension as the concentrations matrix. The equation-based uncertainty dataset is constructed according to the method detection limit (MDL) and error fraction (%):

$$U_{ij} = \frac{5}{6} \times \text{MDL} \quad C < \text{MDL} \quad (1)$$

$$U_{ij} = \sqrt{(\text{ER} \times \text{concentration})^2 + (\text{MDL})^2} \quad C > \text{MDL} \quad (2)$$

Not all fifty-seven ~~56~~ Photochemical Assessment Monitoring Stations (PAMS) VOCs are introduced into the PMF model, there are some rules to decide which species should be included or excluded from the PMF model: (1) highly collinear species, such as propane & *n*-butane, benzene & toluene are included (Fig. A1); (2) species indicating VOC sources (i.e., acetylene is the marker of combustion sources) are retained; (3) species that are highly reactive are excluded (i.e., *i*-pentene), since they are rapidly reacted away in the ambient atmosphere (Guo et al., 2011b; Shao et al., 2016) (Guo et al., 2011; Shao et al., 2016).

Prior to the PMF model base run, the retained species were firstly classified into strong, weak, and bad based on their signal-noise-ratios (S/N). Species with S/N ratios less than 0.5 were grouped into bad and grouped into weak if S/N ratios are in the range of 0.5–1.0 (US EPA, 2014). However, the S/N ratios were not useful to categorize species because all species have S/N ratios greater than 2.0 in this study. Therefore, the percentage of samples below the detection limit (BDL) method limit detection, residual scale, and priority knowledge of VOCs source tracers are used. The species with percent below MBDL greater than 60% were categorized as bad and were excluded from the model (i.e., *trans/cis*-2-pentene, isoprene); species with percent below MDLBDL > 50% were characterized as weak (Callén et al., 2014). Finally, nine species (ethane, propane, *n*-hexane, cyclohexane, methylcyclohexane, *n*-octane, *n*-nonane, *n*-decane, and *u*-undecane) were categorized as strong and eleven species (*i*-butane, *n*-butane, *i*-pentane, *n*-pentane, *n*-dodecane, ethylene, acetylene, benzene, toluene, *m*, *p*-xylene, and *o*-xylene) were characterized as weak due to its residual scale beyond 3.

A2 The optimal number of factors.

Choosing the optimal number of factors (P-value) in modeling is a critical question in PMF analysis. Too many factors will result in meaningless factor profiles, while too few factors will make it difficult to segregate the mixing sources (Bressi et al., 2014). Factors ranging from 3 to 8 were tested in this study. Each model was run for 20 times with a random seed. All the Q values (Q_{true} , Q_{robust} , Q_{except} , and $Q_{\text{true}}/Q_{\text{except}}$), observed versus predicted (O/P) concentrations and scaled residuals were

evaluated. In theory, if the number of sources is estimated properly, the Q_{true} value should be approximately to Q_{except} . If the number of sources is not well determined, the Q value may deviate from the theoretical value— (Bressi et al., 2014; Baudic et al., 2016)(Guo et al., 2011; Bressi et al., 2014; Baudic et al., 2016). However, the Q_{true} always deviates from the Q_{except} in many cases especially in for large dataset (Liu et al., 2016, 2017; Shao et al., 2016). The variation of the Q values to the number of factors is shown in Fig. A2a and the correlation coefficients between O/P values in each factor number solution is shown in Fig. A2b.

As shown in Fig. A2a, Q_{true}/Q_{except} decreased substantially between 2-, 3- and 4-factor solutions, indicating that a substantial amount of the variability in the dataset was accounted for with each additional factor; for $P=5$, the Q_{true}/Q_{except} exhibited the minimum value; as the factor number moved-changed from 6 to 8, the Q_{true}/Q_{except} value increased again. The Pearson correlation coefficients between the observed and predicted total VOCs concentrations for different factor numbers are shown in Fig. A2b, which indicating that the total VOCs concentrations were well reproduced by PMF model. In addition, for the 20 individual VOCs species, the PMF model also well reproduced the predicted concentrations, with the R^2-r^2 ranged from 0.42 to 0.96 (Table A1). Therefore, we considered that the 5-factor solution was the optimum solution for this PMF analysis (Fig. A3).

15 A3 Bootstrap run (BS)

After choosing the 5-factor solution, the bootstrap (BS) method was used to detect and estimate disproportionate effects of a small set of observations on the solution and also, to lesser extent, effects of rotational ambiguity. BS datasets were-are constructed by randomly sampling blocks of observations from the original data set (US EPA, 2014). The base run with the lowest Q_{robust} iswas provided to map with each BS run in minimum Pearson correlation coefficient being 0.6. The number of BS iswas set as 100 to ensure the robustness of the statistics. In this study, the base and boot factors were matched except for factor 3 (combustion) andtwo factors especially due to the factor 5 (fuel evaporation) (Table A2).-The factor 1 (oil refinery) and factor 2 (NG) containing factor 5 species and factor 3 (combustion) also mapped to boot factor 5. Mapping over 80% of the factors indicatesthat BS uncertainties can be interpreted and the number of factors may be appropriate. Seen from the Table A2, the BS results indicated a rotational ambiguity and F-peak should be further applied.

25 A4 BS-DISP error estimation

BS-DISP estimates the errors associated with both random and rotational ambiguity. A key file containing the number of cases accepted, largest decrease in Q , number of swaps in best fit and DISP was generated (Table A3), and s swaps by factor (Table A3) was used to assess the error fraction. There were 99 bootstrap cases accepted and one resample was rejected proved by the largest decrease in Q being -14. The decrease of Q was less than 1%, which indicated that the test of BS was validated and no more testing was required. It suggested that the solution was well constrained and the BS-DISP results can be reported.

Finally, the F-Peak values from -1 to 1 at 0.1 interval were used to remove the rotational ambiguity as discussed above. The F-peak bootstrap was also used to test the mapping between the base model and the F-peak runs. The results indicated that the F-peak ≈ 0.2 was the optimal solutions with all factors mapping 100% and the ~~a~~base run of each ~~the~~ species ~~of~~ was base ~~run~~ within the inter quartile range (IQR) of the BS run.

5 Appendix B The calculation of PSCF and CWT

B1 PSCF

The PSCF values were calculated to explore the potential geographic origins of VOC sources using the source contributions apportioned from the PMF model and the backward-trajectory. The PSCF is defined as:

$$PSCF_{ij} = \frac{m_{ij}}{n_{ij}} \quad (4)$$

10 where i and j are ~~on behalf of~~ the latitude and longitude, n_{ij} is the total number of endpoints that fall in the ij -th cell, and m_{ij} is defined as the number of endpoints in the same cell that exceeded the threshold criterion. The 75th percentile ~~s~~ of each identified source contribution (i.e., 3.9 ppbv for oil refinery, 75.1 ppbv for NG, 15.3 ppbv for combustion, 1.2 ppbv for asphalt, and 33.4 ppbv for fuel evaporation) was used as the criterion value. When each grid average number of trajectory endpoint (n_{ave}) is three times larger than the n_{ij} , the uncertainty of cell is reduced by multiplying a weight function (W_{ij}) into the PSCF value. The weight function is expressed as:

$$WPSCF = \frac{m_{ij}}{n_{ij}} \times W(n_{ij}) \quad (5)$$

$$W(n_{ij}) = \begin{cases} 1.00, & n_{ij} > 3n_{ave} \\ 0.70, & 3n_{ave} > n_{ij} > 1.5n_{ave} \\ 0.40, & 1.5n_{ave} > n_{ij} > n_{ave} \\ 0.20, & n_{ij} > n_{ave} \end{cases} \quad (6)$$

B2 CWT

20 Since PSCF value just gives the proportion of potential sources in a grid with struggles to distinguish the pollution levels of different potential regions, a concentration-weighted-trajectory (CWT) model was employed in this study. The geographical-domain was sliced into grid cell with a resolution of $0.5^\circ \times 0.5^\circ$. The CWT was calculated according to:

$$C_{ij} = \frac{1}{\sum_{l=1}^M \tau_{ijl}} \sum_{l=1}^M C_l \tau_{ijl} \quad (7)$$

25 where C_{ij} represents the average weight concentrations in the grid cell (i, j), C_l is the measured VOCs concentration observed on the arrival of trajectory l , τ_{ijl} is the number of trajectory end points in the grid cell (i, j) associated with the C_l sample. The weighting function described in equation (6) was also used in the CWT ~~analyses~~analysis.

Appendix C ~~The d~~Detailed operation calculating of local emission and regional transport contribution

C1 Choosing the radius to distinguish the local and regional area.

Grids within a given radius were excluded in case they could be too close to the origin ~~to be properly distributed.~~ Usually, the radius was set according to the area covered by first 6 h of trajectories (Bari et al., 2003; Wang et al., 2015; Wang et al., 2016). In this study, we referred to it with modification. 12 h backward trajectories were set as the radius to distinguish the local and regional areas due to the following reasons:

(1) The duration of *m, p*-xylene decreasing from highest concentrations (at 02:00 LT) to lowest (14:00 LT) was 12 h (section 3.4). The atmospheric lifetime of *m, p*-xylene is about 11.8 h assuming the OH radical equals to 10^6 rad cm^{-3} . The compounds with atmospheric lifetime longer than *m, p*-xylene can be transported from long distance ~~or accumulated in the local area.~~

(2) The endpoint of ~~each every 2-h~~ backward trajectories in the first 24 h was tested to find the optimum range of “local and nearby” area (Fig. C1). As the backward time increasing from 1 h to 24 h, the area covered by the long air mass increased significantly. Before the first 5 h, the air masses were mainly from the northwest and the east of the sampling site. From 7 h to 12 h, air masses from the northeast, southeast, and southwest ~~reached of the receptorsampling~~ site and the “shape of local area” formed. After 12h, the air masses, especial for the trajectories from the west transported ~~from-for~~ long distance and reached the sampling site, indicating the regional contribution.

It can be seen from ~~the~~ Fig. C1 that the farthest endpoint of 12_h backward was about 7 degrees away from the sampling site. Therefore, the local and regional area was divided by a circle with the radius being 7 degrees (sampling site as the origin).

C2 Raster analysis

The CWT results obtained by TrajStat software were stored in shapefile format and then were introduced into the Arc GIS software (10.1, Esri, US). The first step was to remove the negative value from the shapefile and then convert the shapefile into raster format. The local and regional area was extracted by a circle with radius being 7 degrees as discussed above. The inner of the circle was defined as the local while the external area was set as the regional transport and an example is shown in Fig. C2. The statistics (count, minimum, maximum, sum, mean, and standard deviation) of the extracted raster were shown in its layer properties in Arc Map. The statistics of each VOCs sources in each season are summarized in Table C1. The percentage of contributions of local source and regional transport of the five VOCs sources in different seasons were calculated according to Eq. (26) in section 2.46.3.

Table A1. Pearson coefficients between the observed and predicted VOCs concentrations for 5-factor solution

Species	Intercept	Slope	SE ^a	r^2
ethane	1.09	0.90	7.69	0.96
propane	0.25	0.98	5.96	0.94
<i>i</i> -butane	0.42	0.86	4.27	0.88
<i>n</i> -butane	0.76	0.82	6.06	0.84
<i>i</i> -pentane	2.50	0.71	7.57	0.50
<i>n</i> -pentane	0.69	0.75	4.20	0.77
<i>n</i> -hexane	0.24	0.84	1.05	0.91
cyclohexane	0.11	0.82	0.37	0.92
methylcyclohexane	0.14	0.81	0.43	0.93
<i>n</i> -octane	0.06	0.84	0.21	0.93
<i>n</i> -nonane	0.04	0.71	0.10	0.85
<i>n</i> -decane	0.05	0.68	0.08	0.79
<i>n</i> -undecane	0.04	0.70	0.09	0.71
<i>n</i> -dodecane	0.17	0.27	0.29	0.49
ethylene	0.25	0.50	0.75	0.53
acetylene	0.57	0.15	0.93	0.42
benzene	0.36	0.33	0.56	0.42
toluene	0.32	0.24	0.48	0.37
<i>m</i> , <i>p</i> -xylene	0.14	0.48	0.32	0.57
<i>o</i> -xylene	0.05	0.36	0.07	0.55

^aSE = standard error

Table A2. Mapping of bootstrap factors to base factors

	Factor 1	Factor 2	Factor 3	Factor 4	Factor 5	Unmapped
Boot Factor 1	100	0	0	0	0	0
Boot Factor 2	0	100	0	0	0	0
Boot Factor 3	2	3	95	0	0	0
Boot Factor 4	0	0	0	100	0	0
Boot Factor 5	14	20	0	0	66	0

Table A3. BS-DISP Diagnostics.

# of Cases Accepted:	99				
% of Cases Accepted:	99%				
Largest Decrease in Q :	-14.10				
%d Q :	-0.014				
# of Decreases in Q :	1				
# of Swaps in Best Fit:	0				
# of Swaps in DISP:	0				
Swaps by Factor:	0	0	0	0	0

Table C1. The statistics of each-VOCs sources in each season obtained by raster analysis

		Oil refinery		NG		Combustion		Asphalt		Fuel evaporation	
		Local	Regional	Local	Region	Local	Region	Local	Region	Local	Region
Autumn	Minimum	0.016	0.00055	0.083	0.005	0.021	0.019	0.022	0.0032	0.012	0.0027
	Mean	2.68	0.48	41.15	4.63	7.6	1.16	0.98	0.17	17.43	2.9
	Sum	816	449	12758	4347	2356	1098	305	160	5315	2468
	Number	304	928	310	939	310	943	310	944	305	851
Winter	Minimum	0.017	0.0007	0.62	0.089	0.092	0.092	0.0052	0.00043	0.13	0.0025
	Mean	1.41	0.32	36.1	7.82	12.34	2.93	0.35	0.076	18.51	4.21
	Sum	492	319	12707	8411	4333	3147	121	79	6406	4421
	Number	348	1010	352	1076	351	1073	345	1036	346	1049
Spring	Minimum	0.0027	0.000094	0.11	0.064	0.48	0.033	0.0066	0.0041	0.002	0.0015
	Mean	1.05	0.19	16.71	2.86	2.6	0.5	0.49	0.093	7.66	1.91
	Sum	360	180	6068	3175	945	553	177	103	2764	1840
	Number	343	954	363	1112	363	1111	363	1109	361	964
Summer	Minimum	0.00044	0.0011	0.036	0.021	0.01	0.0021	0.0082	0.00022	0.0097	0.00028
	Mean	1.92	0.29	19.57	2.6	2.63	0.4	0.51	0.1	9.98	1.87
	Sum	556	242	5714	2250	776	343	149	89	2923	1513
	Number	289	845	292	865	295	863	293	876	293	808
Annual	Minimum	0.0036	0.000094	0.0356	0.011	0.0645	0.0019	0.0023	0.00043	0.0036	0.0015
	Mean	2.16	0.41	35.26	6.52	8.08	1.87	0.73	0.16	16.44	3.8
	Sum	953	821	15973	13338	3653	3805	328	330	7399	7225
	Number	442	1959	453	2047	452	2035	450	2014	450	1899

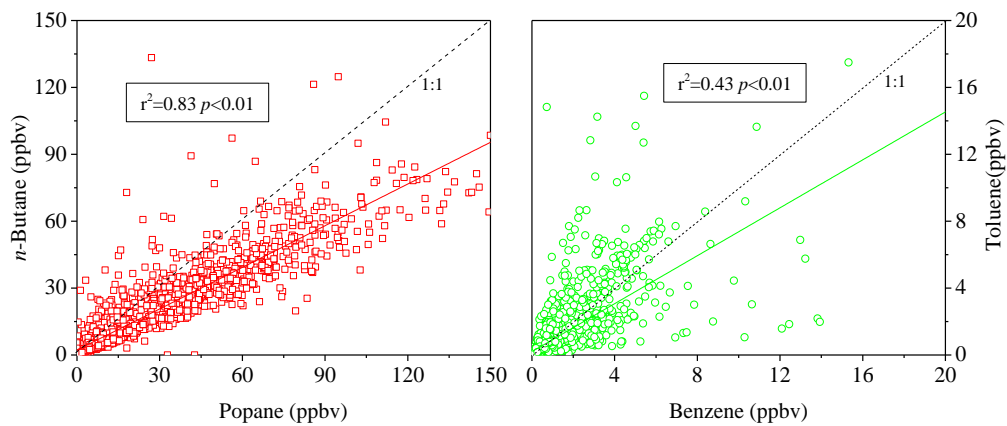


Figure A1. Samples of highly collinear species.

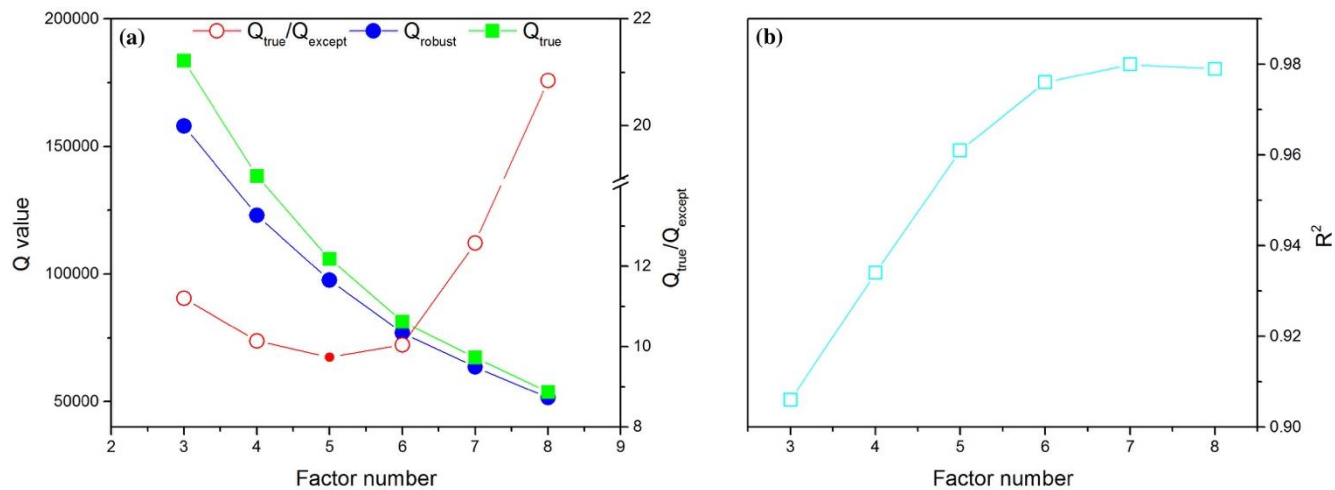


Figure A2. $Q_{\text{true}}/Q_{\text{except}}$, Q_{robust} , and Q_{true} plotted against the number of factors used in the positive matrix factorization (PMF) solution.

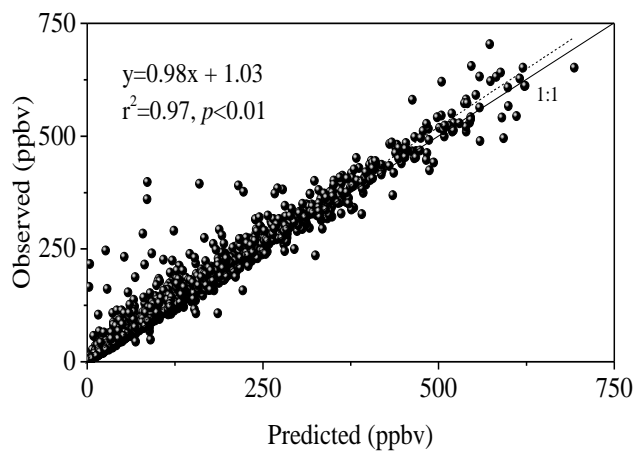


Figure A3. Scatter plots between the total predicted and observed VOC concentrations based on the 5-factor PMF solution.

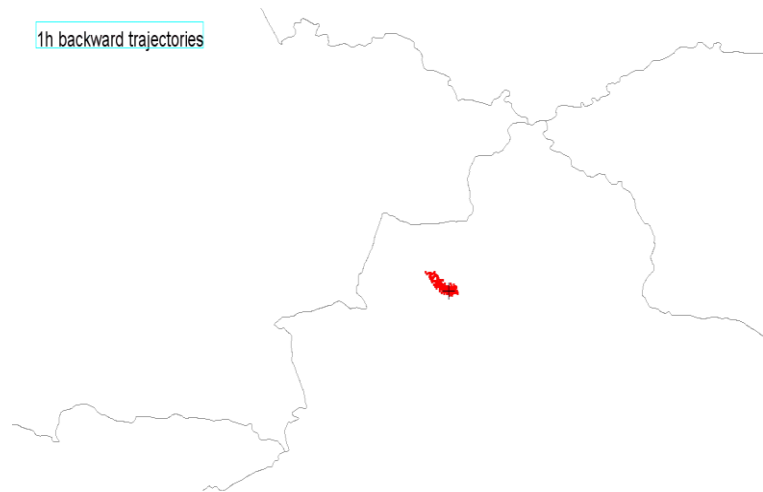
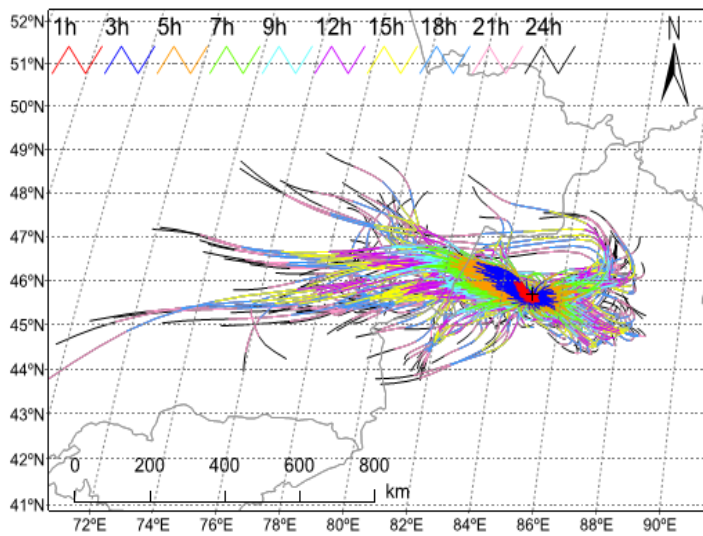


Figure C1. The region covered by the first 24_h backward trajectories. Left: the domain covered by the trajectories. Right: the dynamic variation of backward trajectory-trajectories from 1h to 24h. (Double click to view the GIF)

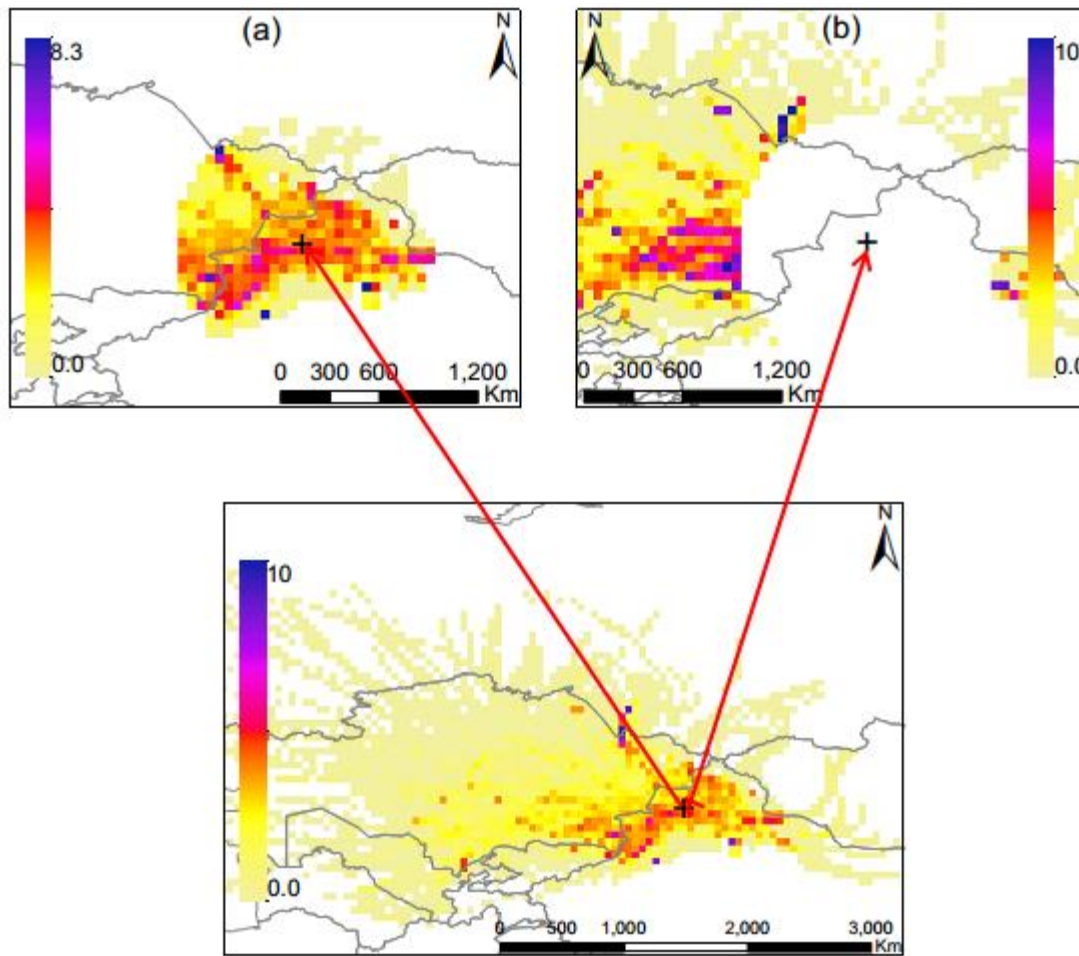


Figure C2. Example of (a) local area and (b) domain of regional transport range extracted by a circle with the radius being seven degrees. The black cross represents the sampling point and is set as the original point.